การผลิตไบโอดีเซลจากสารป้อนปาล์มน้ำมันด้วยกรรมวิธีไฮโดรโพรเซสซิ่งบนตัวเร่งปฏิกิริยานิกเกิลโมลิบดินัมและโคบอลต์โมลิบดินัมบนอะลูมินา

นางสาวนริศรา รอดบุญ

วิทยานิพนธ์นี้เป็นส่วนหนึ่งของการศึกษาตามหลักสูตรปริญญาวิศวกรรมศาสตรมหาบัณฑิต
สาขาวิชาวิศวกรรมเคมี ภาควิชาวิศวกรรมเคมี

คณะวิศวกรรมศาสตร์ จุฬาลงกรณ์มหาวิทยาลัย

ปีการศึกษา 2555

Biodiesel production from different palm-oil feedstocks with hydroprocessing process over Ni-Mo/Al_2O_3 and Co-Mo/Al_2O_3 catalysts

Miss Narisara Rodboon

A Thesis Submitted in Partial Fulfillment of the Requirements
for the Degree of Master of Engineering Program in Chemical Engineering
Department of Chemical Engineering
Faculty of Engineering
Chulalongkorn University
Academic Year 2012

Thesis Title	BIODIESEL PRODUCTION FROM DIFFERENT PALM-OIL FEEDSTOCKS WITH HYDROPROCESSING PROCESS OVER Ni-Mo/Al_2O_3 AND Co-Mo/Al_2O_3 CATALYSTS
By	Miss Narisara Rodboon
Field of Study	Chemical Engineering
Thesis Advisor	Professor Suttichai Assabumrungrat, Ph.D.
Thesis Co-advisor	Assistant Professor Worapon Kiatkittipong, D.Eng.

Accepted by the Faculty of Engineering, Chulalongkorn University Partial Fulfillment of the Requirements for the Master's Degree

.....…….……Dean of the Faculty of Engineering
(Associate Professor Boonsom Lerdhirunwong, Dr.Ing.)

THESIS COMMITTEE

……Chairman
(Assistant Professor Suphot Phatanasri, D.Eng.)

……Thesis Advisor
(Professor Suttichai Assabumrungrat, Ph.D.)

……...Thesis Co-advisor
(Assistant Professor Worapon Kiatkittipong, D.Eng.)

……...Examiner
(Associate Professor Artiwan Shotipruk, Ph.D.)

……...External Examiner
(Associate Professor Navadol Laosiripojan, Ph.D.)

นริศรา รอดบุญ : การผลิตไบโอดีเซลจากสารป้อนปาล์มน้ำมันด้วยกรรมวิธีไฮโดรโพรเซสซิ่งบนตัวเร่งปฏิกิริยา นิกเกิลโมลิบดินัมและโคบอลต์โมลิบดินัมบนอะลูมินา (BIODIESEL PRODUCTION FROM DIFFERENT PALM-OIL FEEDSTOCKS WITH HYDROPROCESSING PROCESS OVER Ni-Mo/Al_2O_3 AND Co-Mo/Al_2O_3 CATALYSTS) อ. ที่ปรึกษาวิทยานิพนธ์หลัก : ศ.ดร.สุทธิชัย อัสสะบำรุง รัตน์, อ.ที่ปรึกษาวิทยานิพนธ์ร่วม: ผศ.ดร.วรพล เกียรติกิตติพงษ์, 101 หน้า.

ในงานวิจัยนี้ใช้สารป้อนจำพวกน้ำมันปาล์ม ได้แก่ น้ำมันปาล์มที่ผ่านการกระบวนการกำจัดยางเหนียว, น้ำมันปาล์มที่ผ่านการทำให้บริสุทธิ์จำพวก ไขปาล์มในการผลิตไบโอดีเซล การทดลองทำในเตาปฏิกรณ์แบบกะขนาดเล็ก ภายใต้สภาวะความดันที่ 50 บาร์ โดยใช้ตัวเร่งปฏิกิริยานิกเกิลโมลิบดินัมและโคบอลต์โมลิบดินัมบนตัวรองรับอะลูมินา จากการทดลองพบว่าเมื่ออุณหภูมิในการทำปฏิกิริยาต่ำ (น้อยว่า 360 องศาเซลเซียส) ตัวเร่งปฏิกิริยา โคบอลต์โมลิบดินัม มีความสามารถในการทำปฏิกิริยาดีกว่า ตัวเร่งปฏิกิริยานิกเกิลโมลิบดินั มและเมื่ออุณหภูมิสูงขึ้น ความสามารถในการทำปฏิกิริยาของตัวเร่งทั้งสองมีค่าใกล้เคียงกัน ผลได้ดีเซลของตัวเร่งปฏิกิริยานิกเกิลโมลิบดินั มมีค่าสูงกว่าผลได้ดีเซล ของตัวเร่งปฏิกิริยา โคบอลต์โมลิบดินัม เนื่องจาก ตัวเร่งปฏิกิริยานิกเกิลโมลิบดินั มมีความสามารถในการเลือกเกิด สารผลิตผลในช่วงที่เป็นดีเซลได้ ดีกว่าภายใต้สภาวะการทำปฏิกิริยาที่กำหนด ปริมาณของไตรกลีเซอไรด์และกรดไขมันที่ถูกใช้ในการทำปฏิกิริยาเรียงตามลำดั บจากมากที่สุดไปน้อยที่สุดได้ดังนี้ ไขมันปาล์มชนิดแข็ง , ไขมันปาล์มชนิดอ่อนและน้ำมันปาล์มที่ผ่านกระบวนการกำจัดยางเหนียว ปริมาณของไตรกลีเซอไรด์และกรดไขมันที่ใช้ในการทำปฏิกิริยาจะมีค่าสูงขึ้นเมื่อ ค่าความอิ่มตัวของสารป้อน มีค่ามาก จากผลการทดลองพบว่าที่อุณหภูมิ 360 องศาเซลเซียส เวลาในการทำปฏิกิริยา 4 ชั่วโมงโดยใช้ตัวเร่งปฏิกิริยาซัลไฟต์ของนิกเกิลโมลิบดินัมไขมันปาล์มชนิดแข็งให้ค่าผลได้ของดีเซลสูงที่สุดคือ 71 เปอร์เซ็นต์.

ภาควิชา.....วิศวกรรมเคมี..... ลายมือชื่อนิสิต.....

สาขาวิชา.....วิศวกรรมเคมี..... ลายมือชื่อ อ.ที่ปรึกษาวิทยานิพนธ์หลัก.....

ปีการศึกษา.....2555..... ลายมือชื่อ อ.ที่ปรึกษาวิทยานิพนธ์ร่วม.....

##5370446421: MAJOR CHEMICAL ENGINEERING
KEYWORDS: HYDROPROCESSING / DEGUMMED PALM OIL / REFINED BLEACHED DEODORISED PALM STEARIN / SULFURIZATION

NARISARA RODBOON: BIODIESEL PRODUCTION FROM DIFFERENT PALM-OIL FEEDSTOCKS WITH HYDROPROCESSING PROCESS OVER Ni-Mo/Al_2O_3 AND Co-Mo/Al_2O_3 CATALYSTS. ADVISOR: PROF. SUTTICHAI ASSABUMRUNGRAT, Ph.D. CO-ADVISOR: ASST.PROF. WORAPON KIATKITTIPONG, D.Eng., 101 pp.

In this research, relevant palm oil i.e. degummed palm oil (DPO), refined palm stearin (RPS) including hard and soft stearin are employed as feedstock to produce bio hydrotreated diesel. The reaction was performed in parallel small batch reactor under reduced pressure of 50 bar catalyzed by sulfided NiMo/γ-Al_2O_3 and CoMo/γ-Al_2O_3 catalyst. CoMo catalyst shows much lower catalytic activity than NiMo catalyst at low opearting temperature (<360 °C) and become comparable to NiMo catalyst at higher temperature. However, NiMo catalyst generally gives higher selectivity of diesel range hydrocarbon therefore higher diesel yield. Under the defined operating condition, conversion (of triglyceride and fatty acid) could be in order of RPS hard > RPS soft > DPO which indicating that higher degree of saturation of feedstock lead to obtain higher conversion. Maximum of diesel range hydrocarbon yield of 71% could be obtained from RPS hard at reaction temperature of 360 ℃ for 4 h with sulfided NiMo/γ-Al_2O_3 catalyst.

Department: Chemical Engineering Student's Signature……..

Field of study: Chemical Engineering Advisor's Signature…….

Academic Year: 2012 Co-advisor's Signature……

ACKNOWLEDGEMENTS

This thesis is made under the sincere guidance of Professor Sutichai Assabumrungrat whose most kindness and gave the life attitude in non-thesis area. An author would like to express her special thanks of gratitude to her co-advisor, Assistant Professor Worapon Kiatkittipong, who gave the golden opportunity to do this project on the topic of production of biodiesel, which also helped a lot of conceptualize the thesis. Without his guidance of co-advisor there wouldn't be able to make it completed in time. Special thanks extended to Assistant Professor Suphot Phatanasri as a chairman, Associate Professor Artiwan Shotipruk, and Associate Professor Navadol Laosiripojan, as the members of thesis committee for precious time, their valuable suggestions and comments.

Secondly the author would also like to thank to the Oleen Company limited and Patum Oil Company who provided raw materials for the thesis. With deep sense of gratitude to her family especially her parents whom pay attention to take care of health along time during the thesis. The most success of graduation is devoted to them.

Moreover, the author wishes to thank the members of the Center of Excellence on Catalysis and Catalytic Reaction Engineering, Chulalongkorn University and the member also the staff of Chemical Engineering Laboratory for their friendship and assistance.

Finally, the big thanks for the Thailand Research Fund (TRF), as well as the Graduate School of Chulalongkorn University for their financial supports.

CONTENTS

Page

CHAPTER

Page

CHAPTER

Page

CHAPTER

Page

CHAPTER

LIST OF TABLE

TABLE Page

LIST OF FIGURES

FIGURE Page

FIGURE Page

FIGURE Page

CHAPTER I

INTRODUCTION

1.1. Rationale

Rapid industrialization and development has continued to heighten the demand for petroleum oil. Consequently, concerns regarding the increase in petroleum prices, energy security, global warming and environmental problem has been raised(Ong et al., 2011). Moreover, many critics have pointed out that fossil fuels are not considered sustainable in terms of economic feasibility, ecology and environment (Kamm et al., 2006). For these reasons, renewable energy resources are urgently explored to substitute the fossil fuels (Dennis Y.C. Leung et al., 2010). One of the alternative fuel options with the highest potential is the biofuel, especially the biodiesel (Fernando et al., 2006). Biodiesel is an alternative fuel for diesel engines produced by the chemical reaction of vegetable oil or animal fat. The physical properties of biodiesel are a clear yellow liquid with similar viscosity to petroleum diesel as shown in Table 1. Biodiesel is non-flammable, non-explosive with a flash point of 423 K compared to 337 K for petroleum diesel (Fernando et al., 2006)

Table 1.1 Physical properties of biodiesel (Demirbas et al., 2009).

Common name	Biodiesel
Common chemical name	Fatty acid (m)ethyl ester
Chemical formula range	C_{14}-C_{24} methyl esters or $C_{15\text{-}25}H_{28\text{-}48}O_2$
Kinematic viscosity range (mm^2/s, at 313K)	3.3-5.2
Density range (kg/m^3, at 288K)	860-894
Boling-point range (K)	>457
Flash-point range (K)	420-450
Distillation range (K)	470-600
Vapor pressure (mm Hg, at 295K)	<5
Solubility in water	Insoluble in water
Physical appearance	Light to dark yellow, clear liquid
Odor	Light musty/soapy odor
Biodegradability	More biodegradable than petroleum diesel
Reactivity	Stable, but avoid strong oxidizing agents

The conventional method for producing biodiesel is trans-esterification of oil and fat. Trans-esterification of triglyceride with methanol or ethanol produced fatty acid methyl or ethyl ester (FAME, FAEE) which is called first generation biodiesel. However, fatty acid methyl ester from trans-esterification, the first generation of biodiesel, have several limitations e.g. low oxidation resistance, low compatibility with diesel engine and a glut of glycerol by-product (Alexander Guzman., 2010, Kiatkittipong et al., 2010).

Nowadays, the advanced biodiesel research is focused on hydrotreated vegetable oil which is called second generation biodiesel. The hydrotreated biodiesel (HBD) becomes more attractive for utilization as renewable energy for diesel engine. For this method, the transformation of triglyceride present in vegetable oils or animal fats are converted to hydrocarbons, mainly to n-alkanes at the temperatures above 300–360 ˚C and pressure at least 3 MPa leaving propane, CO_2 and water as side-products (da Rocha Filho et al., 1993). The main advantages of the hydrotreated biodiesel are the higher heating content than from FAME, high cetane number and low capital costs and operating costs (Mikkonen., 2008).

Palm oil is the highest potential feedstock for biodiesel production in Thailand; however, as the food vs. fuel debate, many researchers are turning their focus to utilizing inedible or waste oil. In order to render the oils to an edible form, the impurities (non-glycerides) were removed. The highest impurities are gums (phospholipids, phosphotides). Firstly, an impurity called gum in crude palm oil (CPO) was removed by precipitation process. At this state, we will get degummed palm oil (DPO). The DPO is then bleached to remove any undesirable impurities such as pigments and trace metals giving a bleached palm oil (BPO). Next, the BPO is deodorized to eliminate free fatty acid content. This step results in refined, bleached, deodorized palm oil (RPSPO) and palm fatty acid distillate (PFAD) as a byproduct. Finally, The RPSPO is fractionated to yield refined palm olein and refined palm stearin. In this study, DPO, and RPS palm stearin are used as raw materials to produce biodiesel.

$NiMo/Al_2O_3$ and $CoMo/Al_2O_3$ were recently employed as catalyst for HBD production. The catalysts are normally activated by sulfur compound to sulphidation catalyst form. It is worthy to note that $NiMo/Al_2O_3$ and $CoMo/Al_2O_3$ were previously employed as hydrodesulfurization (HDS) catalyst successfully. However, some researchers found that bimetallic carbides catalyst showed higher activites in hydrodenitrogenation (HDN) and HDS reactions than that of commercial Ni-Mo/Al_2O_3 and Co-Mo/Al_2O_3 catalysts (Schwartz et al., 2000; Izhar et al., 2006; Sundaramurthy et al., 2007; Diaz et al., 2003; Ramanathan and Oyama 1995).

This present work is investigated in hydroprocessing of DPO and RPS palm stearin catalyzed by Ni-Mo/Al_2O_3, Co-Mo/Al_2O_3 presulfided catalysts in-house prepared catalysts. Two main products are liquid products and gas products. The main liquid products are hydrocarbons which identified as C_{12}- C_{18} alkanes. The calculated of the yield of diesel (range 250 – 380 ˚C) is following by ASTM-2887-D86 procedure. The influence of operating parameters i.e. H_2 pressure, operating temperature and reaction time on the diesel range yield and product composition are also discussed.

1.2 Objective

To find the appropriate catalyst and operating condition for the production of biodiesel via hydroprocessing of different palm-oil feedstocks.

1.3 Scope of work

1. Prepared bimetallic Ni-Mo/Al_2O_3, Co-Mo/Al_2O_3 sulfided catalysts with characterization including Brunauer-Emmett-Teller (BET) surface area analysis, Coupled plasma-optical emission spectrometer (ICP-OES), Scanning Electron Microscope (SEM), X-ray diffraction (XRD), temperature-programmed reduction of hydrogen (H_2-TPR) and NH_3 Temperature programmed desorption (NH_3 –TPD).

2. Perform the experiment of hydroprocessing of, DPO, refined bleached deodorised palm soft stearin and refined bleached deodosized palm hard stearin in a shaking batch reactor under various operating temperature and reaction time by using Ni-Mo/Al_2O_3, Co-Mo/Al_2O_3 sulfided catalysts.

3. The product composition was analyzed by using gas chromatography with flame ionization detector (FID) and yield of diesel range is calculated form simulated distillation following by ASTM-2887D-68 and Fourier transforms infrared Spectroscopic method (FT-IR).

CHAPTER II

THEORY

This chapter describes the background information of hydroprocessing of vegetable oil, the mechanism of reaction, raw-material for biodiesel production, properties of diesel, and simulated distillation method.

2.1 Mechanism of hydroprocessing

Hydrotreating and hydrocracking are occurred in hydroprocessing which hydrotreating is heteroatom removal such as sulfur and nitrogen while hydrocracking, is saturation and breakage of C–C bonds in order to produce high quality gasoline and diesel molecules (Scherzer and Gruia., 1996). Hydrotreating has been used to produce straight chain alkanes ranging from n-C_{15} – n-C_{18} from other vegetable oil and fat. Owing to a removal of oxygen from triglyceride molecule, there are two possible deoxygenation approaches: (i) hydrodeoxygenation and (ii) decarboxylation. For the first approach, oxygen is removed in the form of water while for another one it is removed as CO_2 (Donnis., 2009). The hydrocracking reactions produced not only normal alkanes but also cycloalkanes, aromatics and carboxylic acids where the decarboxylation and decarbonylation are take place (da Roch Filho et al., 1993). Accordingly several reactions have an important role in the hydroproceesing such as hydrodenitrogenation (HDN), hydrodesulfurization (HDS), hydrodeoxygenation (HDO), hydrogenation (HYD) and hydrodemetallization (HDM). The various feed, operating condition and type of catalyst have an effect on these reactions (Furimsky., 2003).

A reaction pathway for conversion of triglycerides into alkanes is shown in Figure 2.1. For the first step, double bonds of triglycerides are at first saturated. The hydrogenated triglycerides are broken down into various intermediates by hydroprocessing. The next step has mainly three pathways for hydroprocessing of triglycerides including hydrodeoxygenation (hydrogenation/ dehydration), decarboxylation and decarbonylation. This process also has another reactions such as water gas shift and methanization as well as isomerization and cracking that can be described as follows (Huber et al., 2007; Mikulec et al., 2010).

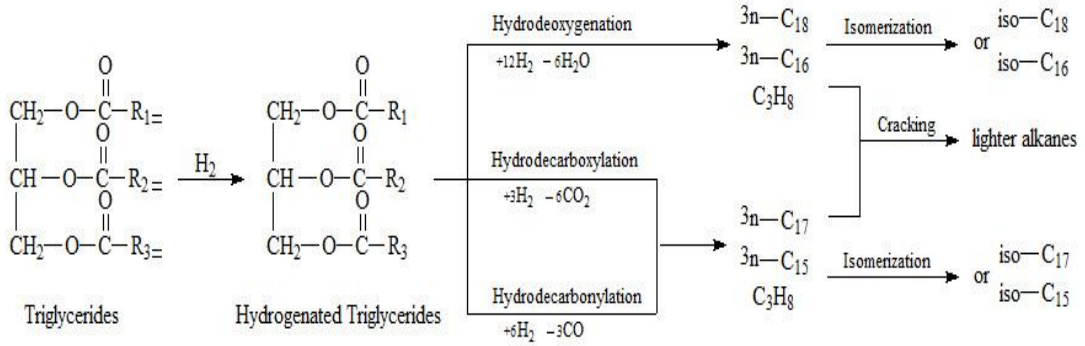

Figure 2.1. Reaction pathway for conversion of triglycerides to alkanes.

2.1.1 Hydrodeoxygenation (hydrogenation/dehydration)

Hydrodeoxygenation (HDO) is a hydrogenolysis process that removes oxygenated compounds from the organic molecule in reaction with hydrogen forming water using commercial hydrotreating catalysts. There is commonly used Ni-Mo or Co-Mo on γ-Al_2O_3, zeolites (ZSM-5), Pd or Pt on carbon as well as alumina. Ni-Mo sites for hydrogenation reactions and acid catalytic sites for dehydration reactions. The summarized reactions are shown in Figure 2.2.

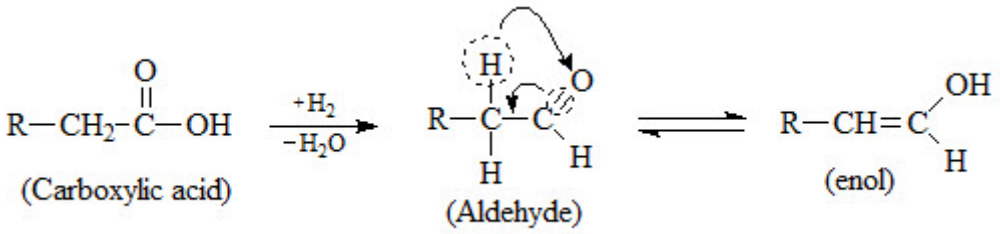

Figure 2.2 Reaction pathway of carboxylic acid to enol form.

The carboxylic acids as a reactant which is hydrogenated can be converted into aldehyde and water. The aldehyde compound is enolized because α-hydrogen can be isomerized to the enol from, which is the reactive intermediate. On the contrary, compounds lacking α-hydrogen cannot be isomerized to the enol form (Donnis et al., 2009).

In Figure 2.3 shown the enol form could either be hydrogenated over the catalyst at the highly reactive oxygen, at the C=C double forming alcohol or forming 1-alkene and water. The alcohol which is dehydrated can be converted into alkane and water. The alkene which is hydrogenated at C=C double can be converted to alkane (Donnis et al., 2009).

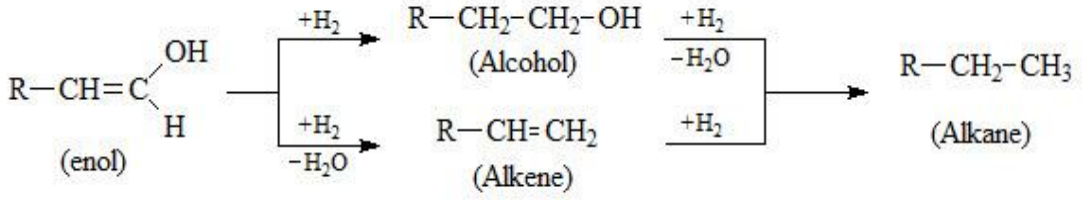

Figure 2.3 Reaction pathway of enol form to alkane.

If non double bond triglycerides are converted by the hydrodeoxygenation route. The products for this mechanism are water, propane and three normal alkanes of the full length of fatty acid chains in Figure 2.4. By this reaction, one mole of triglyceride reacts with 12 moles of hydrogen. The products are forms one mole of propane, six moles of water, and three moles of normal alkanes of the full length of fatty acid (Donnis et al., 2009; Mikulec et al., 2010).

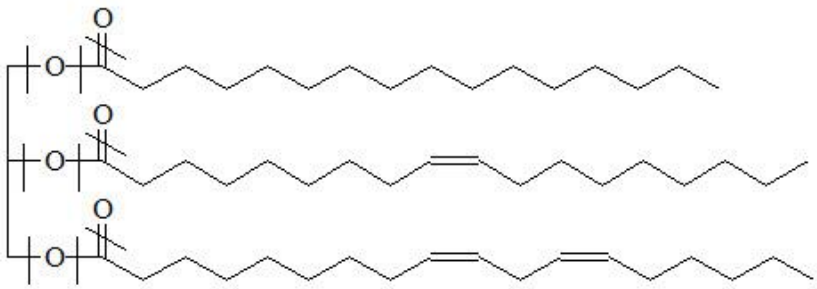

Figure 2.4 Mechanism of the hydrodeoxygenation reaction pathway for the removal of oxygen form triglyceride.

2.1.2 Hydrodecarboxylation

Hydrodecarboxylation (HDC) consists of decarboxylation (CO_2 elimination) of compounds containing carboxylic functional group and hydrogenation of the unsaturated intermediates of CO_2 elimination. The primary product of this reaction is CO_2 and it may undergo further reactions, particularly hydrogenation, which is undesired since it causes significant increase in hydrogen consumption. Therefore, there are many attempts to achieve selective decarboxylation without CO_2 hydrogenation. In this path way, it is required less hydrogen consumption. Due to the saturated triglycerides are converted by the decarboxylation route, the carbon dioxide, propane and three normal alkanes with carbon numbers one less than fatty acid chains are produced as show in Figure 2.5. The products are forms one mole of propane, three moles of carbon dioxide and three moles of a normal alkanes one carbon atom shorter than the full length of fatty acid (Donnis et al., 2009; Mikulec et al., 2010).

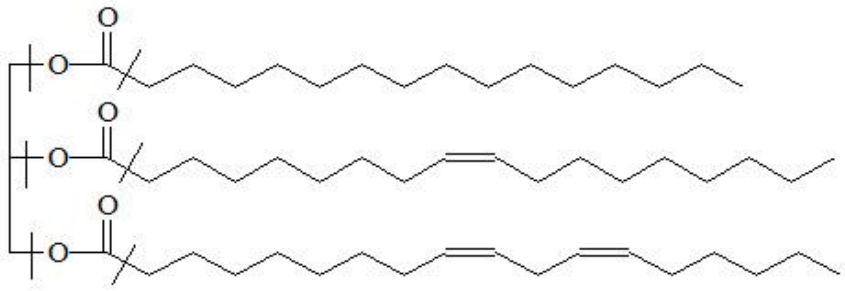

Figure 2.5 Mechanism of the hydrodecarboxylation reaction pathway for the removal of oxygen form triglyceride.

2.1.3 Hydrodecarbonylation

The decarbonylation is chemical reaction which the carboxylic group is reacted with hydrogen for removal one or more carbonyl groups from a molecule to produce a methyl group, carbon monoxide and water. In case of the saturated triglycerides are converted by the decarbonylation route. The products for this mechanism are carbon monoxide, water, propane and three normal alkanes with carbon numbers one less than fatty acid chains in Figure 2.6. As a result of this, one mole of triglyceride reacts with 6 moles of hydrogen. The products are forms one mole of propane, three moles of carbon monoxide, three moles of water and three moles of a normal alkanes one carbon atom shorter than the full length of fatty acid (Donnis et al., 2009; Mikulec et al., 2010).

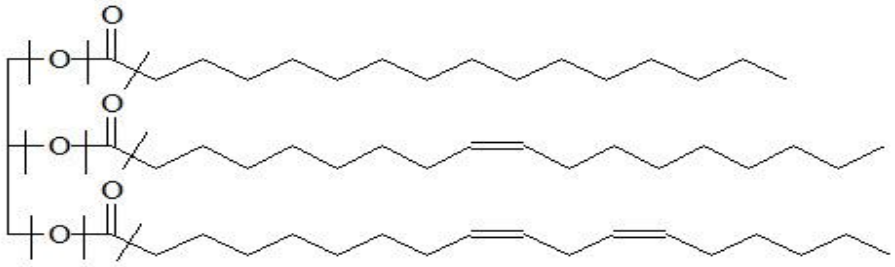

Figure 2.6 Mechanism of the hydrodecarbonylation reaction pathway for the removal of oxygen form triglyceride.

2.1.4 Isomerization and cracking

The isomerization and cracking reaction produce isomerized and lighter alkanes which the normal alkanes from triglyceride can undergo. High cetane number is required for a good diesel production which desired to minimize the isomerization and cracking reactions (Huber et al., 2007).

2.1.5 Water gas shift and methanization

$$CO_2 + H_2 \longleftrightarrow CO + H_2O \quad (2.1)$$

$$CO + 3H_2 \longrightarrow CH_4 + H_2O \quad (2.2)$$

The water gas shift and methanization produce carbon monoxide and carbon dioxide. The water gas shift is a chemical reaction in which carbon dioxide reacts with hydrogen to form carbon monoxide and water vapor as shown in Eq. 2.1. To converted carbon monoxide from water gas reaction reacting with hydrogen into methane and water vapor is the methanization as shown in Eq. 2.2. The influences of both reactions are the hydrogen consumption and product yields (Mikulec et al., 2010).

2.1.6 Hydrodesulfurization

Hydrodesulfurization (HDS) is a catalytic chemical process which removes sulfur (S) from natural gas and from refined petroleum products such as

gasoline or petrol, jet fuel, kerosene, diesel fuel, and fuel oils (Gary et al., 1984). The purpose of removing the sulfur is to reduce the sulfur dioxide (SO_2) emissions that result from using those fuels in automotive vehicles, aircraft, railroad locomotives, ships, gas or oil burning power plants, residential and industrial furnaces, and other forms of fuel combustion.

There is a wide range of organic sulfur compounds, including thiols, thiphenes, organic sulfides and disulfides contain in the refinery HDS feedstocks. These organic compounds are produced by degradation of sulfur containing biological components, present during the natural formation of fossil fuel, petroleum crude oil. In order to prevent poisoning of the noble metal catalysts in the subsequent catalytic reforming of the naphthas, it is necessary to remove the total sulfur down to the parts per million ranges or lower.

The general HDS catalysts are based on molybdenum disulfide (MoS_2) with smaller amounts of other metals (Topsøe H et al., 1996). At the edges of the MoS_2 crystallites, the molybdenum center can stabilize a coordinatively unsaturated site, also known as an anion vacancy. Substrates, such as thiophene, bine to this site and undergo a series a reactions that result in both C-S scission and C=C hydrogenation. Therefore, the hydrogen serves multiple roles to generate of anion vacancy by removal of sulfide, hydrogenation and hydrogenolysis as show in the figure 2.7

(http://en.wikipedia.org/wiki).

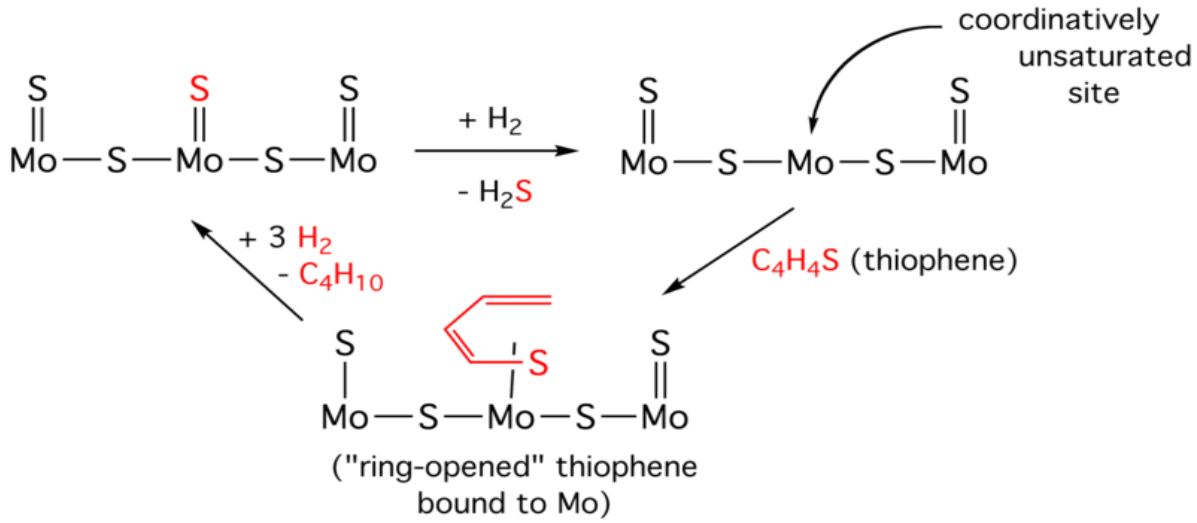

Figure 2.7. A simplified diagram for the cycle.

There are two parallel pathways for the hydrodesulurization reaction. These are hydrogenation and hydrogenolysis which the hydrogenolysis occurs first and the product moieties are hydrogenated the unsaturated heterocycle to a saturated species.

Two reactions occurred in hydrodesulfurization process are:

(I) Hydrogenation of unsaturated compounds which occurs during hydrodesulfurization, and the reaction rates are significant compared with hydrodesulfurization;

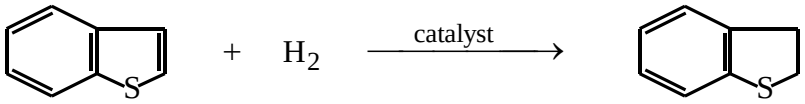

(II) Hydrogenolysis that is results in cleavage of a C-S bond;

$$R-SH + H_2 \longrightarrow RH + H_2S$$

The hydrodesulfurization reactions are practically irreversible at temperatures and pressures ordinary applied, roughly 300 to 450˚C and up to 200 atm. The reactions are exothermic with heats of reaction of the order of 10 to 20 kcal/mol of hydrogen consumed. Coking of catalysts not occur only poisons a catalyst surfaces but also contribute to blocking of the catalyst pores and fixed-bed interstices (Gates et al., 1979).

2.2 Raw material

The most suitable raw material for producing high quality engine fuels is triacylglycerols (TAG) present in vegetable oils or animal fats which give their high molecular weight and low volatility of the use in diesel engines without construction changes of the engines (Mikulec et al., 2010). The sustainable biomass resource as a renewable feedstock being used for production of biofuels is the vegetable oils (Huber et al,. 2007). The source for biodiesel production is usually chosen according to the availability in each country. Malaysia, Indonesia and Thailand also have surplus palm oil and coconut oil which is utilized for the synthesis of biodiesel. However, some Asian countries are not self-sufficient in edible oil and exploring non-edible oil like Jatropha and waste cooking as biodiesel raw materials. For palm oil in Thailand or known as refined palm olein which is achieved from the refinery of crude palm oil, mostly used as bio resource for biodiesel production. Typically, crude palm oil always contains high amount of fatty acids (FFAs) and presence of the soap formation during the transesterification reaction but it could be suitable for hydrotreating reaction. Moreover, the most of FFAs in crude palm oil is removed via the refinement of crude

palm oil (CPO) to purified palm oil (PPO) as called palm fatty acid distilled or PFAD with high contain of FFA is also used as an economically promising feedstock for biodiesel production (Shotipruk et al., 2009). There is a degummed palm oil (DPO) which is resulting from removed gums from crude palm oil also used as a feedstock for biodiesel production.

2.2.1 Degummed palm oil (DPO)

DPO is a byproduct from the refining process of palm oil to palm olein. From the refining process, palm oils were removed gum by precipitant step that give degummed palm oil as a byproduct as shown in Figure .

2.2.2 Refined Bleached Deodorised Palm Stearin (RBD palm stearin)

RBD Palm Stearin ia solid fraction obtained by the fraction of palm oil after crystallization at controlled temperature from the refining process of crude palm oil. The refining process consists of 3 major steps:

1. Degumming: To condition gums (phosphatides) and oxidative trace metals (such as copper and iron) with food grade phosphoric acid, citric acid, EDTA etc, for later removal with the spent earth after the bleaching stage.
2. Bleaching: To remove pigments, oxidation products, residual trace metals and phosphatides and soaps.
3. Steam refining/deodorization: To remove fatty acids, pigments (e.g. caoptenoids)

Fully-refined palm oil (RPO) is an off-white solid in cold climates, a yellowish semi-solid at room temperature, and a yellowish liquid when heated to about 45°C. The RPO may be fractionated into its liquid component, which is called palm olein, and its solid component, which is called palm stearin.

Palm olein is popular used for frying applications and often blended with other oils such as Canola to improve their stability and shelf life and to minimize smoke formation during high-temperature frying applications.

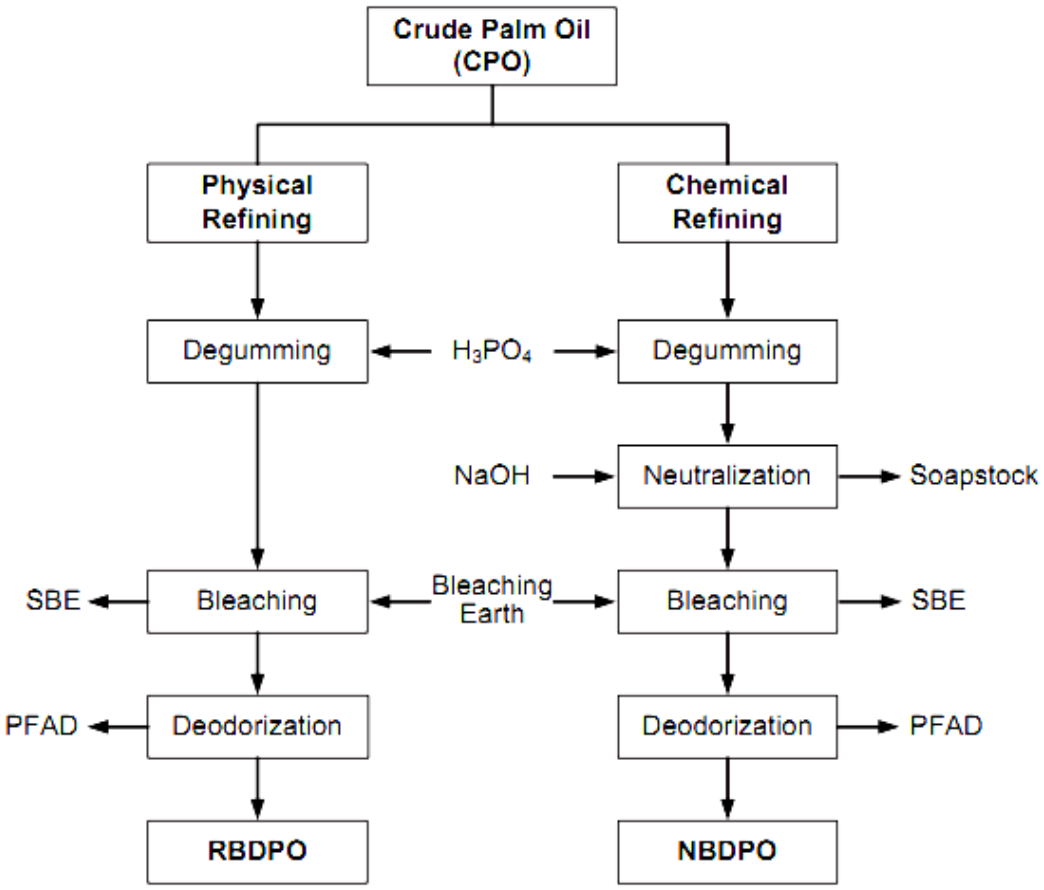

Figure 2.8 Palm oil refining processes (Haslenda et al., 2011).

Palm stearin is utilized for high temperature industrial frying applications such as in the production of instant noodles. Palm stearin is free of trans-fatty acids, and is used as a replacement for hydrogenated oil such as soyabean and Canola and also be utilized in non-edible applications as in the manufacture of soaps and candles. It contains mainly of triglyceride with minimal of fatty acids causing by pass through the refining process. Y.B. Che Man and co-workers are investigated in the composition and thermal profile of crude palm oil and its products which found the triglycerides composition of RPS palm oil were quite similar to triglycerides composition of crude palm oil (CPO). The results showed that CPO, refined palm stearin, refined palm olein and superolein consist mainly of monosaturated and disaturated triglycerides while refined palm stearin consists of mainly of disaturated and trisaturated triglycerides as shown in table 2.1.

Table 2.1 Glyceride Composition of CPO, RBD Palm oil, RBD Palm olein and RBD Palm stearin (Man et al., 1999)

Fatty acid	Glyceride composition (%)			
	CPO	RBD Palm oil	RBD Olein	RBD Stearin
Diglyceride	6.32	5.20	5.55	5.15
Triglyceride	93.60	94.80	94.45	94.85
Triunsaturated	5.12	4.98	5.27	3.95
Monosaturated	34.1	35.18	38.81	16.40
Disaturated	46.43	45.95	47.56	36.61
Trisaturated	7.95	8.69	2.81	35.20

2.3 Standard of biodiesel

The quality of biodiesel fuel can be significantly influenced by numerous factors among others include; the quality of feedstock, fatty acid composition of the vegetable oil, animal fats and waste oil, type of production and refining process employed and post- production parameters (Ong et al., 2011). After the reaction run, aqueous and organic liquid phase were physically separated and, analyzed using several gas-chromatography methods. Gas products (carbon monoxide, carbon dioxide, methane, and propane) were analyzed by gas-chromatography thermal conductivity detector (GC-TCD). Organic liquid products were analyzed by gas-chromatography with flame ionization detector (GC-FID). The physiochemical properties of the organic liquid products are shown in Table 2.2.

The physiochemical properties of the organic liquid products can be comparison with European diesel fuel standard EN590, NExBTL biodiesel, GTL diesel and FAME shown in Table 2.4 and cetane number in Table 2.5.

Table 2.2 Standard test physiochemical properties of the organic liquid products (Walendziewski et al., 2009; Guzman et al., 2010)

Properties	**Solution**	**Method**	
		European diesel fuel standard (EN)	**ASTM**
Total acid number (TAN)	titration of the sample with KOH solution PN 85/C-04066		ASTM D-664 ASTMD974
Carbon and hydrogen			ASTM D-5291
Cetane index			ASTM D-4737
Thermal stability			ASTM D-6468
Thermal stability			ASTM D-6468
Simulated distillation			ASTM D-7213 ASTM-2887-D86
Contents o f ester bonds, aromatic compounds and carboxylic groups in hydrorefined products	FTIR method		
Density (15°C)	aerometer	EN ISO 3675, EN ISO 12185	ASTM D-4052
Kinematical viscosity (40 °C)	Ubbelohde viscosimeter	EN ISO 3104	ASTM D-445
Fractional composition		EN ISO 3405	
Flash point	Pensky-Martens-closed cup	EN ISO2719	ASTM D-93
Cloud point			ASTM D-2500
Pour point			ASTM D-97
Corrosion			ASTM D-130
Color			ASTM D-1500
Cold filter plugging point (CFPP)		EN 116	
Bromine number	PN-68/C-04520		ASTM D-1159

Table 2.3 The physiochemical properties standard of the organic liquid products from hydroprocessing (Technical Research centre of Finland 2005)

Fuel properties	**NExBTL biodiesel**	**GTL diesel**	**FAME**	**EN590/2005**
density @ 15°C (kg/m^3)	775-785	770-785	≈ 885	≈ 835
viscosity @ 40°C (mm^2/s)	2.9-3.5	3.2-4.5	≈ 4.5	≈ 3.5
Cetane index	84-99	73-81	≈ 51	≈ 53
Distillation 10 vol% (°C)	260-270	≈ 260	≈ 340	≈ 200
Distillation 90 vol% (°C)	295-300	325-330	≈ 355	≈ 350
Cloud point (°C)	-5…-30	0…-25	≈ -5	≈ -5
Lower heating value (MJ/kg)	≈ 44	≈ 43	≈ 38	≈ 43
Lower heating value (MJ/litres)	≈ 34	≈ 34	≈ 34	≈ 36
Polyaromatics (wt%)	0	0	0	≈ 4
Oxygen (wt%)	0	0	≈ 11	0
Sulfur (mg/kg)	≈ 0	< 10	< 10	< 10

Table 2.4 Cetane number of normal and iso-paraffins. (Santana et al., 2006)

N-PARAFFINS	CN	ISO-PARAFFINS	CN
n-Butane	22	2-Methylpentane	33
n-Pentane	30	3-Methylpentane	30
n-Hexane	45	2,3-Dimethylpentane	22
n-Heptane	54	2,4-Dimethylpentane	29
n-Octane	64	2,2,4-Trimethylpentane	14
n-Nonane	72	2,2,5-Trimethylhexane	24
n-Decane	77	2,2-Dimethyloctane	59
n-Undecane	81	2,2,4,6,6-Pentamethylheptane	9
n-Dodecane	87	3-Ethyldecane	47
n-Tridecane	90	4,5-Diehtyloctane	20
n-Tetradecane	95	4-Propyldecane	39
n-Pentadecane	96	2,5-Dimethylundecane	58
n-Hexadecane	100	5-Butylnonane	53
n-Heptadecane	105	2,7-Dimethyl-4,5-diethyloctane	39
n-Octadecane	106	5-Butyldodecane	45
n-Nonadecane	110	7,8-Dimethyltetradecane	40
n-Eicosane	110	7-Butyltridecane	70
		7,8-Diethyltetradecane	67
		8-Propylpentadecane	48
		9-Methylheptadecane	66
		5,6-Dibutyldecane	30
		9,10-Dimethyloctadecane	60
		7-Hexylpentadecane	83
		2,9-Dimethyl-5,6-diisopentyldecane	48
		10,13-Dimethyldocosane	56
		9-Heptylheptadecane	88
		9,10-Dipropyloctadecane	47

2.4 Simulated distillation

Simulated distillation (SimDist) is a gas chromatography (GC) method used to characterize petroleum fractions and products that separates the individual hydrocarbon components in the order of their boiling points, and is used to simulate the time-consuming laboratory-scale physical distillation procedure known as true boiling point (TBP) distillation. The determination of the boiling range distribution of petroleum fractions by conventional GC is rapid analytical tool, which is widely used to replace conventional distillation methods for control of refining operations and specification testing. The separation is accomplished with a non-polar chromatography column using a gas chromatograph equipped with an oven and injector that can be temperature programmed. A flame ionization detector (FID) is used for detection and measurement of the hydrocarbon analysts. The result of SimDist is reported as a correlation between the boiling points and the percentages of the sample eluted from the column. The chromatographic elution times of the hydrocarbons are calibrated to the atmospheric equivalent boiling point (AEBP) of the paraffins reference material. The SimDist method ASTM (American Society for Testing and Materials) D2887 covers the boiling range 55–538°C (100–1000°F) which covers the n-alkanes (n-paraffins) of chain length about C_5–C_{44}. The high-temperature simulated distillation (HTSD) method covers the boiling range 36–750°C (97–1382 °F) which covers the n-alkane range of about C_5–C_{120}. A key difference between ASTM D2887 and HTSD is the ability of the latter technique to handle residue-containing samples (i.e. material boiling > 538°C, 1000°F). SimDist and laboratory-scale physical distillation procedures are routinely used for determining boiling ranges of petroleum crude oils and refined products, which include crude oil bottoms and residue processing characterization. The boiling points with yield profile data of these materials are used in operational decisions made by refinery engineers to improve product yields and product quality. Data from SimDists are valuable for computer modeling of refining processes for improvements in design and process optimization. Precise yield correlations between HTSD and crude assay distillation (methods ASTM D2892 and D5236) have allowed HTSD to be successfully used in place of physical distillation procedures. This has given the refiner the ability to rapidly evaluate crude oils for selection of those with economic advantages and more favorable refining margins. SimDist methods are becoming more widely used in environmental applications. HTSD is useful for characterizing hydrocarbons which can be present as soil and water contaminants; for example, to map and follow hydrocarbon removal processes.

SimDist became an ASTM standard method in 1973, with the designation D2887, ‘‘Boiling Range Distribution of Petroleum Fractions by GC’’. The current

edition is designated D2887-97. This method covers the determination of the boiling range distribution of petroleum products and fractions having a final boiling point (FBP) of 538°C (1000°F) or lower at atmospheric pressure. HTSD is a relatively recent method which extends ASTM D2887 determination of the boiling range distribution of hydrocarbons to a FBP of about 750°C (1382°F). Technological advances in capillary GC columns and stationary phases together with either programmed temperature vaporization (PTV) or on-column injection techniques, provide adequate separation from C_5 to C_{120} normal paraffins and allows the characterization of petroleum products from about 36–750°C (97–1382°F). Under the special conditions of HTSD, elution of materials from the GC column occurs at up to 260–316°C (500–600°F) below their AEBP. For instance, the elution of C_{110} (AEBP of 735°C or 1355°F) occurs at a column temperature of about 427°C (800°F). Also under these conditions, little or no evidence of cracking is normally seen in HTSD (Villalanti et al., 2000).

2.4.1 Measurement of boiling point distribution using the total area method

The analysis using a gas chromatograph with a non-polar liquid phase column is applied for a linear temperature programming method. The hydrocarbons will be eluted in the order of boiling point. Since the elution time is more or less directly proportional to the boiling point, a calibration curve of the retention time and boiling point can be created, as shown in Figure 2.9. Otherwise, the retention time can be converted into the boiling point. Therefore, by working out the relationship between the retention time and the boiling point before through the analysis of a hydrocarbon mixture with a known boiling point (with the gas chromatograph analysis conditions kept constant), it becomes possible to convert the retention time of an unknown sample into the boiling point. Furthermore, the total area of the gas chromatogram obtained is divided into fixed time intervals, and the smaller areas comprised by each time period are calculated. Since the time interval can be converted into the boiling point interval, this in effect calculates the gas chromatogram area for the fraction of a particular boiling point (http://www.shimadzu.com).

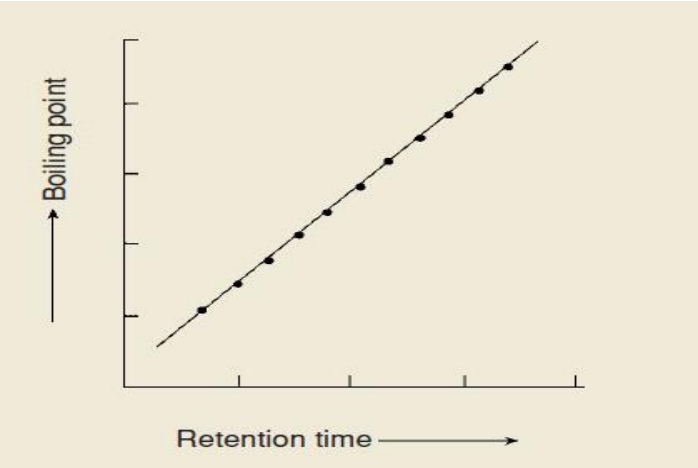

Figure 2.9 Calibration curve (http://www.shimadzu.com)

In this study, used calibration mixture 1%wt/wt -An accurately weighed mixture of approximately equal mass quantities of n-hydrocarbons dissolved in carbon disulfide (CS_2) The mixture shall cover the boiling range from n-C_5 to n-C_{44}, but does not need to include every carbon number shown in Table 2.5 and Figure 2.10.

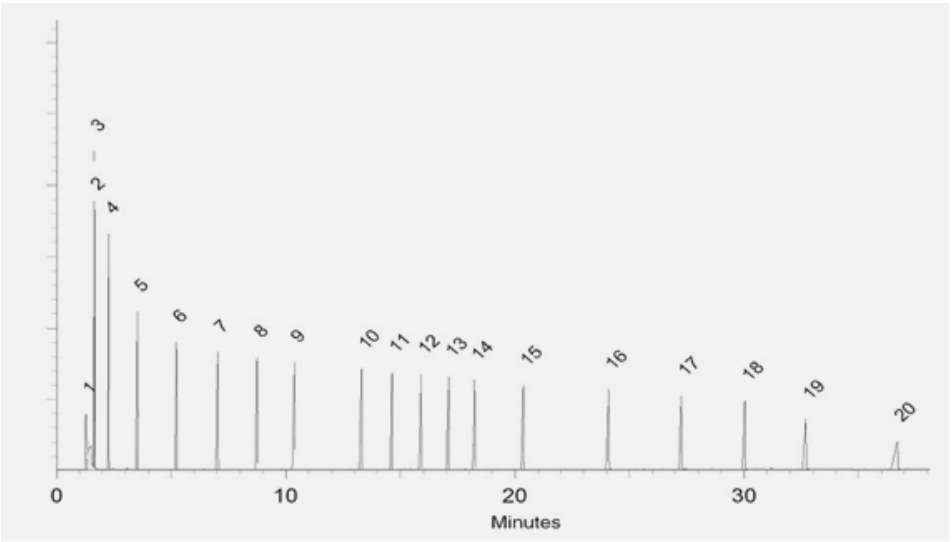

Figure 2.10 Graph of n-C_5 to n-C_{44} alkanes at various times in calibration mixture (http://www.Restek.com).

In addition, by obtaining the cumulative area through the addition of all the small areas from the start point onwards, and expressing it as a ratio of the area of the entire gas chromatogram, the elution amount up to that time will have been calculated. In Figure 2.11 for example, the cumulative area up to 'n' consists of 'S1', 'S2', 'Sn-1', 'Sn'. By figuring out the ratio with respect to the total area 'St', the elution amount at 'tn' is obtained. The data in Figure 2.12 is an example of the elution amount (corresponds to the amount of distillate). This method is applied to samples where all the components of the sample are eluted from the column during high temperature analysis using GC, such as the oil fractions of gasoline, kerosene, and light oil (http://www.shimadzu.com).

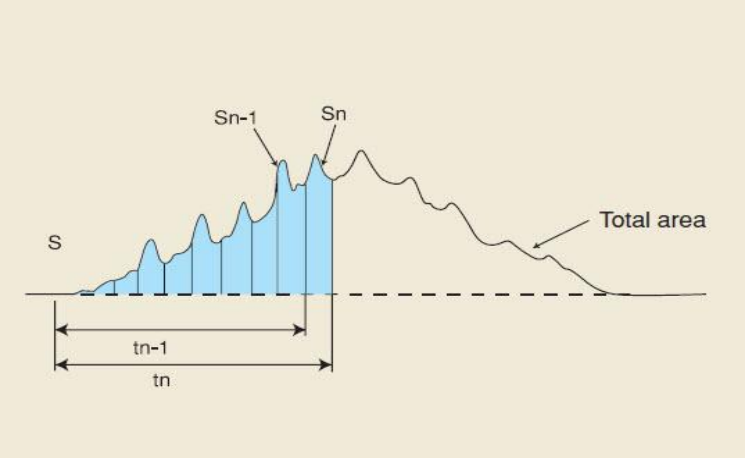

Figure 2.11 Calculating the elution amount. (http://www.shimadzu.com)

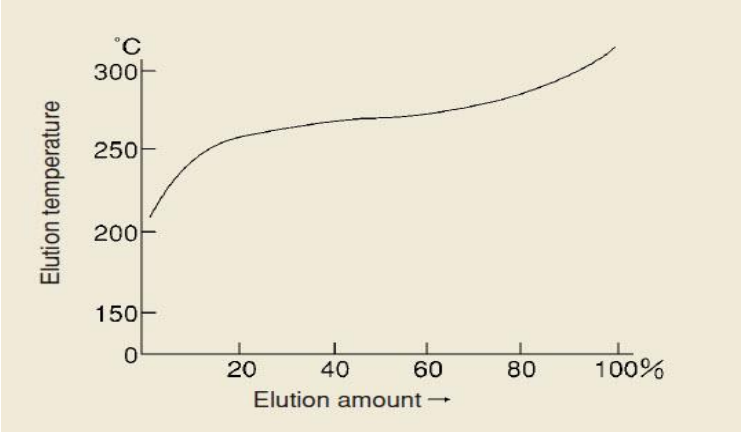

Figure 2.12 Distillation characteristics curve. (http://www.shimadzu.com)

Table 2.5 Component of n-C5 to n-C44 alkanes in calibration mixture. (http://www.Restek.com)

Elution order	Compound	CAS#	Percent Purity	Concentration (weight/weight%)
1	n-Pentane (C5)	109-66-0	99%	0.9995 wt./wt.%
2	n-Hexane (C6)	110-54-3	99%	0.9995 wt./wt.%
3	n-Heptane (C7)	142-82-5	99%	0.9995 wt./wt.%
4	n-Octane (C8)	111-65-9	99%	0.9995 wt./wt.%
5	n-Nonane (C9)	111-84-2	99%	0.9995 wt./wt.%
6	n-Decane (C10)	124-18-5	99%	0.9995 wt./wt.%
7	n-Undecane (C11)	1120-21-4	99%	0.9995 wt./wt.%
8	n-Dodecane (C12)	112-40-3	99%	0.9995 wt./wt.%
9	n-Tetradecane (C14)	629-59-4	99%	0.9995 wt./wt.%
10	n-Pentadecane (C15)	629-62-9	99%	0.9995 wt./wt.%
11	n-Hexadecane (C16)	544-76-3	99%	0.9995 wt./wt.%
12	n-Heptadecane (C17)	629-78-7	99%	0.9995 wt./wt.%
13	n-Octadecane (C18)	593-45-3	99%	0.9995 wt./wt.%
14	n-Eicosane (C20)	112-95-8	99%	0.9995 wt./wt.%
15	n-Tetracosane (C24)	646-31-1	99%	0.9995 wt./wt.%
16	n-Octacosane (C28)	630-02-4	99%	0.9995 wt./wt.%
17	n-Dotriacontane (C32)	544-85-4	98%	0.9991 wt./wt.%
18	n-Hexatriacontane (C36)	630-06-8	99%	0.9995 wt./wt.%
19	n-Tetracontane (C40)	4181-95-7	97%	0.9986 wt./wt.%
20	n-Tetratetracontane (C44)	7098-22-8	99%	0.9995 wt./wt.%
Solvent	Carbon Disulfide	75-15-0	99%	

Table 2.6 Distillation data in specified temperature range. (Huber et al., 2007)

The straight chain alkanes	**Range of temperature (°C)**
Lighter alkanes	-50 to 65
Alkanes C_5-C_8	65-150
Alkanes C_9-C_{14}	150-250
Alkanes C_{15}-C_{18}	250-380
Intermediates and the alkanes < C_{20}	380-520
The tri-glycerides and fatty acids	520-1000

In this study, we used simulated distillation to analyze the temperature range of products following by ASTM-2887-D86 procedure. It was found, at temperature range of 250-380°C is a suitable for diesel range (n-C_{15}-n-C_{18}) shown in Table 2.6. It can be concluded that the products are suitable for diesel fuel blending (Huber et al., 2007).

2.5 Catalysts

The Mo (W)-containing supported catalysts, promoted either by Co or Ni, have been used for hydroprocessing for decades. The γ-Al_2O_3 has been the predominant support. In recent years, other supports such as silica-alumina, zeolites, TiO_2 have been gradually introduced with the aim of improving catalyst performance. The enhancement in the rate of hydrocracking reaction (HCR) and hydroisomerization reaction (HIS) was the reason for using more acidic supports. The operating (sulfide) form of the catalysts contains the slabs of the Mo(W)S_2. The distribution of the slabs on the support from a monolayer to clusters which depends on the method used for the loading of active metals, conditions applied during sulfiding, operating conditions, properties of supports, etc.

Under hydroprocessing conditions, the corner and edge sulfur ions in Mo(W)S_2 can be readily removed. This results in the formation of the coordinatively unsaturated sites (CUS) and/or sulfur ion vacancies, which have the Lewis acid character. Because of the Lewis acid character, CUS can adsorb molecule with the unpaired electrons which present in the feed. They are also the sites for hydrogen

activation. In this case, H_2 may be homolytically and heterolytically split to yield the Mo-H and S-H moieties, respectively.

Catalytic functionality of a catalyst could not be established without its ability to activate hydrogen. The active hydrogen id subsequently transferred to the reactant molecules adsorbed on or near CUS. Part of the active hydrogen can be spilt over on the support and to a certain extent protect slabs of the active phase from deactivation by coke deposits. The promoters, such as Co and Ni decorate $Mo(W)S_2$ crystals at the edges and corners sites of the crystals. In the presence of promoters, CUS are considerably more active than those on the metal sulfide alone. Consequently, the rate of hydrogen activation is enhanced. The H_2S/H_2 ratio is the critical parameter for maintaining the optimal number of CUS. It has been confirmed that above 673 K, the –SH moieties on the catalyst surface possess the Bronsted acid character. The presence of the Bronsted acid sites is desirable for achieving a high rate of hydrodenitrogenation (HDN). In addition, the formation of coke and metal (predominantly V and Ni) deposits on CUS will diminish the availability of active site (Marafi et al., 2010).

2.5.1 Nickel

Table 2.7 Physical properties of nickel (http://en.wikipedia.org/wiki)

Property	Value
atomic number	28
atomic weight	58.69
melting point, ^oC	1453
latent heat of fusion, ΔH_{fus} kJ/mol[a]	7.48
boiling point, ^oC	2732
latent heat of vaporization at bp, ΔH_{vap} kJ/mol[a]	377.5
specific heat, kJ/(mol.K)[a] 25^oC	26.07
coefficient of thermal expansion, $\mu m \cdot m^{-1} \cdot K^{-1}\ ^oC^{-1}$	13.4
thermal conductivity at 27 ^oC, W/(m.K)	90.9
Curie temperature, ^oC355	355
Young's modulus, Gpac	200

Nickel is a chemical element with the atomic number 28. It is a silvery-white lustrous metal with a slight golden tinge. It uses in certain alloys that will retain a high silvery polish. The metal is chiefly valuable in the modern world for the alloys it forms; about 60% of the world production is used in nickel-steels (particularly stainless steel). The most of the remainder of the world nickel use with chemical uses for nickel compounds. As a compound, nickel has a number of niche chemical manufacturing uses, such as a catalyst for hydrogenation. The physical properties of the nickel are shown in Table 2.7 (http://en.wikipedia.org/wiki).

2.5.2 Cobalt

Cobalt is a chemical element with atomic number 27. It is found naturally only in chemically combined form. The free element, produced by reductive smelting, is hard, lustrous, silver-gray metal. Nowadays, some cobalt is produced specifically from various metallic-lustered ores, but the main source of the element is as a byproduct of copper and nickel mining. Cobalt occurs naturally as only one stable isotope, cobalt-59. Pure cobalt is not found in nature, but compounds of cobalt are common. It is a weakly reducing metal that is protected from oxidation by a passivating oxide film and attacked by halogens and sulfur. Physical properties of cobalt are shown in Table 2.8.

Table 2.8 Physical properties of cobalt (Othmer 1991)

Property	Value
Atomic number	27
Atomic weight	58.93
Heat of transformation, J/g[a]	251
Melting point, ^{o}C	1493
Latent heat of fusion, ΔH_{fus} J/g[a]	395
Boiling point, ^{o}C	3100
Latent heat of vaporization at bp, ΔH_{vap} kJ/g[a]	6276
Specific heat, J/(g·^{o}C)[a]	
15-100^{o}C	0.442
molten metal	0.560
Coefficient of thermalexpansion, $^{o}C^{-1}$	
cph at room temperature	12.5
fcc at 417^{o}C	14.2
Thermal conductivity at 25 ^{o}C, W/(m·K)	69.16
Curie temperature, ^{o}C	1121
Young's modulus, Gpac	211

2.5.3 Molybdenum

Molybdenum is a group 6 chemical element with atomic number 42. It readily forms hard, stable carbides, and for this reason it is often used in high-strength steel alloys. Molybdenum does not occur as a free metal on earth, but rather in various oxidation states in minerals. Industrially, molybdenum compounds are used in high-pressure and high-temperature applications, as pigments and catalysts (http://en.wikipedia.org/wiki). Table 2.9 is shown the physical properties of molybdenum.

Table 2.9 Physical properties of molybdenum (http://en.wikipedia.org/wiki)

Property	**Value**
atomic number	42
atomic weight	95.96
melting point, ^{o}C	2610
latent heat of fusion, ΔH_{fus} kJ/mol	37.48
boiling point, ^{o}C	4825
latent heat of vaporization at bp, ΔH_{vap} kJ/mol	598
specific heat, J/(mol·K) 25^{o}C	24.06
coefficient of thermal expansion, $^{o}C^{-1}$	4.8 μm·m^{-1}·K^{-1}
thermal conductivity at 27 ^{o}C, W/(m·K)	138
Young's modulus, GPa	329

2.5.4 Aluminium oxide

Aluminium oxide is an amphoteric oxide with the chemical formula Al_2O_3. It is commonly referred to as alumina (α-alumina), or corundum in its crystalline form, as well as many other names, reflecting its widespread occurrence in nature and industry. Alumina can exist in many metastable phase before transforming to the stable form of alumina in which the stable form of alumina was well known as α-alumina or corundum from. There are six principle phase namely by the Greek letters, composed that chi (χ), kappa (κ), eta (η), theta (θ), delta (δ), and gamma (γ). Each of their phases, has a unique crystal structure and properties. The several phases depend on many factors such as calcination temperature, heating environment, as called heat treatment condition. Additionally, Aluminum hydroxide minerals are the main component of bauxite, the principal ore of aluminium. A mixture of the minerals comprise bauxite ore, including gibbsite ($Al(OH)_3$), boehmite (ɣ-AlO(OH)), and diaspora (α-AlO(OH)), along with impurities of iron oxides and hydroxides, quartz and clay minerals which effect to the nature of the product as illustrated in Figure 2.13. It shows thermal transformation scheme of different types of starting material that among of various crystalline phases of alumina, ɣ-Al_2O_3 is probably the most important inorganic oxide refractory of widespread technological importance in the field of catalysis, also used as catalyst support. In addition, ɣ-Al_2O_3 is an exceptionally good choice for catalytic applications because of a defect spinel crystal lattice that imparts to it a structure that is both open and capable of high surface area (Yang et al., 2007, http://en.wikipedia.org/wiki).

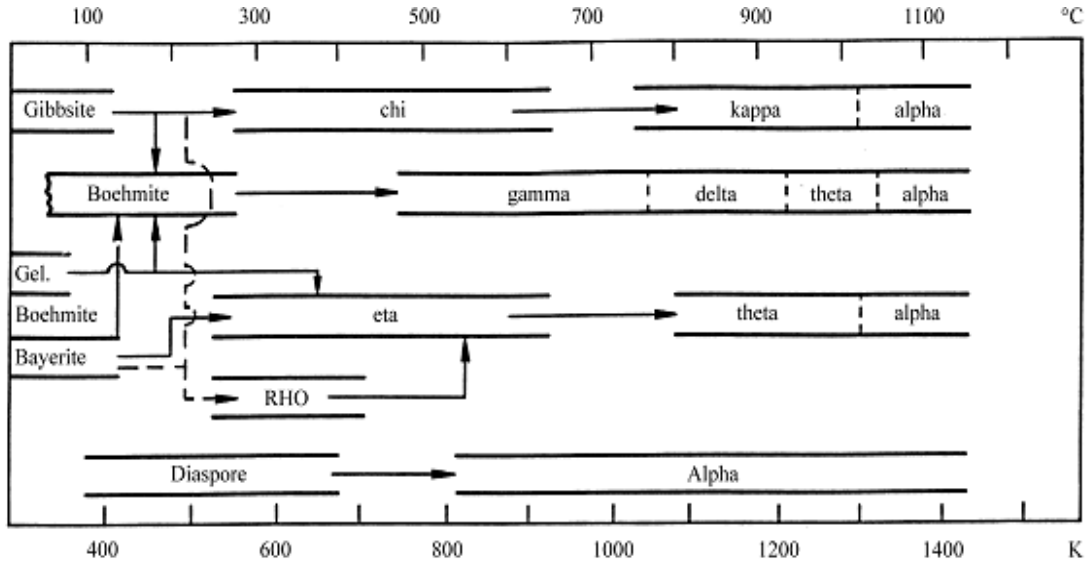

Figure 2.13 Thermal transformations of different types of starting material (Santos et al., 2000).

2.6 Presufurization method

The hydrotreating catalysts are commonly sulfided $CoMo/Al_2O_3$ and $NiMo/Al_2O_3$. The promoter may be added to lower the acidity of the catalyst and improve Mo dispersion and sulfidability. Mo and Ni are regarded as the active species in hydrotreating catalysts. The form of active metal species in the sulfurized catalysts is rather complicated, and the precise structure of sulfided catalyst is still under debate. Nominally, MoS_2, Ni_3S_2, and mixed sulfides (Co-Mo-s, etc) are some of examples. Presulfurization is an essential process for activation of hydrotreating catalyst in the oxidic form. There are many procedures for presulfiding catalyst. The conventional process is insitu presulfurization (IPRES), which used to sulfurize the pre-loaded catalyst in the reactor by introducing a sulfurizing agent. Moreover, ex situ presulfurization (EPRES) is the process in which the catalyst is sulfuruzed or partially sulfurized before loading the catalyst into the reactor. Comparing two of these procedures, ex situ presulfurization takes much shorter of treating time, hence significantly increases production efficiency. The key point with the ex situ presulfurization (EPRES) process of hydrotreating catalysts is to take advantage of using combined sulfur-containing agents as the sulfur source and the reducing the loss of sulfur from the EPRES catalysts. The impregnation method was mainly used for introducing sulfurizing agent and different kinds of solvents are essential to dissolve the sulfurizing agent.

The more accomplish of different ex situ presufurization were investigated since 1980s'. Staring with EURECAT first adopted organic polysulfide as sulfurizing agent to achieve presulfurization in two steps (Berrebi et al., 1991). Later on EURECAT also used $(NH_4)_2S$ as sulfur-containing additives and elemental S or H_2S as the sufurizing agents (Berrebi et al., 1992, Dufresne et al., 1995, Dufressne et al., 2002). CRITEIRON used element S as the sulfurizing agent and high boiling point oil or liquid hydrocarbon as the solvent (Seamans et al., 1990).

CHAPTER III

LITERATURE REVIEW

This chapter consists of the research reviews of the biodiesel production via hydroprocessing reaction. In this reviews, there are many useful knowledge such as raw material, operating condition, and catalyst selection, analysis of product, advantages and drawback of their strategies.

3.1 Raw material

The sustainable biomass resource as a renewable feedstock being used for production of biofuels is the vegetable oils (Huber et al,. 2007). Because of the food and fuel debate, there are many attempts has been made to produce biodiesel from non-edible plant oils such as mahua (Ghadge and Raheman, 2005), tobacco (Veljkovic et al., 2006), rubber seed oil (Ramadhas et al., 2005), Jatropha curcas (Ong et al., 2011), waste oils such as waste cooking oils (Leung and Guo, 2006), waste tallow (Bhattie etal., 2008) and animal fats (Canakci and van Gerpen, 2001) as cheap feedstocks for biodiesel production. Malaysia, as one of the biggest palm oil producers and exporters in the world, is producing large amounts of low-grade oil from palm oil industries such as degummed palm oil (DPO), palm fatty acid distillate (PFAD) and sludge palm oil (SPO). The DPO is a byproduct of degumming step with mainly composes of gums and free fatty acid (http://www.andrew.cmu.edu). Similarly with degummed palm oils, PFAD recovered from deodorization process which rich in free fatty acid content. It is commonly used as raw materials in producing medium-grade cleaners, animal feeds, plastics and other intermediate products for the oleochemical industries (Haslenda, Jamaludin, 2011). There are many studies that demonstrated the potential use of the local palm fatty acid distillate (PFAD) as alternative feedstock for fatty acid methyl ester (FAMEs) production such that the study of the possibility to replace the conventional acid-catalyzed esterification process (with H_2SO_4) with non-catalytic process in supercritical methanol by esterification of palm fatty acid distillate (Shotipruk et al., 2009). Another research PFAD, a byproduct from the production of consumable palm oil, with a free fatty acid content of 93 wt% was used as a feedstock for biodiesel

production with mild operating conditions and continuous overflow production (Chongkhong et al., 2009).

3.2 Reaction condition of hydroprocessing process

Hydroprocessing of triglycerides includes the following major reactions: hydrogenation of unsaturated bonds in alkyl chains of carboxylic acid and hydrodeoxygenation of fatty acids (Kikhtyanin et al., 2010). The hydrogenation reaction is quite similar to those of hydrodesulfurization (HDS), which is convert sulfur-containing molecules into H_2S. Therefore, the hydrogenation of oils and fats can take place desulfurization unit. Donnis et al., 2009 studied mechanism of overall reaction for the hydrogenation between triglycerides and hydrogen. This study describes the three carboxylic acids are stepwise liberated and hydrogenated into straight chain alkanes of the same length or one carbon atom shorter. Then the backbone of the triglycerides is converted into propane, water, carbon monoxide, carbon dioxide and methane. These products will be considerable due to appropriated conditions and suitable catalyst. The proposed reaction mechanism, which can be explained the path way of these products, involve at least three reaction pathways as hydrodeoxygenation, decarboxylation and decarbonylation.

One mechanism is hydrodeoxygenation (HDO) reaction (see the unbroken red lines in Figure 3.1), which occurs via the absorbed enol intermediate. The products for this mechanism are water, propane and three normal alkanes of the full length of fatty acid chains. The others mechanism, which are called decarboxylation and decarbonylation (see the broken blue lines in Figure 3.1). The triglycerides are broken down the products, which are propane, carbon monoxide and/or carbon dioxide and three normal alkanes with carbon numbers one less than fatty acid chains (Filho et al., 1993).

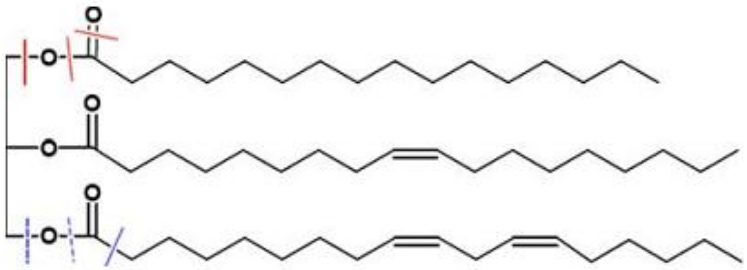

Figure 3.1 Schematic representation of the different reaction pathways for the removal of triglyceride oxygen by hydrodeoxygenation (--) and decarboxylation (--)

3.3 Thermodynamic balance

Smejkal et al., 2009 studied the thermodynamic model derived for the total hydrogenation and its predictions were compared with the experimental of rape-seed oil transformation into hydrocarbons. Tristearate was chosen as a model compound to represent vegetable oils in the calculations. As the thermodynamic data for tristearate were not available in literature, their values were estimated by using the Joback's contribution method. Based on the comparison to a relevant known system (butyl stearate) it was concluded that the chosen method is suitable for the assessment of thermodynamic data of triglycerides. The Joback's contribution method has been demonstrated to estimate accurately the thermodynamic data of tristearate (ΔH_{f° = -2176.9 kJ/mol and ΔG_{f° = -504.5 kJ/mol) from Aspen plus. A thermodynamic model for the total hydrogenation of tristearate was derived for temperatures between 250-450 C and hydrogen pressures ranging from 7 to 70 bar. The reaction was assumed to enable isothermal reaction conditions. Phase equilibrium liquid-gas was considered in the model too (Peng–Robinson and Ideal EOS = Equation of State).The basic reaction mechanism of the proposed catalytic transformation is summarised and consists of two main reactions: hydrodeoxygenation and hydrodecarboxylation, completed by water-gas-shift reaction and CO formation. The thermodynamic balance of the system was used to predict the composition of the liquid phase, namely to predict the distribution of $C_{17}$and C_{18} hydrocarbons. The predictions suggest that C_{18} hydrocarbons are the main reaction

products and that their concentration is affected by temperature and particularly by pressure. Moreover, the model predictions were found to be in good agreement with experimental data. The estimations suggested that the reaction were limited by hydrogen and triglyceride diffusivity through the liquid film on catalyst particles

The study of hydroprocessing of crude palm oil (CPO) using conventional hydrotreating with NiMo/γAl_2O_3 catalyst where they obtained products was characteristic by GC-MS. It was found when pressure is decreased (15 bar), product yields from n-C16 to n-C18 increased due to increasing number of products and cannot specified exactly products like octadecenes, octadecanol, n-hexadecanoic acid, actadecanal and hexa-actadecyl hexadecanoate (Guzman et al., 2010). On the other hand, pressure is increased (90 bar), decreasing number of products can be indentified because intermediates were not found and fatty acids is reduced as well. Subsequently, test pressure effect and hydrogen consumption via simulated in Aspen plus. It was found that. The hydrodeoxygenation reaction is better than decarboxylation and decarbonylation when pressure increased (10-100 bar) and increasing hydrogen consumption. Moreover, time analysis was obtained by simulated distillation curves, the best diesel yields (95.3 %vol) was observed at 4 hours.

3.4 Effect of operating condition

The hydroprocessing studies related to the renewable fuel production involve complete conversion of the vegetable oils to alkanes. The composition of hydroprocessed vegetable oil depends on reaction conditions and the catalyst used. A key parameter for reaction activity and properties of product are temperatures, hydrogen pressure, time of stream and feedstock. Hydroprocessing of vegetable oils is usually carried out in the temperature range of 300–400˚C and under the hydrogen pressure of 6–20 MPa**.**

A study of noble metal cstslyst was investigated by Murzin et al. on liquid-phase deoxygenation reaction over a Pd/C catalyst under constant pressure and temperature, 15-27 bar and 300-360 ˚C, respectively. Deoxygenation of unsaturated renewable, such as oleic acid, methyl oleate and linoleic acid, with high selectivity to saturated diesel fuel range hydrocarbons, was successfully accomplished over Pd/C. Under hydrogen rich atmosphere the hydrogenation was enhanced and the deoxygenation reaction became predominant. Sebos et al. hydroprocessed desulphurized (S < 50 ppm) mineral diesel containing 10 wt.% of cotton-seed oil. Hydroprocessing was carried out over a commercial $CoMo/Al_2O_3$ and under common hydrotreating conditions (305–355˚C, 3 MPa). The feed was artificially sulphurized by adding DMDS. The obtained product containing renewable diesel had a benefit of +3 cetane units compared to the pure mineral diesel used as a matrix. The cloud point of the product was the same as cloud point of the summer-type diesel matrix (0˚C).

According to a commercial catalyst for hydrotreating process, bimetallic catalyst was studied by Huber et al. on the hydroprocessing of sunflower oil and heavy vacuum oil–sunflower oil mixtures (5–50 wt.% of sunflower oil) over a wide range of reaction temperatures (300–450˚C). Their experiments were carried out over a $NiMo/Al_2O_3$ and under the pressure of 5 MPa. The total conversion of sunflower oil into hydrocarbons was observed at a reaction temperature of 350˚C and above, at which no acidity was detected. For the wide range of reaction temperatures general trends of increasing n-alkane isomerization and cracking at higher reaction temperatures were well illustrated as was the increasing decarbonylation/decarboxylation selectivity. It was found, that desulfurization of petroleum-derived feed component is significantly slower than hydrocarbon formation from vegetable oil. However, mixing the sunflower oil with petroleum-derived feed did not decrease the rate of desulfurization. Co-processing vegetable oil with conventional petroleum fractions on an industrial scale has been reported by Petrobras. The process is known under the name H-Bio.

Donnis et al., 2009 were conducted the hydroprocessing by feed 0, 15 and 25 vol% rapeseed oil in light gas oil (LGO) with reaction temperature 350ºC and under

hydrogen pressure of 45 bar. A commercial TK-565 (Ni-Mo based) catalyst was used. The products obtain 100% conversion from rapeseed oil and the same final boiling point (FBP) of all three products were analyzed by the simulated distillation curves, which is also the FBP of the LGO feed. The HDO route and the decarboxylation route can be calculated from the yields of CO, CO_2, and CH_4. The triglycerides reacted via the decarboxylation rate about 66-74%. Increased rapeseed oil mixed in LGO; properties of the diesel product were a low density and a high cetane index. The cloud point is important because the car manufactures observed filter plugging from the tank to the engine when operated at low temperatures. Therefore, the production of rapeseed oil will be improved product properties as concern cloud and pour point.

Walendziewski et al., 2009 studied hydroprocessing of 10 and 20 wt.% of rape oil and 90 and 80 wt.% of LGO fraction mixtures in continuous reactor with the same parameter sets, temperature 320, 350 and 380ºC as well as under hydrogen pressure 3 and 5 MPa. A commercial $NiMo/Al_2O_3$ catalyst was used. As the result of process the temperature range 350-380ºC and hydrogen pressure 5 MPa are good efficiency. In comparision to the product yields for hydrotreating of vegetable oil (sunflower oil) used simulated distillation to analyze with the same as catalyst, temperature and pressure. It was obtained the maximum theoretical products carbon yields and carbon yields of C_{15}-C_{18} are 95% and 75%, respectively. The yields of gaseous (propane, carbon monoxide and carbon dioxide), isomerized and cracked products are minimum at the same temperature (Huber et al., 2007).

The obtained liquid product was approximately 95 wt% yields of all products and 5 wt% of gaseous light hydrocarbons. Hydrogenation of unsaturated hydrocarbons and hydrogenolysis reactions of ester and carboxyl acid bonds results in fatty acid chains were converted to saturated linear hydrocarbon (paraffins), which are higher melting temperatures. It leads to undesirable increasing in boiling point, cloud point and CFPP. Bromine number decreased but acid number increased because ester bonds in fatty acids was hydrogenolized giving carboxylic group, which is loss because of hydrogenation of the carbonyl group (Filho et al., 1993). Then partial hydrocracking of paraffins hydrocarbons were transformed to light hydrocarbons

whose flash point, density and kinematics viscosity are lower. There are improvement by the separation and removal of low boiling hydrocarbons from the product distillation. More research which conducts Ni-Mo catalyst for hydroprocessing of rapeseed oil as a source of hydrocarbon-based biodiesel (Šimáčˇek et al., 2010). The Rapeseed oil was hydroprocessed in a laboratory flow reactor under four combinations of reaction conditions at temperatures 310 and 360˚C and under hydrogen pressure of 7 and 15 MPa. Reaction products contained mostly n-heptadecane and n-octadecane accompanied by low concentrations of other n-alkanes and i-alkanes. Reaction product obtained at 360˚C and 7 MPa was blended into mineral diesel fuel in several concentration levels ranging from 5 to 30 wt.%. It was found, that most of the standard parameters were similar to or better than those of pure mineral diesel. On the other hand, low-temperature properties were worse, even after addition of high concentrations of flow improvers.

Under high hydrogen pressure and relative high temperature vegetable oils can be converted into paraffins (from n-C15 up to n-C18) having water, propane and CO_x gases as by-products. Intermediates as monoglycerides, diglycerides, ketenes, aldehydes, acrolein and carboxylic acids have been proposed these are formed in the initial step and subsequently hydrogenated or broken down via decarboxylation, decarbonylation or hydrodeoxygenation (Chang and Wan. 1947, Stumborg et al., 1996 and Hodge. 2008). In addition, cyclization and aromatization reactions can take place especially when fatty acids that compose the triglycerides in the vegetable oil are polyunsaturated as linoleic and linolenic acids (Filho et al., 1993). The hydroprocessing of rapeseed oil at various temperatures (260–340˚C) under a pressure of 7 MPa in a laboratory flow reactor over three Ni–Mo/alumina hydrorefining catalysts were dealing by Kubicka et al. The main components of OLP were identified as C17 and C18 n-alkanes and i -alkanes. At a low reaction temperature, OLP contained also free fatty acids and triglycerides. At reaction temperatures higher than 310˚C, OLP contained only hydrocarbons of the same nature as hydrocarbons present in diesel fuel. The content of reactants and intermediates decreased with increasing reaction temperature. At temperatures higher than about 310˚C, the mentioned

reactants and intermediates were not detected in the reaction mixture. However the absence of triglycerides and free fatty acids was observed already at lower reaction temperatures (290–300˚C). Conclude that the reaction temperature has a relatively strong influence on the ratio of n-alkanes with even and odd carbon atom number which is increasing reaction temperature the content of n-heptadecane were increases at the expense of n-octadecane. It is apparent that with increasing reaction temperature decarboxylation comes into play more prominently. For more investigated the hydroprocessing of palm oil using conventional hydroteating catalyst ($NiMo/\gamma Al_2O_3$), Guzman et al are observed at 40–90 bar hydrogen pressure crude palm oil (CPO) can be deeply converted into paraffins in the diesel range. However, at lower pressures hydrodeoxygenation cannot be fully reached and the appearance of intermediates as C16–C18 alcohols, C16–C18 acids and esters were preliminary identified in the reaction product. Times of stream (TOS) experiments have shown that conventional hydrotreating catalyst suffers of slight deactivation as the reaction proceeds. As more work with another triglycerides such as sunflower oil Hancsók et al. are carried the process of hydrotreating of sunflower oil on $CoMo/Al_2O_3$ catalyst which found (380˚C, 40–60 bar, 500–600 Nm^3/m^3 H_2/sunflower oil ratio, 1.0 h^{-1}), where the conversion of triglycerides was 100% and the yield of the target fraction (high paraffin containing (>99%) gas oil boiling range product) was relatively high (73.7–73.9%). The deoxygenation of triglycerides the reduction as well as the decarboxylation/decarbonylation reactions took place.

The several degummed edible/non-edible oil are also studies for production of biodiesel fuel. Degumming is an economical chemical process that is done by concentrated phosphoric acid. This process is applied to the non-edible oils to remove the impurities for the improvement of viscosity, cetane number and better combustion in the diesel engine up to certain blend of diesel and non-edible vegetable oils. Gomes et al. demonstrated that the degummed soybean oil can be used to obtain biodiesel by transesterification with ethanol and basic catalyst (NaOH 1%, w/w). Due to the free fatty acids of degummed soybean oil used in the experiments (0.87%), it was

found that a temperature lower than 40 ˚C and an oil: alcohol molar ratio higher than 1:7 give the maximum ester yield.

Palm fatty acid distillate has been explored as a feedstock for biodiesel production only via transesterification techniques. Shotipruk et al. demonstrated the potential use of local palm fatty acid distillate (PFAD) as alternative feed-stock for fatty acid methyl esters (FAMEs) production and the possibility to replace the conventional acid-catalyzed esterification process (with H_2SO_4), which was industrially proven to suffer by several corrosion and environmental problems, with non-catalytic process in supercritical methanol. The esterification of PFAD in supercritical methanol gave FAMEs production yield of 95% at 300˚C with the PFAD to methanol molar ratio of 1:6 and the reaction time of 30 min. Compared with the conventional acid catalyzed esterification of PFAD, only 75% FAMEs yield was obtained in 5 h. Laosiripojana et al. was studied the esterification of palm fatty acid distillate (PFAD), a byproduct from palm oil industry, in the presence of three modified zirconia-based catalysts. It was found that, among all synthesized catalysts, the reaction in the presence of SO_4– ZrO_2 and WO_3–ZrO_2 (with 1.8 %SO_4 calcined at 500 °C and/or 20 %WO_3 calcined at 800 °C) enhances relatively high fatty acid methyl ester (FAME) yield (84.9 –93.7%). Production of fatty acid methyl ester (FAME) from palm fatty acid distillate (PFAD) having high free fatty acids (FFA) was investigated by Chongkhong et al. The optimum condition for the continuous esterification process (CSTR) was molar ratio of methanol to PFAD at 8:1 with 1.834 wt% of H 2 SO4 at 70˚C under its own pressure with a retention time of 60 min. The amount of FFA was reduced from 93 wt% to less than 2 wt% at the end of the esterification process. The final FAME product met with the Thai biodiesel quality standard, and ASTM D6751-02.

The product yields for hydrotreating of vegetable oil were analyzed by using the simulated distillation. The products at temperature less than 350ºC was observed which contained small amounts of reaction intermediate and reactant. It was obtained that temperature at 350ºC is suitable due to no oxygenated compounds and achieved 100% conversion (Simacek et al., 2010), the maximum theoretical products carbon

yields and carbon yields of C_{15}-C_{18} are 95% and 75%, respectively. The yields of gaseous (propane, carbon monoxide and carbon dioxide), isomerized and cracked products are minimum (Huber et al., 2007). It was observed by GC-MS when pressure is decreased to15 bar, product yields from n-C16 to n-C18 was increased due to increasing number of products and cannot specified exactly products like octadecenes, octadecanol, n-hexadecanoic acid, actadecanal and hexa-actadecyl hexadecanoate so there are several intermediates of this reactions. On the other hand, when pressure is increased (90 bar), decreasing number of products can be identified because intermediates were not found and fatty acids is reduced as well. Subsequently, pressure effect and hydrogen consumption were tested via simulated in Aspen plus. It was found that the hydrodeoxygenation reaction is better than decarboxylation and decarbonylation when pressure increased and increasing hydrogen consumption. Moreover, time analysis was obtained by simulated distillation curves, the best diesel yields (95.3 %vol) was observed at 4 hours (Guzman et al., 2010).

Influence of temperature to the conversion and pathway of process was show on the study effect of temperature at 350, 370 and 390ºC, the conversion and product yields are estimated from the simulated distillation data of the total liquid product at the each temperature by Bezergianni and Kalogianni. The produced liquid biofuels (gasoline and diesel) increase. This is expected as hydrocracking activity rises with increasing temperature. Furthermore gasoline yield increases monotonically with temperature, while diesel yield is smaller at the middle temperature (370ºC). The minimum diesel yield observed at 370ºC is attributed to the fact that increasing temperature. The cracking reactions favored by increasing temperature. These hydrocracking reactions convert heavier molecules including some diesel molecules into lighter gasoline molecules (Bezergianni et al., 2010). Bezergianni et al., 2010 was observed that as the temperature increases the amount of paraffins decrease, while the amount of iso-paraffins increases. The decrease of n-paraffins vs. the increase of iso-paraffins indicate that isomerization reactions are favored by hydrotreating temperature, which is expected as higher temperatures because hydrocracking type of reactions (which include isomerization and cracking).

A small percentage of DMDS (di-methyl-di-sulfide) and TBA (tetra-butyl-amine) is added in the feedstock. Heteroatom removal (mainly sulfur, nitrogen and oxygen) is expressed as the percentage of the sulfur (27,200 wppm), nitrogen (219.8 wppm) and oxygen (3.9 wt%) contained in the feed which has been removed during hydrotreatment reactions at operating temperature 330, 350, 370, 385 and 398ºC. As the result, Sulfur and nitrogen is most effectively removed by over 99.4% for all cases. Furthermore, the most difficult element to remove is oxygen. In low temperatures the oxygen removal is low (78.3%). However, by increasing the temperature, the oxygen removal gradually reaches over 99%. It is evident that higher temperatures favor all heteroatom removal from the final products (Bezergianni and Kalogianni 2009; Bezergianni et al., 2010).

3.5 Catalyst selection

The beginning of thermo catalytic processing of vegetable oil dates back to twenties of 20th century. The first catalysts used for cracking in gas phase were MgO, Al2 O3, CaO and Cu. Chlorides of Zn, Cu and Ba were used for cracking in liquid phase. The pro-cesses were carried out at temperatures 400–450˚C Bezergianni and Kalogianni, 2009; Kubicˇka et al., 2009; Šimácˇek et al., 2009 were investigated the applicability of a transition metal/metals containing heteroatom (sulphur and nitrogen) removal catalyst which is from the petroleum industry or expediently modified for the oxygen removing reaction (HDO, hydrodeoxygenation, reduction). Another research group (Simakova et al., 2009) were investigated the decarboxylation or decarbonylation reaction route on supported noble metal catalysts (Pd or Pt/activated carbon). Generally the bimetallic aluminium oxide supported catalysts in sulphided form (usually $NiMo/Al_2O_3$ and less $CoMo/Al_2O_3$) were investigated for the HDO reaction (Craig and Sorevan, 1991; Donnis et al., 2009; Gusmao et al., 1989; Krár

et al., 2010; Liu et al., 2009).

Hydroprocessing of vegetable oils is usually carried out in the temperature range of 300–400˚C and under the hydrogen pressure of 6–20 MPa. Traditional hydrogenation catalysts of the type Ni/Al_2O_3, $Ni–Mo/Al_2O_3$, $Co–Mo/Al_2O_3$ or Ni/SiO_2 are used. Laurent and Delmon have studied the catalytic performance of CoMo sulfide catalysts of various supports for the hydrodeoxygenation of oxygen-containing molecules. Murzin et al. using a variety of model compounds resembling vegetable oils investigated the performance of a number of catalysts for the production of renewable diesel. According to their results, Pd supported on active carbon catalysts displayed superior deoxygenation properties, yielding diesel-like hydrocarbons. Krause and co-workers studied HDO of sulfided $CoMo/Al_2O_3$ and $NiMo/Al_2O_3$ on heptanoic acid, heptanol and heptanoate methyl and ethyl esters. Sulfidation by addition of H_2S instead of CS2 shifted the selectivity from C7 to C6 hydrocarbons. It was found that NiMo, but not CoMo was very sensitive to the sulfidation conditions and that the unsulfided catalysts were neither very active nor selective to C6 and C7 alkane formation. Kubicˇka and co-workers evaluated the conversion of rapeseed oil over sulfided catalysts in a number of studies. When the activity and selectivity of sulfided $NiMo/Al_2O_3$ catalyst was compared to that of unsulfided Ni/Al_2O_3 at 270–350˚C, the sulfided catalyst was found to be much more active. However, the unsulfided catalysts primary yielded odd number hydrocarbons (decarboxylation/ decarbonylation) while the sulfided yielded primarily even num-bered (complete reduction). The activity of sulfided $NiMo/Al_2O_3$ surpassed that of Mo/Al_2O_3 and Ni/Al_2O_3 separately in liquid phase HDO below 300˚C in H_2 atmosphere (Kubicˇka et al., 2010). Rapeseed oil HDO over commercial sulfided $NiMo/Al_2O_3$ at 70 bar H_2 achieved full conversion above 300˚C, while higher temperatures yielded higher selectivity towards odd-number hydrocarbons (Šimácˇek et al., 2009). Supporting sulfided CoMo on mesoporous Al_2O_3 rather than MCM-41 resulted in higher yields of alkanes, but incorporating Al into the framework of MCM-41 did improve yields due to support acidity (Kubicˇka and Šimácˇ ek, 2009, Kubicˇka et al., 2010).

Resasco et al. concluded that HDO of methyl octanoate and methyl stearate over Pt/Al_2O_3 at 330˚C proceeds in inert atmosphere, but addition of H_2 suppresses formation of higher self-condensates of both compounds. Decarbonylation was found always to be the primary reaction route. The deoxygenation of methyl octanoate over H-ZSM-5 at 500˚C resulted in lighter hydrocarbon gases and aromatization, the latter of which proceeded through self-condensation products (tetradecane, 8-pentadecanone, octyloctanoate) (Danuthai et al., 2009).

3.6 Properties of production

From the refinery point of view, all hydrocarbons present in hydroprocessed vegetable oil belong to middle distillates and are thus suitable for production of diesel fuel. Hydroprocessed vegetable oil can be called hydrocarbon-based or oxygen-free bio-diesel. Oxygen-free biodiesel eliminates some drawbacks of the traditional FAME-type biodiesel relating mostly to fuel stability. Car manufacturers would probably also prefer hydrocarbon-based biodiesel to FAME as it offers full compatibility with current diesel fuel for which the diesel engine systems are optimized (Šimáčˇek et al., 2010). Thanks to its high content of n -alkanes, oxygen-free biodiesel has an excellent cetane number ranging from 55 to 90 (Stumborg et al., 1996) depending on degree of branching. The worsened low-temperature properties seem to be the only disadvantage in comparison with FAME-type biodiesel. Low-temperature properties can be improved either by choice of proper catalyst and reaction conditions or by isomerisation (Hodge, 2006 and Hancsók et al., 2007) following the hydroprocessing. The production of biodiesel takes place in two stages. Product of vegetable oil hydroprocessing (stage 1) proceeds to an isomerisation unit (stage 2) where its low-temperature properties are improved. The final product called NExBTL is used as renewable component for production of diesel fuel. Neste Oil guarantees that its Neste Green diesel, which suits all diesel engines, contains at least 10% of NExBTL.

The analyses of products were analyzed by gas chromatography. The reaction products mostly are aqueous phase which separated in to liquid phase and gaseous phase. Gaseous products and all organic liquid products were analyzed by gas-chromatographic methods. Physiochemical properties of the organic liquid products and mixed fuels were determined using standard test procedures designated for diesel fuel or petroleum products. As a result of Šimácˇ ek et al. experiment, hydroprocessing of rapeseed oil yielded water, gaseous hydrocarbons and organic liquid product (OLP). The conversion of rape-seed oil was >99% at 310˚C and complete conversion was achieved at 360˚C. The yields of the main products were as follows: OLP–83 wt.%, water – 11 wt.% and gaseous hydrocarbons 6 wt.%. Beside hydrogen, the reaction gas contained mainly propane (0.8–2.5 vol.%) and small amounts of carbon dioxide (0.05–0.3 vol.%), carbon monoxide (up to 0.5 vol.%) and methane.

CHAPTER IV

EXPERIMENTAL

This chapter presents the overview of the hydroprocessing of different palm oil for biodiesel production. First part of this chapter about materials and chemicals are provided for the experiments, catalyst preparation, and products analysis. The procedure of the catalyst preparation by the incipient wetness co-impregnation method was then described. Next part was explained the catalyst characterization. The experimental set up and the procedure were described. Finally, feedstock and Product Characterization were also including in this chapter.

4.1 Materials and Chemicals

The different palm oil was obtained from Oleen Company limited as the feedstock for the reaction. $Ni(NO_3)_2 \cdot 6H_2O$ (Aldrich, 99.9%), $Co(NO_3)_2 \cdot 6H_2O$ (Aldrich, 99.9%) and $(NH_4)_6Mo_7O_{24} \cdot 4H_2O$ (March, 99.9%) were used as precursors. The Alumina (γ-Al_2O_3) from Aldrich was supports in this work. The 2-propanol (Sigma-Aldrich, 99.9%) was used as a solvent for dilute liquid product. Hydrogen (Linde Gases, 99.999%) was used as reactant in the reaction. Helium ultra high purity (Linde Gases, 99.999%) was used as purge gas. Hydrogen (Linde Gases, 99.999%), Nitrogen (Linde Gases, 99.999%) and H_2S/H_2 (Linde Geses , 10vol% of H_2S) were used to presulphidation process.

4.2 Catalyst Preparation

4.2.1 Preparation of bimetallic oxide supported on γ-Al_2O_3

The catalysts were prepared by impregnating commercial γ-Al_2O_3 with heated deionized water solution of ammonium heptamolybdate ($(NH_4)_6Mo_7O_{24}\cdot 4H_2O$, March) and nickel nitrate hexahydrate ($Ni(NO_3)_2\cdot 6H_2O$, Aldrich) or cobalt nitrate hexahydrate ($Co(NO_3)_2\cdot 6H_2O$, Aldrich) followed by the atomic ratio [x/(x+Mo)] = 0.3 (x = Co, Ni). The solution was dropped to γ-Al_2O_3 support with a surface area of 141.8 m^2/g (Kubicka and Kaluza, 2010). The method of incipient wetness co-impregnation was divided in to three steps with three times drying and calcinations. Each of three steps was impregnated by 40%, 35% and 25% of the total amount of precursor. After the dropping of the first step precursor, the sample were dried at 120°C for 12 hours and calcined at 500°C for 5 hours (ramp rate 3°C/min). And the calcined sample was re-impregnated with the next step of aqueous precursor then does it again with the same procedure till finish the third step. Both of NiMo/Al_2O_3 and CoMo/Al_2O_3 oxide catalysts were activated into sulfides form.

4.2.2 Presulfidation process

The sulfidation catalysts were prepared with 5vol. % H_2S/H_2 mixture at 400°C under atmospheric pressure. The sulfidation reactions were conducted under atmospheric pressure in fixed bed reactor (Pyrex glass). The 0.1 grams of oxide catalyst was placed in to a fixed bed reactor with a temperature controller. First the sample was heated to 400°C at heating rate of 10°C /min under N_2 gas flow. The gas flow was switched to 5vol. % H_2S/H_2 mixture when the temperature rose to 400°C (Dumeignil, 2003). The presulfidation was continued for 4 hours with 50ml/min of 5vol. % H_2S/H_2. The catalyst sample was cool down to room temperature with N_2 flow (Viljava, 2000). The Figure 4.1 was showed a flow diagram of sulfided catalyst.

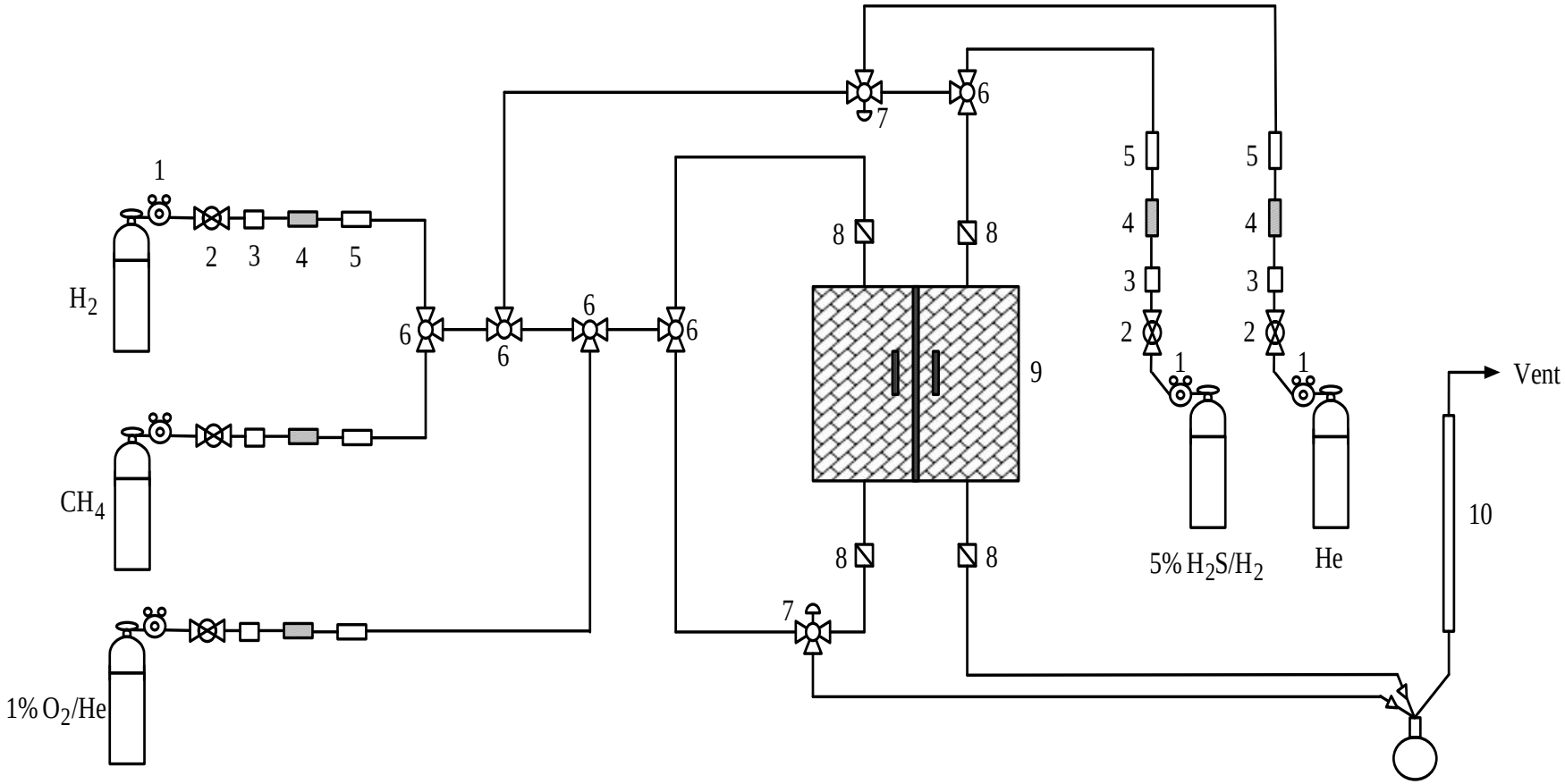

1. Pressure Regulator 2. On-Off Value 3. Gas Filter 4. Mass Flow Meter 5. Check Valve

6. 3-way 7. 3-way Valve 8. Sampling point 9. Furnace 10. Bubble Flow Mete

Figure 4.1 Flow diagrams of synthesis metal sulfided catalysts.

4.3 Catalyst Characterization

4.3.1 Inductively coupled plasma-optical emission spectrometer (ICP-OES)

The percentage of metal loading of catalyst was analyzed by inductively coupled plasma-optical emission spectrometer (ICP-OES). The amount of metal on the surface of catalyst was measured with an inductively coupled plasma atomic emission spectrometer (ICP-AES) Perkin Elmer model PLASMA-1000. The 0.03 g of an exactly amount of catalyst was dissolved in 10 ml of hydrofluoric acid 49%, hydrochloric acid and nitric acid with ratio 3:1:1 respectively. The mixture were stirred until all solid become a solution then make volume up to 100 ml using de-ionized water by the 100ml volumetric flask. The concentration of the sample after volume adjustment is about 5-20 ppm (mg/l).

4.3.2 Nitrogen physisorption (BET surface area)

The BET apparatus for the multiple point method from Micromeritics ASAP 2020 was used for analysis surface area of catalysts. The mixture gases of helium and nitrogen will flow through the system at the nitrogen relative in the range of $0.05 < P/P_0 < 0.35$. The catalyst sample (cat. 0.1 g) will be placed in the sample cell to degassed, which will be then heated up to 150°C and will hold at this temperature for 3 h. After the catalyst sample was cooled down to room temperature, nitrogen uptakes will be measure. Adsorption measurements were carried out using liquid nitrogen at 77K (-196°C). The specific surface area was calculated on the basis of the BET isotherm. Volume distributions and pore size were performed by BJH (Barrett-Joyner-Halenda) desorption branch analysis.

4.3.3 Scanning Electron Microscope (SEM)

A Hitachi S-3400N Scanning Electron Microscope (SEM) was used to observe the surface morphology of the sample with an acceleration voltage of 15 kV.

4.3.4 X-ray diffraction (XRD)

The X-ray diffraction characterization was carried out on a D8 Advance of Bruker AXS, equipped with a long fine focus ceramic Cu K_α X-ray source. The pattern was recorded in the range of $20^\circ < 2\Theta < 80^\circ$ with incremental steps of 0.04°, and scan speed of 0.5 s/step.

4.3.5 Temperature-programmed reduction (TPR)

Temperature-programmed reduction (TPR) analyses of the oxide catalysts were performed on Micrometritics Chemisorb 2750. The catalyst sample (0.1 g) to be tested was pretreated in N_2 stream at 150°C for 1 h and then cooled to room temperature. Then the N_2 flow was switched to a 10% H_2/Ar flow (15ml/min), and catalyst sample was heated to 800°C at a rate of 10°C/min. The hydrogen consumption of the catalyst reducing was detected by a thermal conductivity detector (TCD).

4.3.6 NH_3 Temperature programmed desorption (NH_3 –TPD)

The study of NH_3-TPD was performed in a Micrometric ChemiSorb 2750 automated system attached with ChemiSoft TPX software. The amount of NH_3 adsorbed on the surface was determined by thermal conductivity detector. The 0.05 g of catalyst sample was placed in quartz tube in temperature controlled furnace. Then helium gas with flow rate of 15 ml/min was fed through sample and heating temperature up from room temperature to 500°C with heating rate of 10°C/min after that held for 2 hour to remove moisture. The catalyst sample was cooled down to room temperature and flowed 15%vol of NH_3 in helium gas through a sample at flow rate of 15 ml/min then held for 15 minutes. Subsequently, helium gas was fed through the sample for 3 hours. Finally, the catalyst sample was heated from room temperature to 500°C (10°C/min). The signal was recorded every one second and stored on a microcomputer. The acid property of catalysts was determined by this method.

4.4 Raw material characterization

4.4.1 Individual fatty acid content (GC/MS/MS)

Degummed palm oil, RPS-palm hard stearin and RPS-palm soft stearin were evaluated the fatty acid content by GC/MS/MS at the Halal Science Center Chulalongkorn University. Using capillary column TR-Fame size 30 m × 0.25 mm ID, film thickness 0.25μm and Mass Spectrometry detector (MS) followed by inhouse method: based on Lepage, G. and Roy, C.C., 1986.

4.4.2 Fourier transforms infrared Spectroscopic method (FT-IR)

FTIR were used to estimate the unconverted carboxyl groups. The NICOLET MODEL IMPACT 6700 of the IR spectrometer was presented in this study. The spectra were recorded in the 400-4000 cm^{-1} region.

4.5 Experimental Setup

The reaction was carried out with six cylindrical batch reactor (14 mm ID, 150 mm in length with a volume of 23 cm^3) placed in a furnace with temperature controller as shown in Figure 4.2. The temperature gradient does not significantly with the position of the cylindrical reactor but some temperature gradient between the furnace and inside of the reactor.

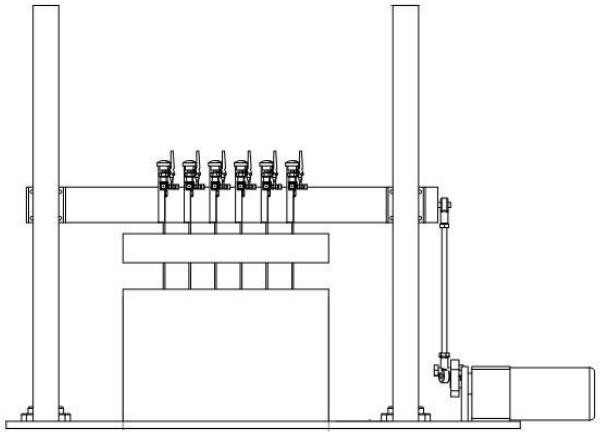

Figure 4.2 Illustrated of Shaking Batch Reactor.

4.6 Experimental Procedure

4.6.1 Preparation of Feed Stock

Degummed palm oil and two kinds of RPS palm stearin were used as a feed for the biodiesel production. Degummed palm oil (DPO) was kindly provided by Patum Oil, Thailand. The DPO was past the process of degumming of the crude palm oil to remove proteins, pigments and other unwanted substances but still contains mainly free fatty acid (FFA) as palmitic (5% max). The DPO has red-yellow liquid at room temperature that can be use for the reaction without any treatment. RPS palm oil has light-yellow liquid and semi-solid at room temperature which is formed during fractionation of palm oil after crystallization process at a specific temperature. Before the reaction, the RPS palm oil was melted to clear-yellow liquid on slightly heating (40-45° C).

4.6.2 Reaction Performance Testing

Several feed stock and catalysts were measured and fill in six tubular reactors with the condition for hydroprocessing experiments as follow in Table 4.1.

To perform the reaction, the reactor was purged with Helium gas for 3 times to get rid of air in the reactor then compressed hydrogen pressure of 50 bars into the reactor. After that, the reactor was put into the furnace by shacking 30 rpm. The reactor was put out of the furnace at the interval time and dipped into the water immediately for stop the reaction after that taken the reaction products.

Table 4.1 Operating condition for hydroprocessing

Variable	Condition
Amount of Feed stock	2 ml
Temperature	330, 360, 390 and 415°C
Hydrogen pressure	50 bar
Reaction time	0, 0.5, 1.5 and 3.5 h
Catalyst type	Ni-Mo/Al_2O_3 and Co-Mo/Al_2O_3 sulfided
Amount of catalyst	0.02 g

4.7 Product Characterization

The hydroprocessed products were contained two phase that gaseous phase and liquid phase. The composition of the total organic products, obtained from the catalytic conversion of the triglycerides were determined.

The liquid product was centrifuged to separate the liquid phase and solid phase (catalyst) then analyzed using gas-chromatography method.

Organic liquid products were analyzed by gas-chromatography equipped with flame ionization detector (GC-14B, Shimadzu). In addition, the distillation temperature was determined by simulated distillation according to the ASTM-2887-D86 procedure. Table 4.2 is shown the operating condition for gas chromatograph equipped with flame ionization detector and operating condition temperature program.

Product yields of desired product (middle distillate yield) were used to describe the effectiveness of hydrotreating reaction. The conversion and selectivity was determined by similated distillation data as follows:

$$\text{Conversion}(\%) = \frac{\text{Feed}_{360+} - \text{Product}_{360+}}{\text{Feed}_{360+}} \times 100$$

Where: Feed_{360+} is the weight percent of the feed which have a boiling point higher than 360°C. Product_{360+} is the weight percent of the product which have a boiling point higher than 360°C.

As middle distillate (Diesel) is the desired product, the measure of Diesel selectivity is based on the boiling point range and defined by the following equation:

$$\text{Diesel selectivity}\ (\%) = \frac{\text{Product}_{180-360} - \text{Feed}_{180-360}}{\text{Feed}_{360+} - \text{Product}_{360+}} \times 100$$

Where: $\text{Feed}_{180\text{-}360}$ and $\text{Product}_{180\text{-}360}$ are the weight percentage of feed and product respectively, which have a boiling point between 180-360°C (Diesel range) (Bezergianni et al., 2010)

Table 4.2 Operating condition for gas chromatograph equipped with flame ionization detector.

Gas Chromagraph	SHIMADZU GC-14B
Detector	FID
Column	Capillary DB-2887 (Agilent J&W GC Columns)
- Column material	Silica
- Length	10 m
- Outer diameter	0.53 mm
- Film thickness	3 µm
Spilt flow rate	30 ml/min
Purge flow rate	4 ml/min
Carrier gas	He (99.999%)
Carrier gas flow	70 kPa
Hydrogen gas flow	60 kPa

Table 4.2 Operating condition for gas chromatograph equipped with flame ionization detector (cont.)

Gas Chromagraph	SHIMADZU GC-14B
Air gas flow	50 kPa
Primary gas flow	500 kPa
Make up flow	60 kPa
Temperature limits (^{o}C)	-60 - 350
Injector temperature (^{o}C)	250
Column oven temperature program	
- initial column temperature (^{o}C)	40
- ramp rate (^{o}C/min)	10
- final column temperature (^{o}C)	330
Detector temperature (^{o}C)	340
Analyzed liquids	Hydrocarbon normal C_5-C_{44} alkanes

CHAPTER V

RESULTS AND DISCUSSION

This chapter presents the results with a discussion about the characteristics and catalytic properties in the hydrotreating activity for biodiesel production. The selectivity and conversion of diesel like hydrocarbon under condition (330- 415°C, H_2 pressure = 50 bar, time = 0.5, 1, 2 and 4 h) are also discuss in this chapter.

5.1 Characterization of Catalysts

5.1.1 Inductively coupled plasma-optical emission spectrometer (ICP-OES)

The compositions of metal in catalysts were confirmed by inductively coupled plasma optical emission spectroscopy (ICP-OES). The catalysts were loaded of 2.5 wt% of Ni, 2.5 wt% of Co and 10 wt% of Mo. Table 5.1 was showed the compositions of catalysts.

Table 5.1 The compositions of catalysts as determined by ICP-OES

Sample	Ni content (%wt.)		Co content (%wt.)		Mo content (%wt)	
	Calculated	Measured	Calculated	Measured	Calculated	Measured
$NiMo/Al_2O_3$	2.5	2.4	-	-	10	9.25
$CoMo/Al_2O_3$	-	-	2.5	2.55	10	9.39

5.1.2 Nitrogen physisorption (BET surface area)

Table 5.2 Typical properties of the catalysts.

Samples	Surface area (m^2/g)	Pore volume (cm^3/g)	Pore size (nm)
Al_2O_3	141.88	0.23	3.91
$NiMo/Al_2O_3$	100.19	0.16	4.54
$CoMo/Al_2O_3$	100.84	0.18	4.52

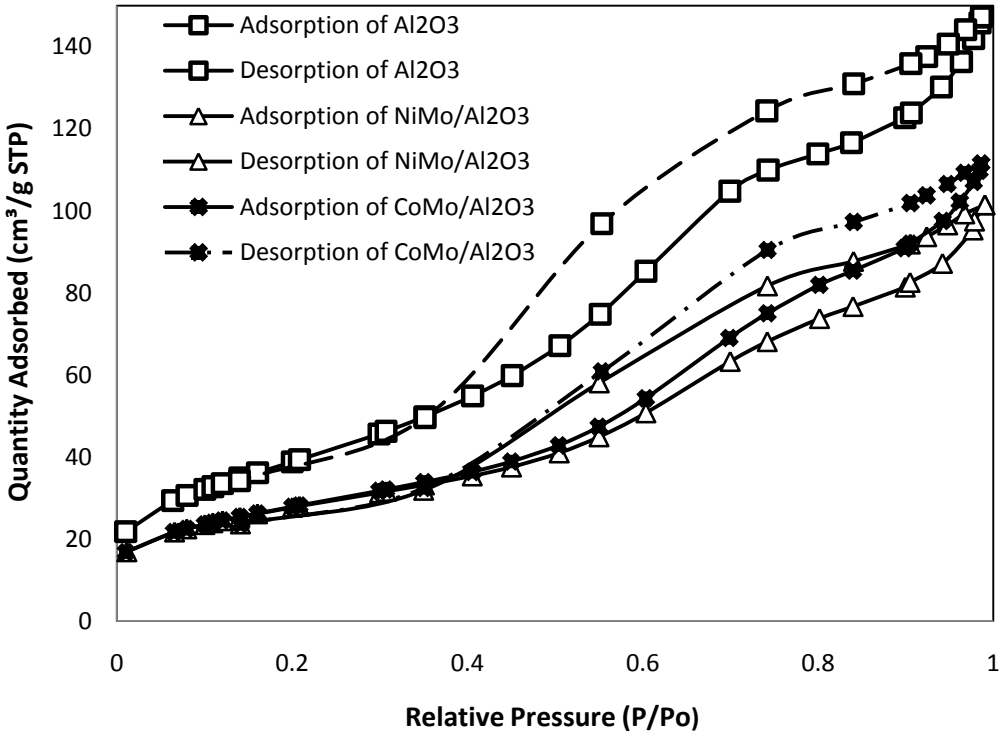

Figure 5.1 N_2 adsorption-desorption isotherm of Al_2O_3, $NiMo/Al_2O_3$ and $CoMo/Al_2O_3$.

The isotherms of nitrogen adsorption-desorption is shown in Figure 5.1. All catalysts and support exhibit a type IV N_2 adsorption isotherm, which is typical for mesoporous materials (S. Rana et al., 2004). The diminished shape of hysteresis loop of $NiMo/Al_2O_3$ and $CoMo/Al_2O_3$ are shown in the fiuure 5.1 indicating that structure of material is change a bit after Mo and Ni loading. The decrease in the height of hysteresis loops indicates the loss of pore volume, due to the filling of pores by Ni and Mo species. BET surface areas, pore volume and pore size are shown in Table

5.2. which indicates the decrease in the surface area and pore volume upon loading of nickel and molybdenum oxide. This could be explained by substantial blocking of pore opening by large MoO_3 crystallites (Badoga et al., 2012).

5.1.3 Scanning Electron Microscope (SEM)

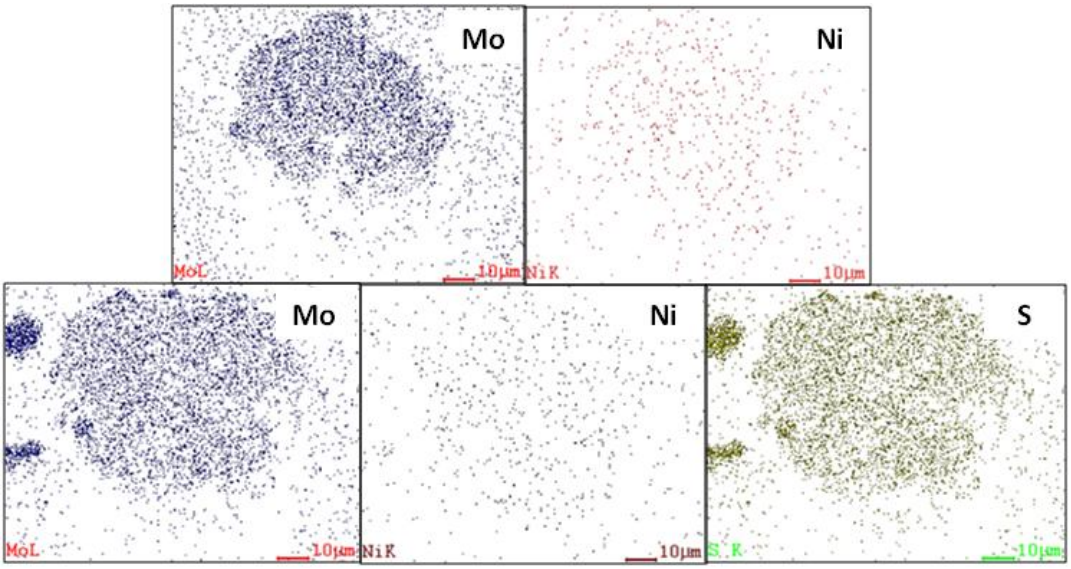

Figure 5.2 SEM-EDX images of NiMo/γAl_2O_3 catalysts in an oxide (upper) and sulfided (lower) form.

Figure 5.2 is shown the SEM-EDX images of NiMo/γ-Al_2O_3**.** The upper block of Mo and Ni are indicated as an oxide catalyst which representing Mo and Ni are well distributed on the alumina surface. The three lower block shows the mapping of Mo, Ni and S on NiMo/γ-Al_2O_3 sulfided catalyst. As seen, the location S atom is matched very well with Mo atom which could imply that Mo atoms are adjacent with S atoms. The possible species of Mo-S species will be discussed laterin the XRD section.

Figure 5.3 is shown the SEM-EDX images of CoMo/γ-Al_2O_3. Similarly, good dispersion of metal could be observed. Sulfided CoMo/γ-Al_2O_3 show a presence of Mo accompany with S atoms.

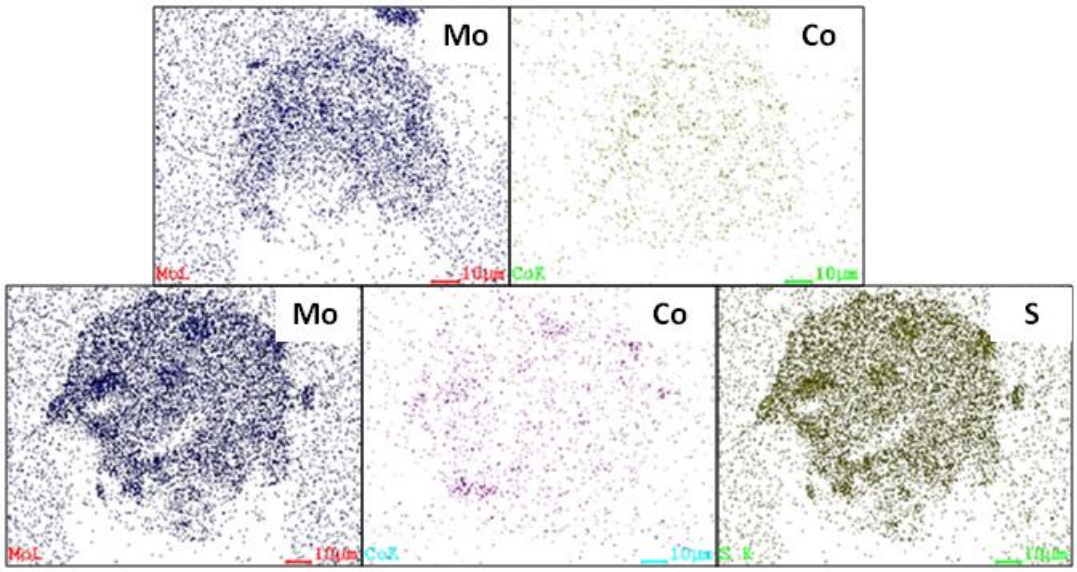

Figure 5.3 SEM-EDX Images of $CoMo/Al_2O_3$ oxide and sulfided catalysts.

5.1.4 X-ray diffraction (XRD)

The XRD patterns of alumina support and oxide catalysts were shown in Figure.5.4. The diffraction patterns show broad peaks at 37.5, 46.2 and 67°, which can be attributed to γ-alumina phase (Lai and Pang, 2013). For $NiMo/Al_2O_3$ catalyst was showed four prominent reflections at 2θ = 23.5, 37.7, 46.2 and 67°, typically at 37.7, 46.2 and 67° are assigned to γ-alumina phase and 23.5 is a characteristic of MoO_3. The peak at 13.1, 23.3, 25.5, 27.9 and 33.7° correspond to crystalline orthorhombic α-MoO_3 (Zhou and Chen et al, 2012). However, no peaks corresponding to nickel and cobalt species, which could be due to the high dispersion of these species. The disappearance of nickel and cobalt observed with low loadings of Ni and Co species (Zhou and Chen, 2012)

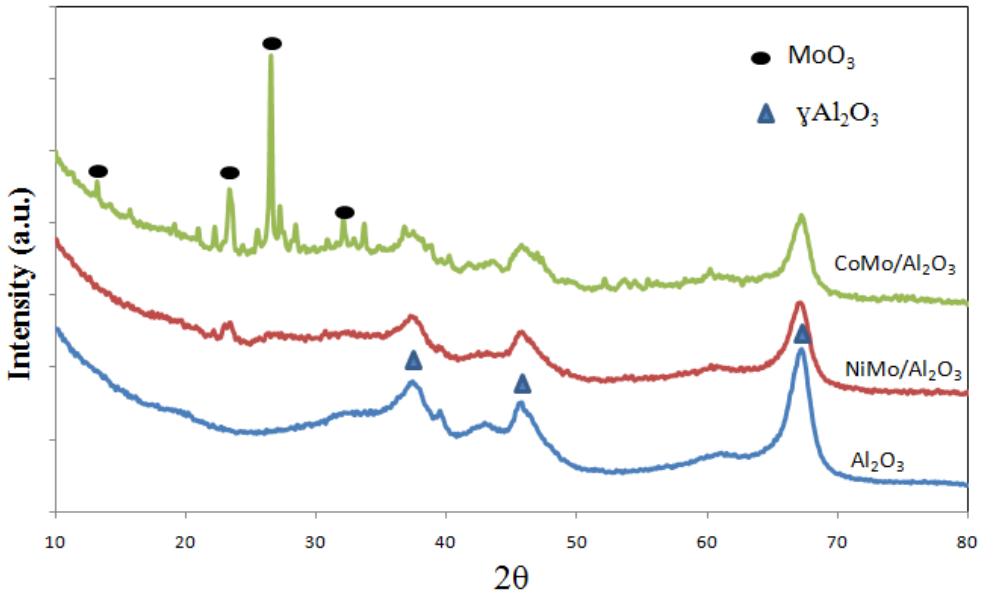

Figure 5.4 XRD patterns of Al_2O_3 support, $NiMo/Al_2O_3$ and $CoMo/Al_2O_3$ catalysts.

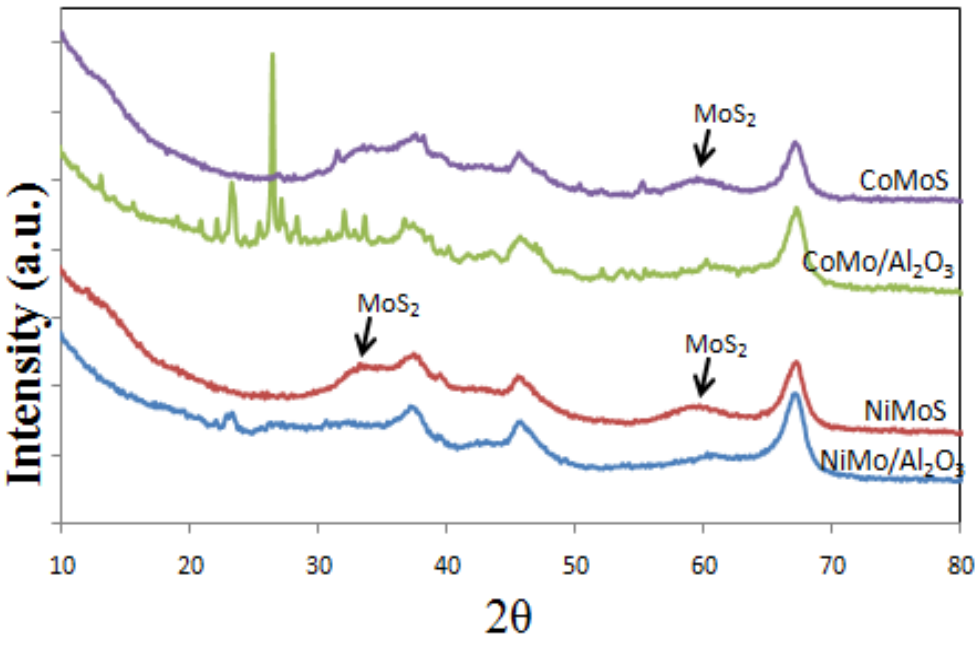

Figure 5.5 XRD patterns of $NiMo/Al_2O_3$ and $CoMo/Al_2O_3$ oxide and sulfided catalysts.

For more clear difference between two forms of catalysts can be found by comparing the XRD patterns of both $NiMo/Al_2O_3$ and $CoMo/Al_2O_3$. As shown in the figure 5.5, two peaks at 33° and 59° were observed for $NiMo/Al_2O_3$ sulfided catalyst such as MoS_2, and $NiMo_2S_4$ (Monteiro-Gezork et al., 2007). Puello-polo and co-worker reported Mo^{4+} species could be the active center for converted to MoS_2. The peak of Ni was not exhibit significant as its low loading. For $CoMo/Al_2O_3$ sulfided catalyst, only peaks of MoS_2 at 33° were observed but not show for peak at 59° indicating that the MoS_2 phases are highly dispersed over the support and their particle sizes are below the detection limit of XRD technique or the amorphous form of MoS_2 (Sundaramurthy et al., 2008).

5.1.5 Temperature-programmed reduction (TPR)

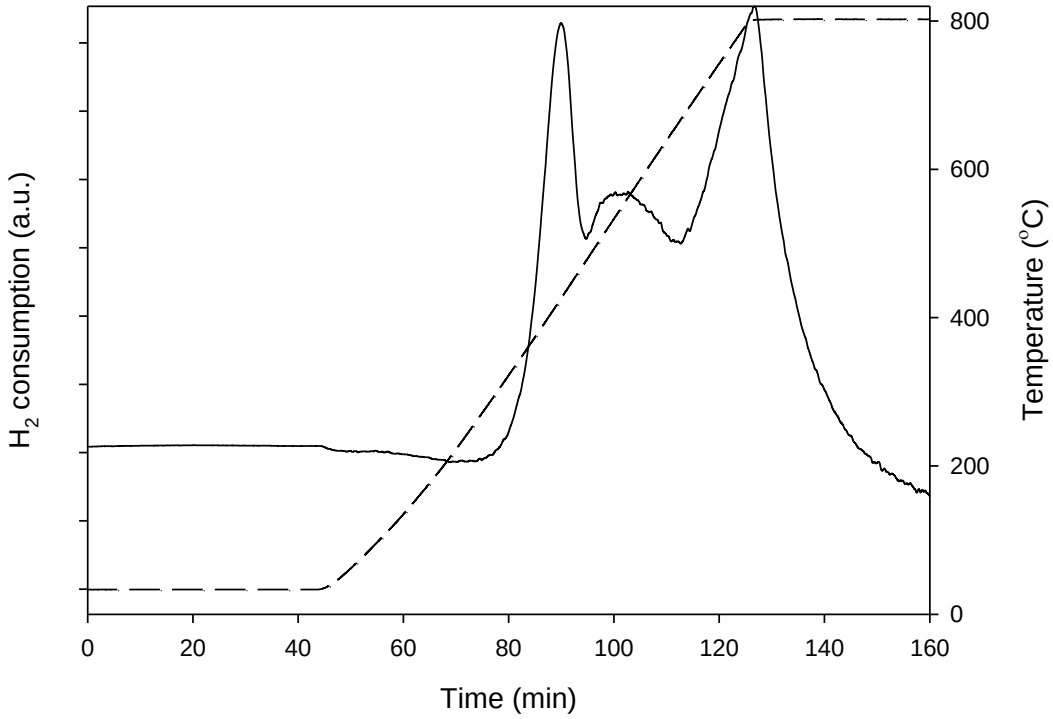

Figure 5.6 TPR profiles of the $NiMo/Al_2O_3$ oxide catalyst

Temperature-programmed reduction of hydrogen (H_2-TPR) was performed in order to determine the reducibility of oxide catalysts. Figure 5.6 and Figure 5.7 are shown the H_2-TPR profile of $NiMo/Al_2O_3$ and $CoMo/Al_2O_3$ oxide catalysts. There are two main reduction peaks where the first is located at around 420°C, related to the reduction of Mo^{6+} species in polymolybdate structures to Mo^{4+} species (Badoga et al., 2012) and the second peak located at around 800°C, which can be attributed to the reduction of the Mo^{+4} to Mo^0 (Kaluza and Gulkova et al., 2007). The shoulder observed at about 520°C could be assigned to the reduction of Ni^{2+} to Ni^0 species on the alumina surface.

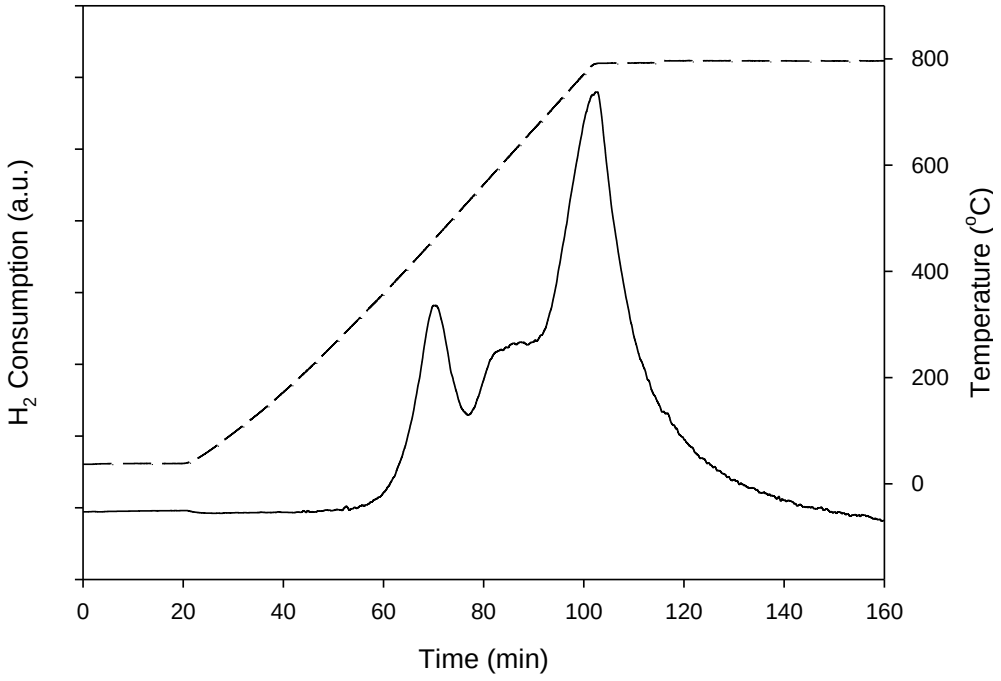

Figure 5.7 TPR profiles of the $CoMo/Al_2O_3$ oxide catalyst

The TPR patterns and trend in the reducibility of $CoMo/Al_2O_3$ oxide catalyst are presented in figure 5.7. $CoMo/Al_2O_3$ shows two principal reduction peaks where the first is attributed to the partial reduction of Mo^{6+} to Mo^{4+} at 420°C while the subsequent peaks are the stepwise reduction of the bulk MoO_3 (Leyva and S. Rana et al., 2008).

5.1.6 NH_3 Temperature programmed desorption (NH_3 –TPD)

To investigate the acidity of the catalysts, the NH_3-TPD measurement of the catalysts was carried out. Two spectra in Figure 5.8 show a broad peak in the temperature range 110-500°C, which indicates the combination of weak-intermediate-strong acid centers (Zhu et al., 2010). The strength of the acid sites can be determined by the temperature at which the adsorbed NH_3 desorbs. As seen, it is most likely that no significant different in the strength of acidity between both catalysts. Total acidity shown in Table 5.3 was determined from the amount of ammonia desorbed from the entire temperature region. The result shows $NiMo/Al_2O_3$ contains higher acidity than $CoMo/Al_2O_3$ catalyst.

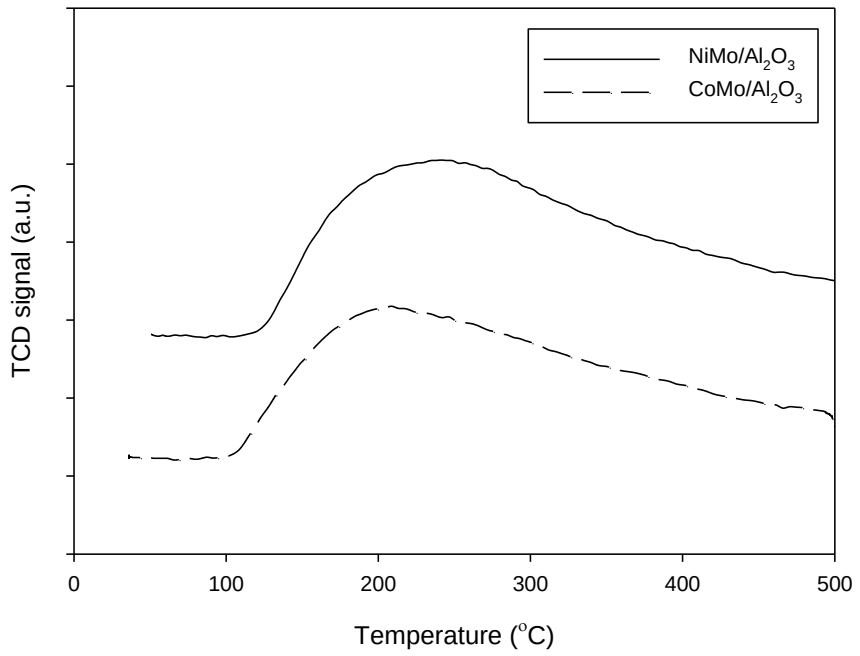

Figure 5.8 NH_3 profiles of reduced catalysts $NiMo/Al_2O_3$ and $CoMo/Al_2O_3$.

Table 5.3 Total acid sites of oxide catalysts.

Catalyst	Total acid site (mmol NH_3/g)
$NiMo/Al_2O_3$	1.415
$CoMo/Al_2O_3$	1.253

5.2 Raw material characterization

5.2.1 Individual fatty acid content (GC/MS)

The weight percentages of fatty acid composition in triglyceride were characterized by the Research and Service Laboratory of Halal Science Center Chulalongkorn University which shown in Table 5.4. From the GC-MS analysis, it was observed that DPO, RPS hard and RPS soft contain mainly palmitic acid and oleic acid. Palmitic acid content (saturated fatty acid) could be ordered as RPS hard > RPS soft > DPO while oleic and linoleic content (unsaturated ones) could be inversely ordered as DPO > RPS soft > RPS hard. The degree of unsaturation could be expressed by iodine value as shown in Table 5.5 could be ordered as DPO > RPS soft > RPS hard, which are corresponding well with the fatty acid composition in Table 5.4. As shown in Tale 5.5, DPO contain the highest free fatty acid content while RPS soft and hard are similar and much lower than that of DPO.

Table 5.4 The weight percentages of fatty acid composition in DPO, RPS Hard and RPS Soft.

FATTY ACID	DPO (wt.%)	RPS Hard (wt%)	RPS Soft (wt.%)
C 12:0 (Lauric)	0.8	0.08	0.11
C 14:0 (Myristic)	1.2	0.69	0.71
C 16:0 (Palmitic)	45.4	61.40	54.86
C 16:1 (Palmitoleic)	0.1	-	-
C 18:0 (Stearic)	3.8	5	4.26
C 18:1 (Oleic)	39.0	27.07	32.47
C 18:2 (Linoleic)	9.1	5.52	7.26
C18:3 (Linolenic)	0.2	-	-
C 20:0 (Arachidonic)	0.3	0.25	0.33
C 20:1 (Eicosenoic)	0.1	-	-

Table 5.5 The properties of DPO, refined bleached deodorisied palm soft and hard stearin (From OLEEN Company Limited).

Parameter	DPO	RPS Soft	RDB Hard
Free Fatty Acid (%)	5% Max.	0.06	0.06
Iodine Value (Wijs method)	51.1	43.94	31.24

5.2.2 Fourier transforms infrared Spectroscopic method (FT-IR)

The FTIR spectra used to determine the glycerides molecules present in the feed. The intensity of the stretching peak at 1742.8, 1742.5 and 1738.3 cm^{-1} of DPO, RPS Soft and RPS Hard respectively are corresponding to the carboxyl group (C-C=O) in FTIR. The CH stretching peaks in the region of 2750-3150 cm^{-1} was taken as the reference for monitoring the decreasing of carboxyl peak because this peak remains nearly unaffected by the reaction and carboxyl peak decrease as the reaction proceeds (Jitendra K.Satyarthi and Darbha Srinivas, 2011).

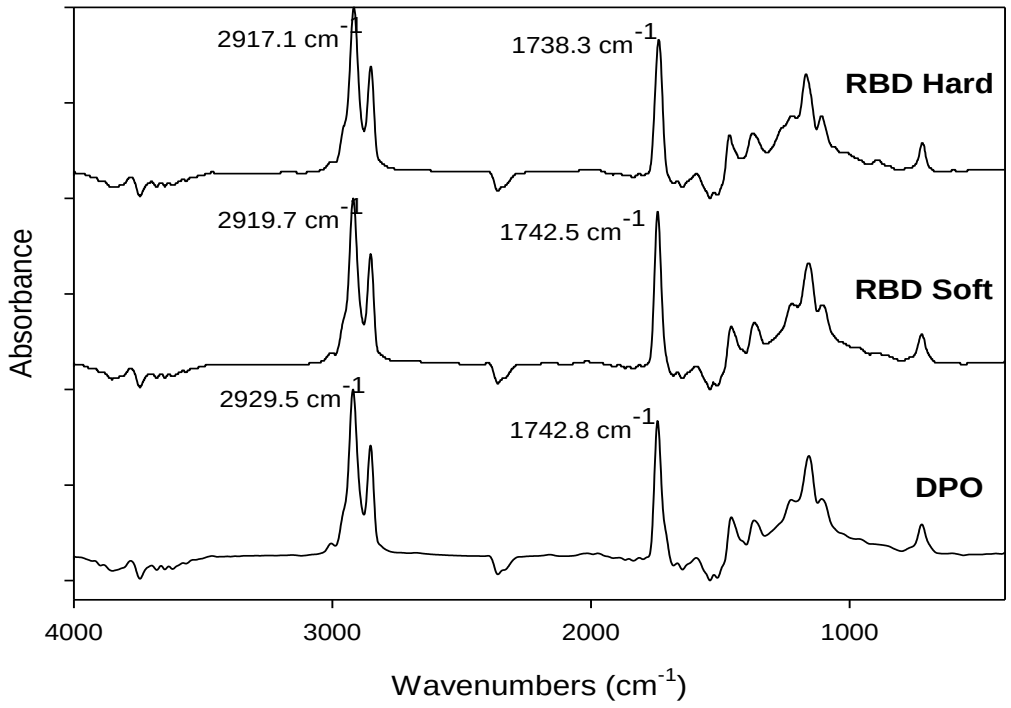

Figure 5.9 FTIR spectra of DPO, RPS Soft and RPS Hard.

5.3 Hydroprocessing of different palm oil feed stock

5.3.1 Influence of process conditions

Several sequential and concurrent reactions occur during the hydroprocessing of triglyceride feeds. These reactions pathways are consist of parallel and/or consecutive reaction steps, including saturation, cracking, decarboxylation, decarbonylation, and/or hydrodeoxygenation (Veriansyah et al., 2012). There are many of researcher aim to study on the process condition of hydroprocessing such as operating temperature, pressure, and reaction time.

The diesel yield and gasoline yield as a function of reaction temperature are shown in Figure 5.10. When the temperature was increased from 330°C to 360°C, the diesel yields of RPS soft and hard palm stearin increased from 47.4% to 65.9% and 49% to 70.8% respectively. As the temperature continued to increase above 360°C, the diesel yield began to decrease. According to Figure 5.10, there is little effect the diesel yield of DPO when temperature rises from 330°C to 360°C, in which the yield only changes from 56.9% to 61.3%. The maximum diesel yield of degummed palm oil (DPO) is 65.1% at reaction temperature 390°C; whereas, the maximum diesel yield for both types of refined bleaching deodorised palm stearin are 65.9% and 70.8% respectively at reaction temperature of 360°C. Comparing between two different catalysts, at low temperature NiMo sulfided catalyst show much higher activity than CoMo sulfided catalyst but CoMo sulfided catalyst become comparable at high temperature.

Figure 5.10 shows that at temperature below 360°C, the gasoline yield of the several feedstocks show a similar trend. The gasoline yield of the several feedstocks increases as the temperature increase. The result show the same as Huber et al studied of reaction temperature general trends of increasing n-alkane isomerization and cracking at higher reaction temperature cause high gasoline yield of product.

Figure 5.11 shows the temperature effect for CoMo sulfided catalyst. At 390°C of reaction temperature, degummed palm oil and refined bleaching deodorised soft and hard palm stearin shown the maximum of diesel yield at 62%, 63.3% and 51.2% respectively. Gasoline yield of several feed were observed the maximum at the same temperature (415°C) which yield of gasoline are 27.6% of RPS Soft, 23.7% of RPS Hard and 19.9% of DPO.

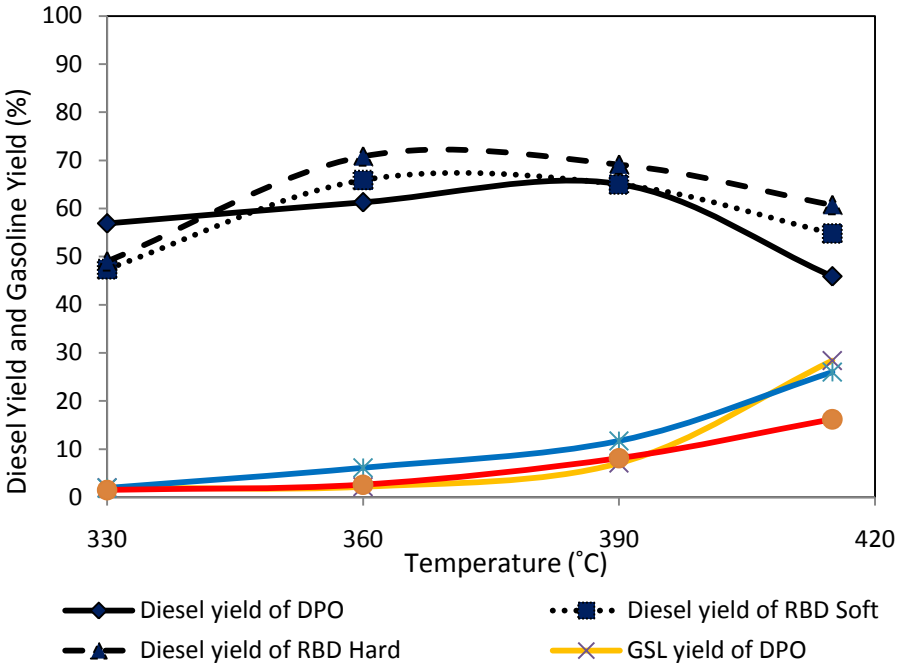

Figure 5.10 Temperature effect on diesel yield and gasoline yield (as vol% of total liquid product). All experiment were perform at P=50 bar, $NiMo/Al_2O_3$ sulfided catalyst and time of reaction 4 hr.

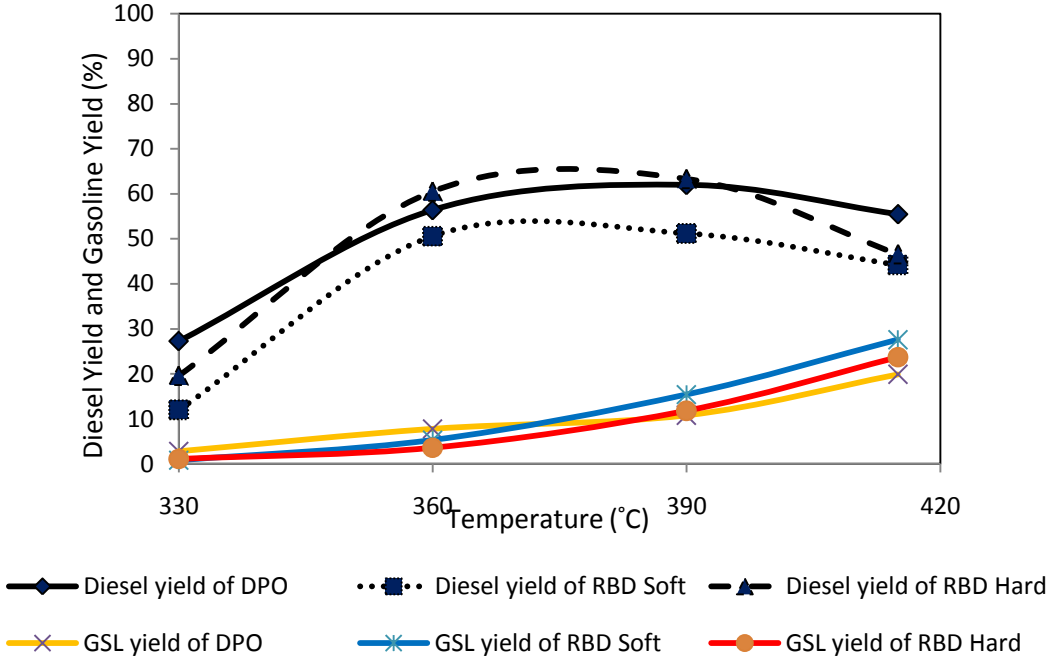

Figure 5.11 Temperature effect on diesel yield and gasoline yield (as vol% of total liquid product). All experiment were perform at P=50 bar, $CoMo/Al_2O_3$ sulfided catalyst and time of reaction 4 hr.

Diesel conversion of DPO tends to increase with increasing reaction time at reaction temperature of 390°C of NiMo sulfided and CoMo sulfided as shown in figure 5.12 and Figure 5.13. For NiMo sulfided catalyst, the maximum conversion are 65.8% at 2 h of DPO, 76.76% at 4 h of RPS soft palm stearin and 75.81% at 4 h of RPS hard palm stearin. For CoMo sulfided catalyst, the maximum conversion at 4 h is 72.8% of DPO, 69.2% of RPS soft palm stearin and 75.2% of RPS hard palm stearin. The increasing of reaction time leads to increase in conversion of triglycerides and fatty acids to C_{12}-C_{18} alkanes. Moreover, a long period of reaction time may cause to increase of light hydrocarbons (less than C_{12} alkanes from cracking of C_{12}-C_{18} alkanes) which decrease of diesel selectivity. As shown in Figure 5.13 the decreasing trend of diesel selectivity over a long period time of reaction implies that the cracking reaction can cause light hydrocarbon.

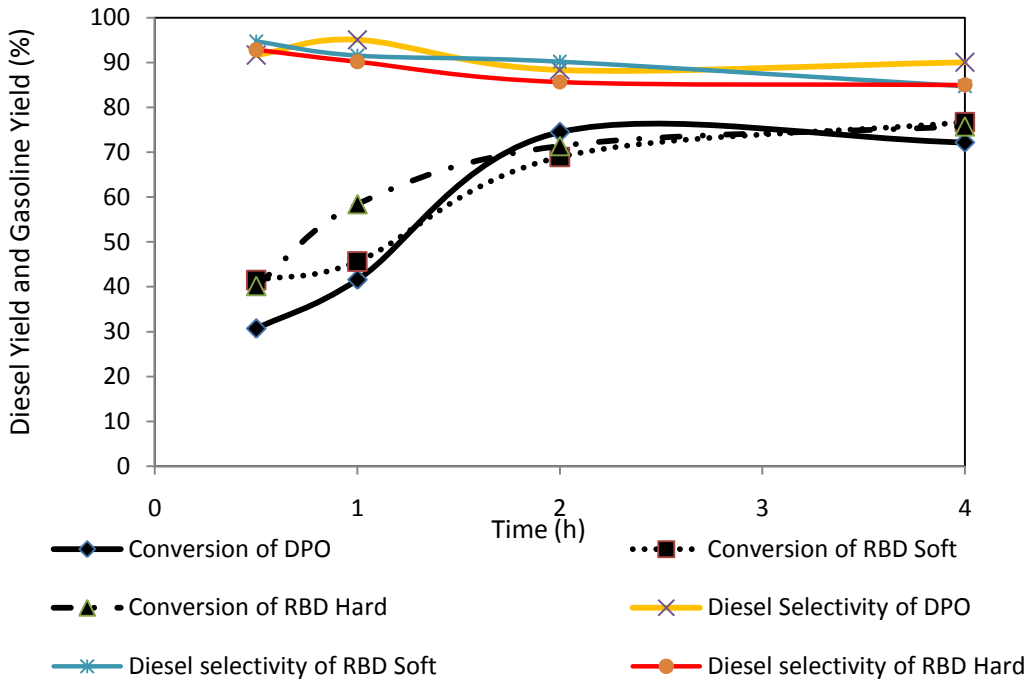

Figure 5.12 Time effect on diesel conversion and diesel selectivity. All experiment were perform at P=50 bar, NiMo/Al_2O_3 sulfided catalyst and reaction temperature at 390°C.

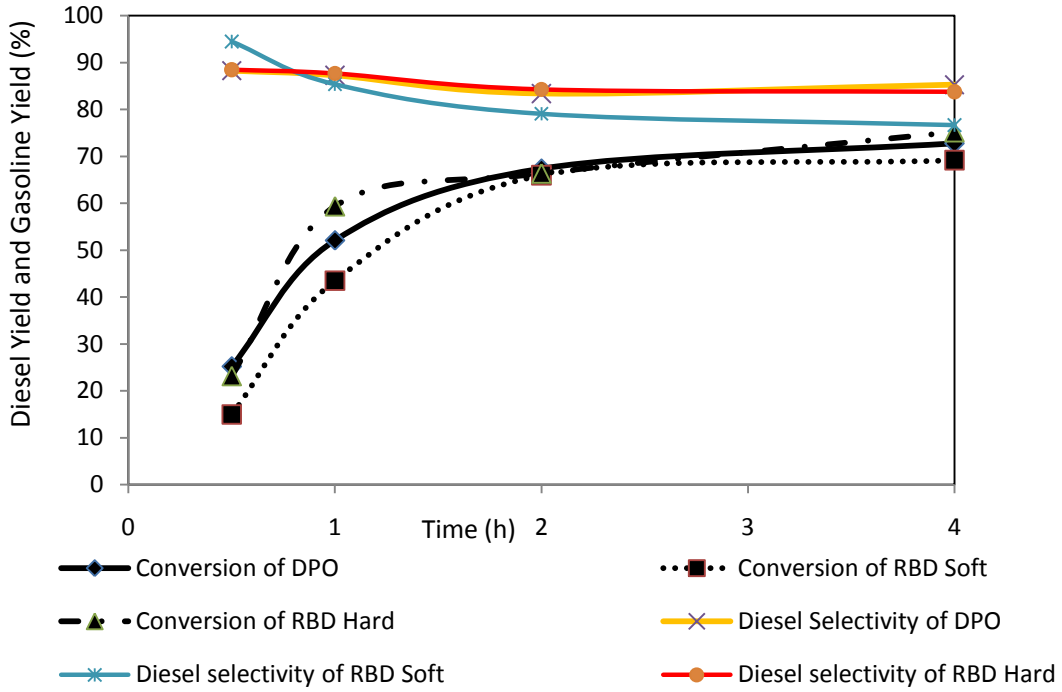

Figure 5.13 Time effect on diesel conversion and diesel selectivity. All experiment were perform at P=50 bar, $CoMo/Al_2O_3$ sulfided catalyst and reaction temperature at 390°C.

5.3.2 Influence of feed composition.

The main compositions of all feed are mostly palmitic acids (C16:0) and Oleic acids (C18:1) as shown in figure 5.14. The studies of hydroprocessing have shown the product alkanes contain equivalent or one less carbon than the parent fatty acids. The renewable diesel product composition of vegetable oil hydroprocessing reaction can thereby be roughly estimated based on the fatty acids composition of the feed. However, depending on the chain length and degree of saturation of the vegetable oil, some differences have been observed in the product yields (Filho et al., 1992). Y.B. Che Man and co-worker were determined that RPS palm stearin has similar triglycerides composition of crude palm oil as further explaining on the chapter 2. RPS palm stearin has small amount of free fatty acid contain than degummed palm oil via the neutralization step in the refining process (Haslenda, 2011).

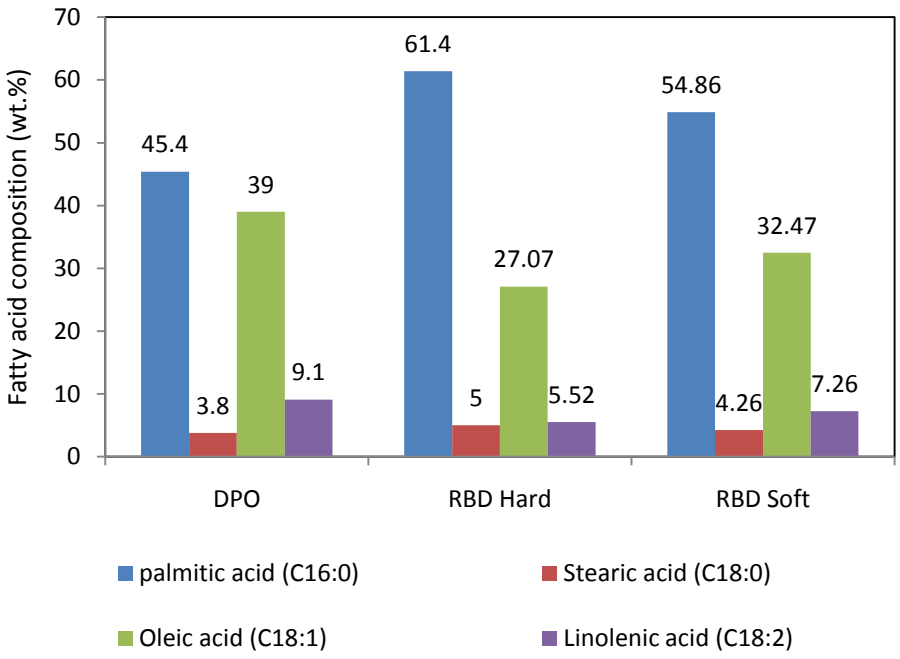

Figure 5.14 Fatty acid compositions of various feeds.

Figure 5.15A showing at reaction temperature of 360°C, the DPO has lower conversion and diesel yield than RPS soft and hard stearin. While the reaction temperature at 390°C and reaction time 4 hour in figure 5.15B, the diesel yield and conversion of DPO are higher and become comparable to the RPS soft and hard stearin. At the reaction temperature of 390°C with 2 hour of reaction time has the maximum conversion and diesel yield of DPO as show in figure 5.15C which explain that the DPO use high reaction temperature for converting the reactant because of many of impurity than those of RPS stearin. The gasoline yield is increase when the reaction temperature increased as shown in the figure 5.15A, B and C.

For CoMo sulfided catalyst in figure 5.16A, the conversion of DPO is nearly the same as the conversion of RPS hard stearin at the reaction temperature of 360°C with 4 hour of reaction time. At 390°C of reaction temperature, DPO show higher conversion than those of RPS stearin which this condition (390°C, 50bar and 4 hour) of all feedstocks has the maximum diesel yield. In case of gasoline range (C5-C11), the increasing of reaction temperature effected to increase of the gasoline yield.

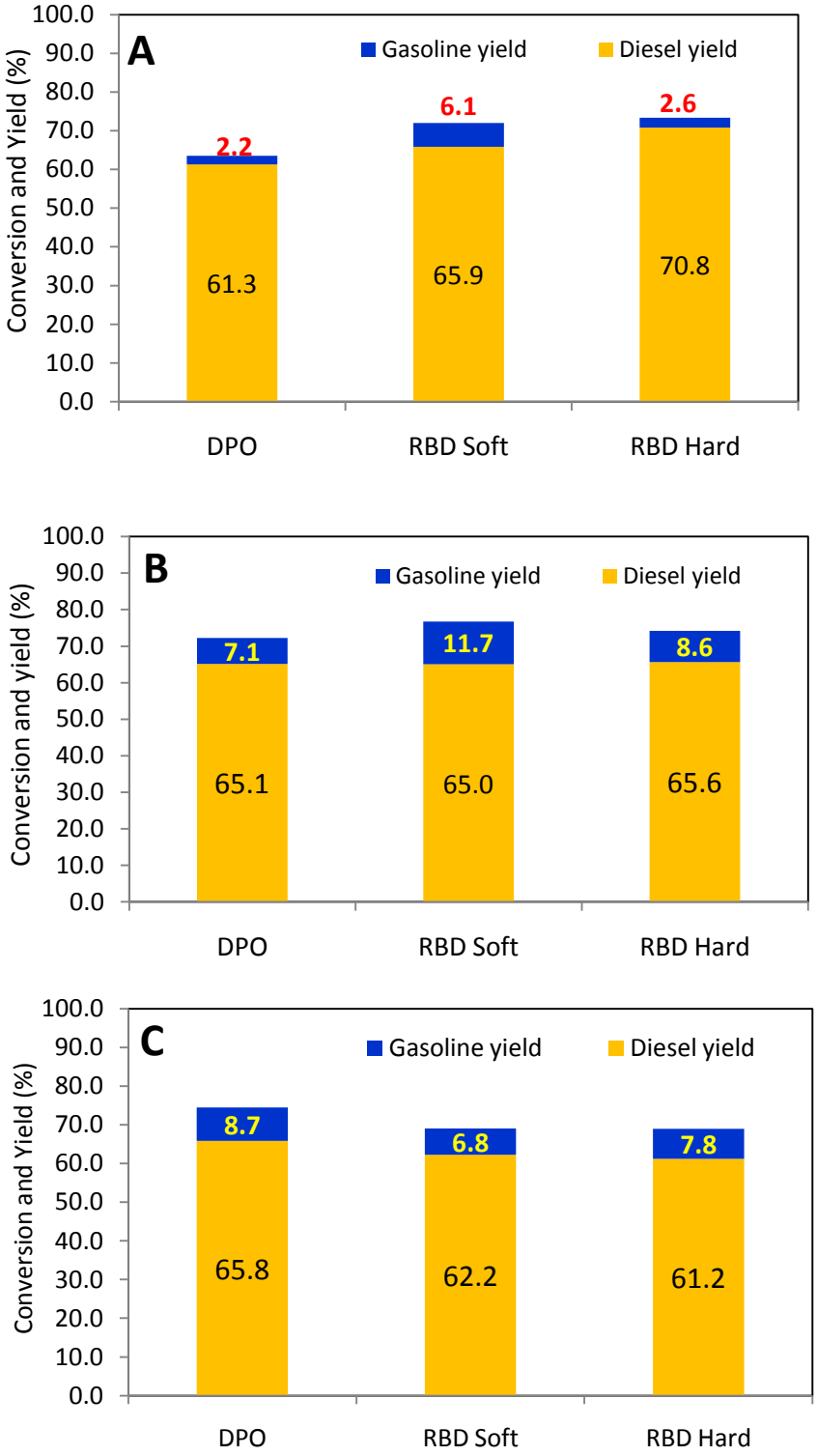

Figure 5.15 The conversion, diesel yield and gasoline yield of various feed stocks of NiMo sulfided catalysts. (Figure 5.15A. 360°C 50 bar 4 hours, Figure 5.15B 390°C 50bar 4hour and Figure 5.15C 390°C 50bar 2hour)

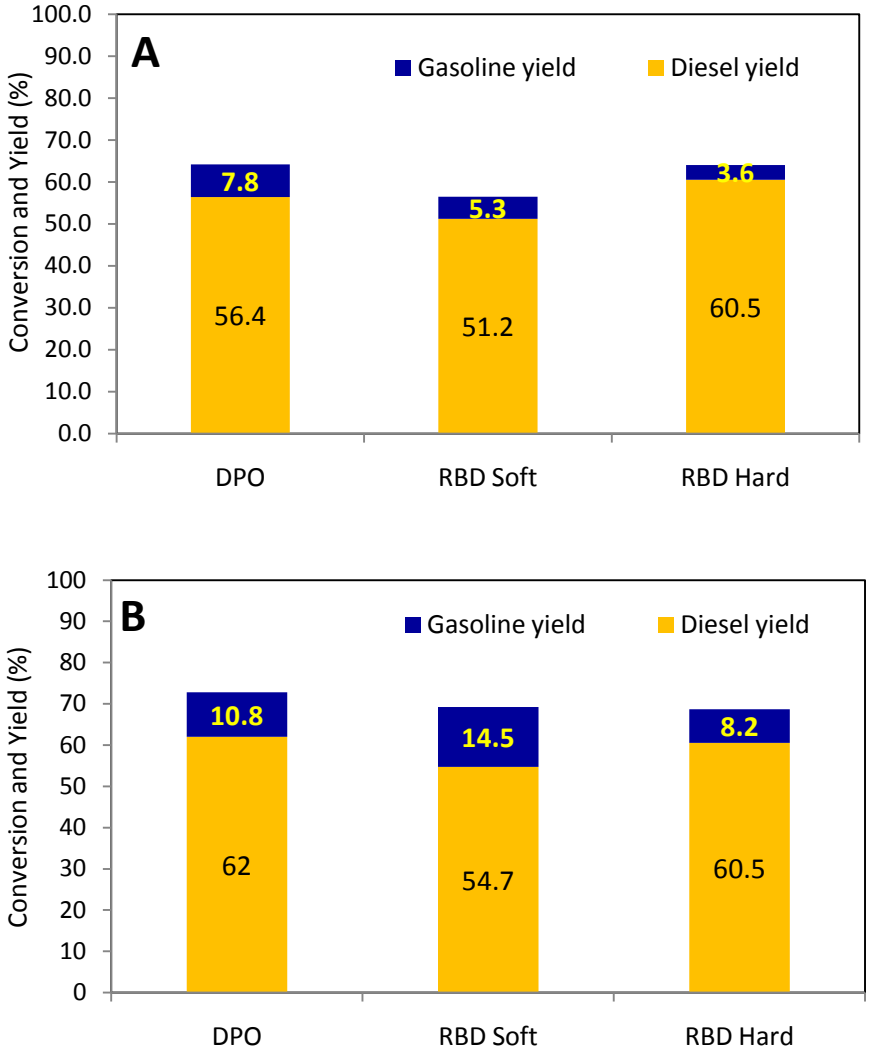

Figure 5.16 The conversion, diesel yield and gasoline yield of various feed stocks of CoMo sulfided catalysts. (Figure 5.15A. 360°C 50 bar 4 hours and Figure 5.15B 390°C 50bar 4hour)

Table 5.6 The optimum value of various feeds and catalysts.

	$NiMo/Al_2O_3$ sulfided			**$CoMo/Al_2O_3$ sulfided**		
	DPO	RPS Soft	RPS Hard	DPO	RPS Soft	RPS Hard
Temperature(°C)	390	360	360	390	390	390
Time (h)	2	4	4	4	4	2
Conversion (%)	74.5	69	73.4	72.8	69.2	66.4
Diesel selectivity (%)	88.4	91.1	96.5	85.3	79.1	87.7
Diesel yield (%)	65.8	65.9	70.8	62	54.7	63.3
GSL selectivity (%)	11.6	8.9	3.5	14.9	20.9	12.3
GSL yield (%)	8.7	6.1	2.6	10.8	14.5	8.2

As concluded in the above table, the optimum of process condition at the highest desirable product (diesel yield), the value were shown in table 5.6. For NiMo sulfided catalyst, the optimum of reaction temperature at 390°C with 2 h of DPO and reaction temperature 360°C with 2 h of RPS palm soft and hard stearin is 65.8%, 65.9% and 70.8% respectively. For used of CoMo sulfided catalysts at 390°C of reaction temperature of RPS palm hard stearin with 2 h, DPO and RPS palm soft stearin with 4 h was observed to reach the optimum of desired product. RPS hard has always the highest of diesel selectivity and diesel yield indicating that higher degree of saturation high diesel selectivity of the liquid product.

5.3.3 Influence of catalyst

As a carbon number of the fatty acids of the triglycerides was mainly 16 and 18 in the applied feedstocks (and it is know that the several feedstocks do not contain C15 and C17 fatty acids) that is why we present only the results which were obtained from the investigation of the deoxygenation ratio by reduction and decarboxylation/decarbonylation (so C15/C16 and C17/C18 paraffin ratio)

The hydrotreated of NiMo sulfided catalyst were show the activity for hydrodeoxygenation route that resulted alkane product had the same carbon as the parent fatty acids or triglycerides (Donnis et al., 2009). The C_{n-1}/C_n for NiMo sulfided catalyst is less than 1 but in the batch reactor with limited mole of hydrogen in the reactor can lead to another route such as decarboxylation and decarbonylation reaction. The show of drop in hydrogen pressure was observed by Veriansyah and co-worker explained the double bonds that were present in the triglycerides and fatty acids were saturated with hydrogen at this step. Figure 5.17A indicated the ratio of C_{15}/C_{16} which explaining that NiMo sulfided catalyst has the activity for deoxygenation reaction than for decarboxylation and decarbonylation as followed by the lower C_{15}/C_{16} ratio in NiMo sulfided catalyst than CoMo sulfided catalyst. In figure 5.16A and figure 5.16B, DPO is shown C_{n-1}/C_n less than 1 which is hydrodeoxygenation pathway occurs via hydrotreating of DPO on NiMo sulfided catalyst (Veriansyah et al., 2012). Pathways of decarboxylation and decarbonylation may show when C_{n-1}/C_n more than 1 as indicated for RPS soft and RPS hard stearin which C_{n-1}/C_n of RPS Soft is more than the C_{n-1}/C_n of RPS hard for all catalysts. From the resulting, RPS Soft can occur the decarboxylation and decarbonylation pathways because use more hydrogen to hydrogenate the unsaturated molecule in their component bring to insufficient of hydrogen for hydrodeoxygenation pathway. The saturation of feed can lead to high C_{n-1}/C_n as in RPS soft than RPS hard since RPS hard was more saturated components than RPS soft.

The effect of CoMo sulfided catalyst was shown in figure 5.17B. RPS soft shows high C_{n-1}/C_n ratio is due to high odd carbon number of alkanes products from decarboxylation and decarbonylation as CoMo sulfided catalyst favor or causing from cracking of even carbon number of alkane products as favor cracking activity of CoMo sulfided catalyst. For ratio more than 1 of DPO and RPS hard are due to selective occur decarboxylation and decarbonylation pathways of CoMo sulfided catalyst and/or less surplus of hydrogen in the reactor after hydrogenated unsaturated molecules

G.M. da Rocha Filho et al observed that the decarboxylation process can either thermal or catalytic, where as the deoxygenation is only a catalytic process. Figure 5.18A and figure 5.18B are confirming that increase the reaction temperature increase of C_{n-1}/C_n ratio for CoMo sulfided catalyst. There is not clearly trend to explanation for NiMo sulfided catalyst which could be an influence of catalytic process.

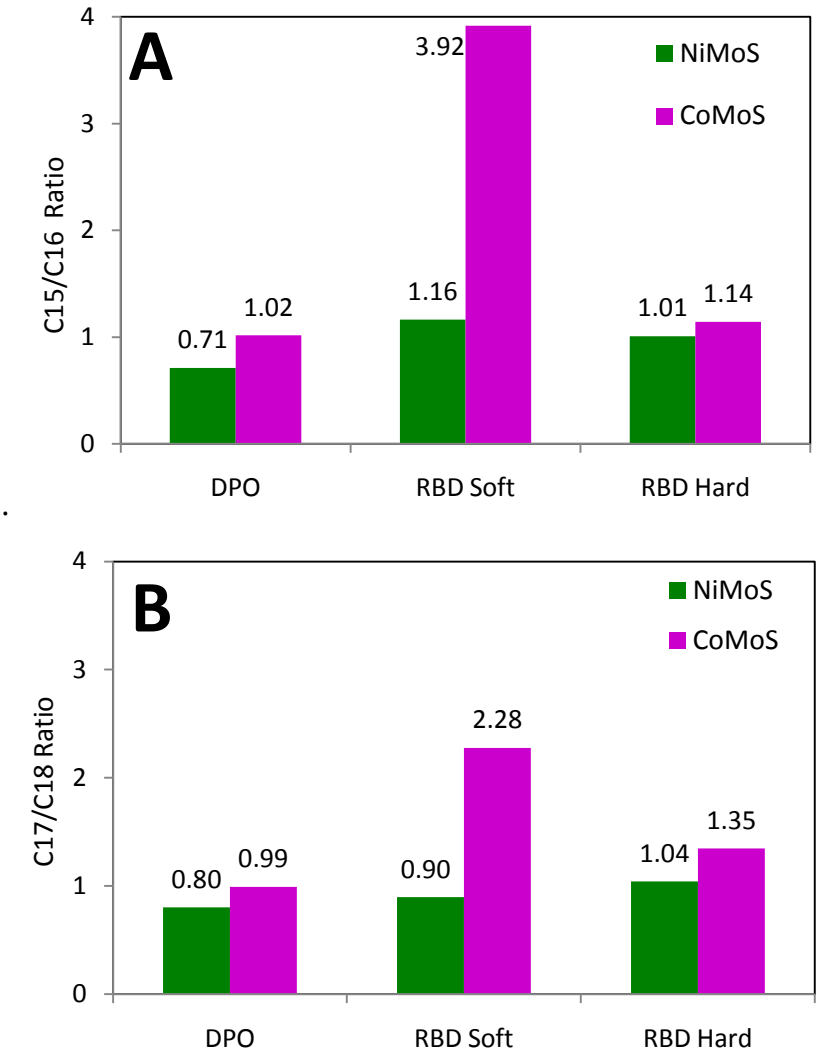

Figure 5.17A Ratios of C_{15}/C_{16} and **B.** Ratio of C_{17}/C_{18} to study of catalyst effect (360 °C 50 bar 4h).

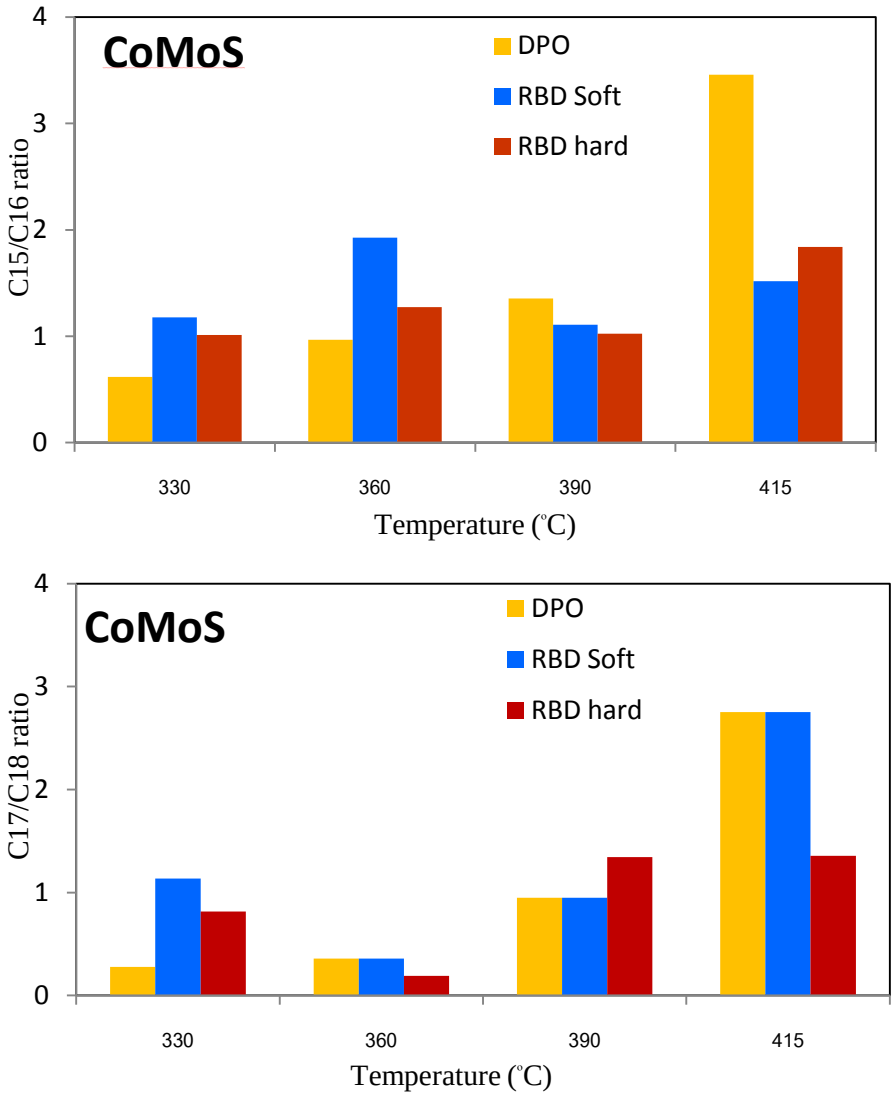

Figure 5.18A Ratios of C_{15}/C_{16} and **B** Ratios of C_{17}/C_{18} for effect of temperature to CoMo catalyst (50 bar with 4h).

5.3.4 FTIR spectra of product

FTIR was used to estimate the unconverted carboxyl groups, which are present in tri-, di-, and monoglycerides of feed. By increasing temperature of the reaction, the intensity of the stretching peak (at about 1740 cm^{-1}) corresponding to the carboxyl group continues to decrease as shown in figure 5.19. Observing that intensity of the stretching peak of acid groups (at about 1708 cm^{-1}) occur at 330°C was disappeared at high temperature range because it converted faster than triglyceride molecules. Following by Veriansyah et al investigation, first drop of hydrogen due to saturated double bond in the fatty acids and triglycerides after that hydrogenated triglyceride degraded into various intermediates was followed by the conversion of the intermediates into deoxygenated products. Figure 5.20 shows clearer the converted step of triglyceride and fatty acid as the effect of reaction time. Starting with the RPS soft has the intensity at 1742.5 cm^{-1} corresponding to triglycerides, at 0.5 hours of reaction time appeared the intensity of acid group at 1707.2 cm^{-1}, which explained by the degraded of triglyceride molecule. After passed through first hour of the reaction, the intensity of acid was disappeared specifying at that time fatty acid completely converted.

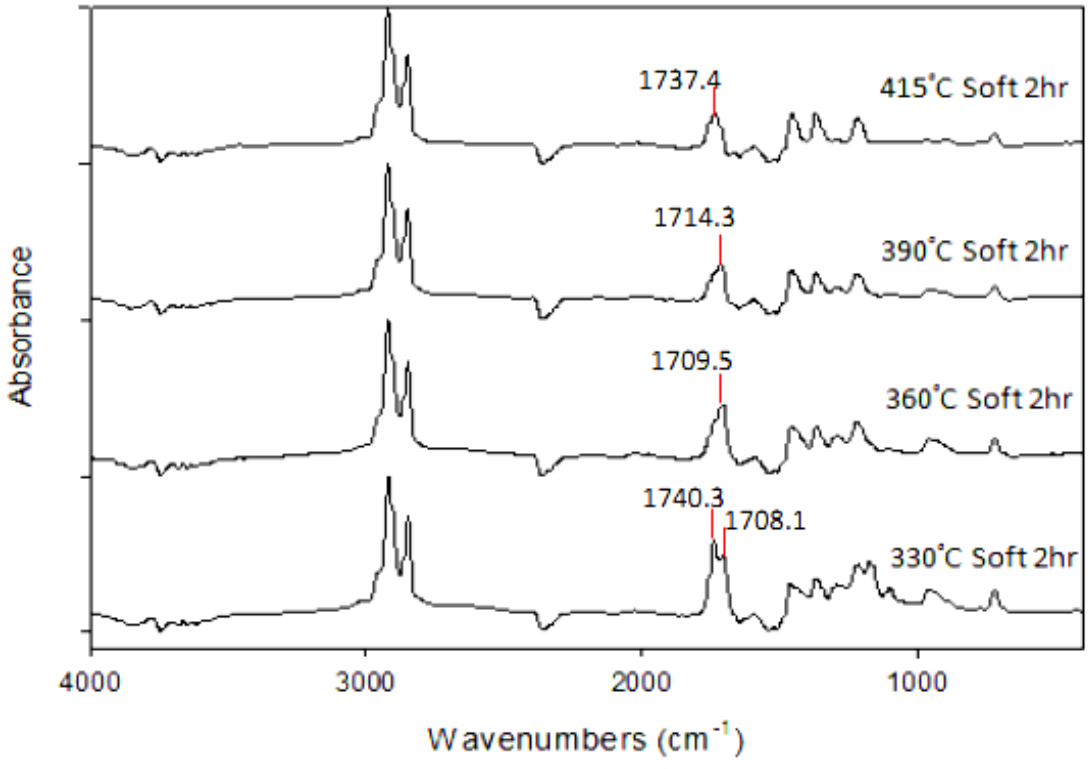

Figure 5.19 FTIR spectra of product of RPS soft stearin of 2 hours and NiMo sulfided catalyst.

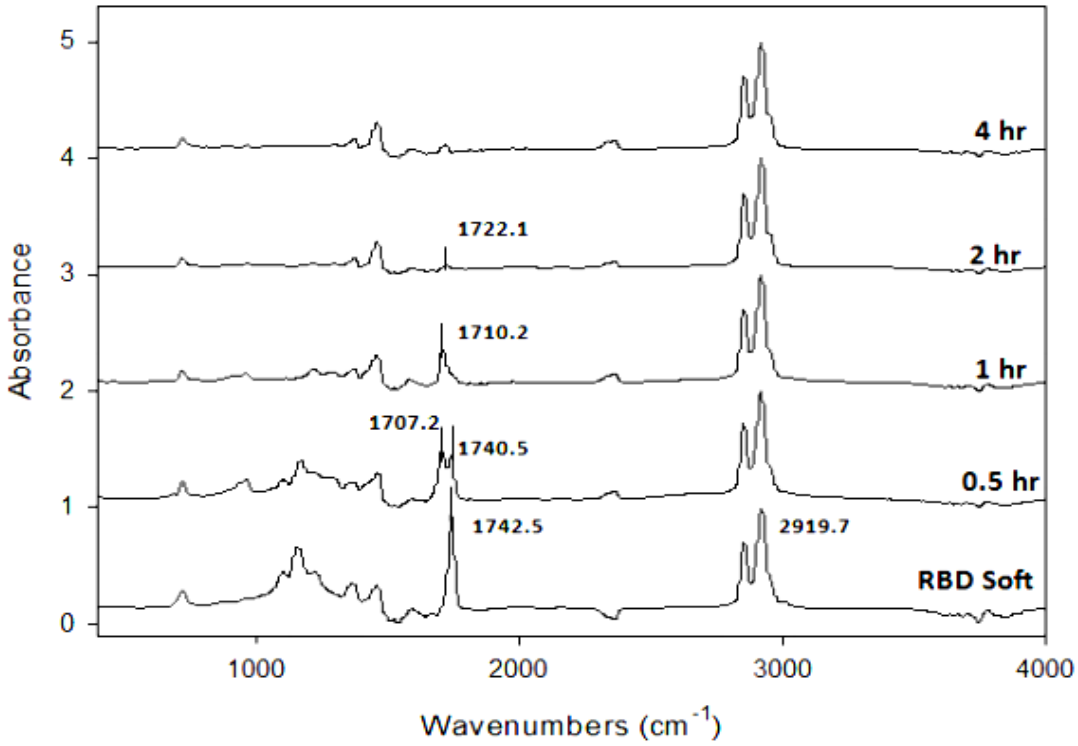

Figure 5.20 FTIR spectra of product of RPS soft stearin 360°C 50bar on CoMo sulfided catalyst.

CHAPTER VI

CONCLUSIONS AND RECOMMENDATIONS

6.1 Conclusions

Production of biodiesel can help in tackling the increasing greenhouse gas emissions from transportation and diminish the depletion of fossil fuel. Hydroprocessing of RPS palm stearin is an effective and promising process for the production of biodiesel. The hydroprocessing is occurs via the several pathways. The first step is the saturation of double bonds in the triglycerides molecule then saturated triglycerides molecule is hydrogenated and cracked to C15 or C17 compound depending on the chain length of the triglyceride molecule. The step of hydrogenated is provided into three reaction pathways: deoxygenation, decarboxylation and decarbonylation.

The optimum process condition for biodiesel production via hydroprocessing of degummed palm oil with reaction temperature of 390°C, hydrogen pressure of 50 bar, reaction time of 2 h and NiMo sulfided catalyst was observed to maximize the diesel yield. Refined bleached deodorized palm soft and hard stearin shows the same condition in maximum diesel yield of 360°C, hydrogen pressure of 50 bar, reaction time 4 h and NiMo sulfided catalyst. The process condition suggests that CoMo sulfided catalyst at maximum diesel yield is reaction temperature of 390°C, hydrogen pressure of 50 bar and reaction time of 4 h for DPO, RPS soft and RPS hard. The highest gasoline yield is found at maximum temperature (415°C) for all kind of feedstocks.

In conclusion, this work indicates the effect of temperature, time of reaction, different feed composition and catalyst for hydroprocessing of DPO, RPS soft and RPS hard. The effect of temperature for the conversion is shown that increasing temperature of reaction increase the conversion, which the highest conversion of DPO, RPS soft and RPS hard are 63.6%, 69% and 73.4% respectively. At low temperature NiMo sulfided catalyst show much higher activity than CoMo sulfided catalyst but CoMo sulfided catalyst become comparable at high temperature. The

study of reaction time observed that long period of reaction time lead to the decreases in diesel yield, which the highest diesel selectivity for DPO, RPS soft and RPS hard are at 2 h of the reaction time. Highest trend of diesel selectivity is found in the hydroprocessing of RPS hard. NiMo sulfided catalyst promotes the hydrodeoxygenation reaction while CoMo sulfided catalyst promotes higher decarboxylation and decarbonylation. Since hydrodeoxygenation is the catalytic process while hydrodecarboxylation and hydrodecarbonylation are thermal and catalytic process (Filho et al, 1992)

6.2 Recommendations

1. Develop the reactor or add more design to perform the study of pressure effect.
2. Modify the reactor to become a semi batch, in order to increase more hydrogen to last through the length of the reaction, for more study of deoxygenation reaction.
3. Study with gas products to minimized the effect of side reaction.
4. Use FTIR to indicate the amount of converted triglycerides.

REFERENCES

A.P.E. York, J.B. Claridge, V.C. Williams, A.J. Brungs, J. Sloan, A. Hanif, H. Al-Megren, M.L.H. Green., Synthesis of high surface area transition metal carbide catalysts. Surface Science and Catalysis 130 (2000): 989-994.

A.J. Brungs., A.P.E. York, M.L.H. Green, Catal. Lett. 57 (1999): 65.

Alexander Guzman, Juan E. Torres, Laura P. Prada, Manuel L. Nunez., Hydroprocessing of crude palm oil at pilot plant scale. Catalysis Today 156 (2010): 38–43.

Arno de Klerk., Hydroprocessing peculiarities of Fischer–Tropsch syncrude. Catalysis Today 130 (2008): 439–445.

Artiwan Shotipruk, Mitsuru Sasaki, Motonobu Goto, Duangkamol Yujaroen., Esterification of palm fatty acid distillate (PFAD) in supercritical methanol: Effect of hydrolysis on reaction reactivity. Fuel 88 (2009): 2011–2016

Badoga Sandeep, K. Chandra Mouli, Kapil K.Soni, A.K. Dalai, J. Adjaye., Beneficial influence of EDTA on the structure and catalytic properties of sulfided NiMo/SBA-15 catalysts for hydrotreating of light gas oil. Applied CatalysisB: Environmental 125 (2012): 67-84

B.C. Gates, J.R. Katzer, and G.C.A. Chuit., Chemistry of catalytic Processes. New York: McGraw-Hill, 1979.

B. Diaz, S. J. Sawhill, D. H. Bale, R. Main, D. C. Phillips, S. Korlann, R. Self and M. E. Bussell., Hydrodesulfurization over supported monometallic, bimetallic and promoted carbide and nitride catalysts. Catalysis Today 86 (2003): 191–209.

B. Donnis, R.G. Egeberg, P. Blom, and K.G. Knudsen., Hydroprocessing of Bio-Oils and Oxygenates to Hydrocarbons Understanding the Reaction Routes, Top Catalyst (2009) 52:229–240.

Berrebi G., Process for presulfurizing with phosphorous and/or halogen additive. US Patent 4 (1991).

Berrebi G., Process of presulfuration of hydrocarbon processing catalyst and catalyst produced by the process. US Patent 5 (1992)

Bezergianni Stella, Aggeliki Kalogianni., Hydrocracking of used cooking oil for biofuels production. Bioresource Technology 100 (2009): 3927-3932.

Bezergianni Stella, Aggeliki Kalogianni, Athanasios Dimitriadis., Catalyst evaluation for waste cooking oil hydroprocessing. Fuel 93(2012): 638-641.

Bhatti, H.N., Hanif, M.A., Qasim, M., Rehman, A.U., Biodiesel from waste tallow. Fuel 87(2008): 2961–2966.

C. Chang, S. Wan., China's motor fuel from tung oil, Industrial and Engineering Chemistry 39 (1947): 1543–1548.

Canakci, M., van Gerpen, J., 2001. Biodiesel production from oils and fats with high free fatty acids. Trans. ASAE 44 (6)(2001): 1429–1436.

Centeno A, Laurent E, Delmon B., Influence of the support of CoMo sulfide catalysts and of the addition of potassium and platinum on the catalytic performances for the hydrodeoxygenation of carbonyl, carboxylic and guaiacol-type molecules. Catalyst 154(1995): 288–98.

Craig, K.W., Sorevan, W.D., Production of hydrocarbons with a relatively high cetane rating. US 4(1991): 992,605.

C.W. Colling, and L.T. Thompson., The structure and function of supported molybdenum nitride hydrodenitrogenation catalysts. Journal of Catalysis. 146 (1994) 193-203.

D.C. Villalanti, J.C. Raia, and J.B. Maynard., High-temperature Simulated Distillation Applications in Petroleum Characterization. Encyclopedia Analytical Chemistry R.A. Meyers (Ed.) pp. 6726-6741@John Wiley&Sons Ltd, Chicherter, 2000.

Danuthai T, Jongpatiwut S, Rirksomboon T, Osuwan S, Resasco DE. Conversion of methylesters to hydrocarbons over an H-ZSM5 zeolite catalyst. Appl Catal A 361 (2009): 99–105.

Demirbas A., Progress and recent trends in biodiesel fuels. Energy Convers Manage 50 (2009):14–34.

Dennis Y.C. Leung, Xuan Wu, M.K.H. Leung., A review on biodiesel production using catalyzed transesterification. Applied Energy 87 (2010): 1083–1095.

D.J. Sajkowski, and S.T. Oyama., Catalytic hydrotreating by molybdenum carbide and nitride: unsupported Mo_2N and Mo_2C/Al_2O_3. Applied Catalysis A: 134 (1996): 399-349.

Dufresne P., B. Legall, G. Berrebi., Process for the presulphurization of hydrocarbon treatment catalysts. US Patent 5 (1995)

Dufresne P., F. Labruyere, Ex-siyu presulfuration in the presence of hydrocarbon molecule. US Patent 6 (2002).

Dumeignil Franck, Hiroshi Amano, Danhong Wang, Eika W. Qian, Atsushi Ishihara, Toshiaki Kabe., Study of the sulfidation process of CrO_3–Al_2O_3 hydrodesulfurization catalysts by a ^{35}S-labeled H_2S pulse tracer method., Applied Catalysis A: General 249 (2003): 255–263.

D.Yu. Murzin, M. Sna˚re, I. Kubicˇkova´, P.Ma¨ki-Arvela, D. Chichova, K. Era¨nen., Catalytic deoxygenation of unsaturated renewable feedstocks for production of diesel fuel hydrocarbons. Fuel 87 (2008): 933–945.

Do PT, Chiappero M, Lobban LL, Resasco DE. Catalytic deoxygenation of methyl-octanoate and methyl-stearate on Pt/Al_2O_3. Catal Lett 130 (2009): 9–18.

E. Laurent, B. Delmon., Deactivation of a Sulfided NiMo/γ-Al_2O_3 during the Hydrodeoxygenation of Bio-Oils: Influence of a High Water Pressure. Applied Catalyst A: General 109 (1994): 97–115.

Fernando S, Hall C, Jha S., NO_x reduction from biodiesel fuels. Energy Fuels 20 (2006): 376–382.

Ferrari M, Maggi R, Delmon B, Grange P., Influence of the hydrogen sulfide partial pressure and of a nitrogen compound on the hydrodeoxygenation activity of a CoMo/carbon catalyst. Catalyst 198(2001): 47–55.

Ferrari M, Bosmans S, Maggi R, Delmon B, Grange P., CoMo/Carbon hydrodeoxygenation catalysts: influence of the hydrogen sulfide partial pressure and of the sulfidation temperature. Catalyst Today 65 (2001): 257–64.

Filho G.N. da Rocha, D. Brodzki, G. Djega-Mariadassou., Formation of alkanes, alkylcycloalkanes and alkylbenzenes during the catalytic hydrocracking of vegetable oils. (1992).

Franco A, Diaz AR., The future challenges for ‘‘clean coal technologies’’: joining efficiency increase and pollutant emission control. Energy 34 (2009):348–354.

Ghadge, S.V., Raheman, H., Biodiesel production from mahua (Madhuca indica) oil having high free fatty acids. Biomass Bioenergy 28(2005): 601–605.

Gusmao, J., Brodzki, D., Djéga-Mariadassou, G., Frety, R., Utilization of vegetable oils as an alternative source for diesel-type fuel: hydrocracking on reduced Ni/SiO_2 and sulphided Ni-Mo/c -Al_2O_3. Catalysis Today 5(1989): 533–544.

G.N. da Rocha Filho D.N, Bentes M.H.S, Brodzki D, Djega-Mariadassou G, Catalytic conversion of Hevea brasiliensis and Virola sebifera oils to hydrocarbon fuels. Journal of the American Oil Chemists' Society 69-(3) (1992): 266–271.

G.N. da Roch Filho G.N, Brodzki D, Djéga-Mariadassou G., Formation of alkanes, alkylcycloalkanes and alkylbenzenes during the catalytic hydrocracking of vegetable oils. Fuel 72 (4) (1993), 543–549.

H.C. Ong, T.M.I. Mahlia, H.H. Masjuki and R.S. Norhasyima., Comparison of palm oil, Jatropha curcas and Calophyllum inophyllum for biodiesel: A review. Renewable and Sustainable Energy Reviews 15 (2011): 3501– 3515.

Haslenda H., Industry to Industry By-products Exchange Network towards zero waste in palm oil refining process. (2011).

H. Haslenda, M.Z. Jamaludin., iIndustry to Industry By-products Exchange Network towards zero waste in palm oil refining processes. Resources, Conservation and Recycling 55 (2011): 713–718

H.O. Pierson., Handbook of Refractory Carbides and Nitrides. Noyes Publ., Westwood, NJ, USA 1996.

Hancsók J, Krár M, Magyar S, Boda L, Holló A, Kalló D. Investigation of the production of high cetane number bio gas oil from pre-hydrogenated vegetable oils over Pt/HZSM-22/Al_2O_3. Micropor Mesopor Mater 101 (2007): 148–52.

Hodge C. California Energy Commission, workshop on bioenergy, 9 March 2006.

Huber G.W, O'Connor P, Corma A., Processing biomass in conventional oil refineries: production of high quality diesel by hydrotreating vegetable oils in heavy vacuum oil mixtures. Applied Catalysis A: General 329 (2007): 120–129.

Immer Jeremy G., M. Jason Kelly, H. Henry Lamb., Catalytic reaction pathways in liquid-phase deoxygenation of C18 free fatty acids. Applied Catalysis A: General 375 (2010): 134–139.

J. Walendziewski, M. Stolarski, R. Luzny, and B. Klimek., Hydroprocesssing of light gas oil- rape oil mixtures. Fuel Processing Technology 90 (2009): 686–691.

Jacques Monnier, Hardi Sulimma, Ajay Dalai, Gianni Caravaggio., Hydrodeoxygenation of oleic acid and canola oil over alumina-supported metal nitrides. Applied Catalysis A: General 382 (2010): 176–180.

Jeno Hancsók, Márton Krár, Sándor Kovács, Dénes Kalló., Fuel purpose hydrotreating of sunflower oil on $CoMo/Al_2O_3$ catalyst. Bioresource Technology101(2010): 9287–9293.

Jitendra K., Satyarthi and Darbha Srinivas., Fourier Transform Infrared Spectroscopic Method for Monitoring Hydroprocessing of Vegetable Oils to Produce Hydrocarbon-Based Biofuel. Energy & Fuels article.

Jozef Mikulec ‚Ja´ n Cvengrosˇ, Lˇ udmila Jorı´ kova´, Marek Banicˇ, Andrea Kleinova., Second generation diesel fuel from renewable sources. Journal of Cleaner Production 18 (2010): 917–926.

K. Othmer., Encyclopedia of chemical technology. Vol 6. 4th ed. New York: A Wiley Interscience Publication, John Wiley&Son, 1991.

Kamm B, Gruber P.R, Kamm M., Biorefinery Industrial Processes and Products. Status and Future Direction, vols. 1 and 2.Wiley-Verlay Gmbtt and Co KGaA, Weinheim (2006).

Kaluza L., D. Gulkova ´,Z.Vı ´t, M. Zdraz ˇil., Effect of support type on the magnitude of synergism and promotion in CoMo sulphide hydrodesulphurisation catalyst. Applied Catalysis A General 324 (2007): 30-35.

Kobayashi K, Yamaguchi E., Artificial petroleum from fish oils. Journal Chemical Industries Japan 24 (1921): 1399–420.

Kojima R, Aika KI., Molybdenum nitride and carbide catalysts for ammonia synthesis. Applied Catalyst A: General 219 (2001):141–147.

Krár, M., Thernesz, A., Tóth, Cs., Kasza, T., Hancsók, J., Investigation of catalytic conversion of vegetable oil/gas oil mixtures. In: Halász, I. (Ed.), Silica and Silicates in Modern Catalysis. Trans world Research Network, Kerala, India, (2010): 435–455.

Kubicˇka D, Šimácˇek P, Kolena J, Lederer J, Šebor G. Catalytic transformations of vegetable oils into hydrocarbons. In: ICP2007 proceedings–43rd international petroleum conference, Bratislava, Slovakia; 2007. p. 1–7.

Kubicˇka D, Kaluzˇa L. Deoxygenation of vegetable oils over sulfided Ni, Mo and NiMo catalysts. Appl Catal A 372 (2010): 199–208.

Kubicˇka D, Bejblová M, Vlk J. Conversion of vegetable oils into hydrocarbons over CoMo/MCM-41 catalysts. Top Catal 53 (2010): 168–78.

Kumar R, Rana B.S, Tiwari R, Verma D, Kumar R, Joshi R.K, Garg M.O, Sinha A.K., Hydroprocessing of jatropha oil and its mixtures with gas oil. Green Chem 12 (2010): 2232–2239.

Lai Weikun, Liqing Pang, Jinbao Zheng, Juanjuan Li, ZhongfangWu, Xiaodong Yi, Weiping Fang, Lishan Jia., Efficient one pot synthesis of mesoporous NiMo–Al_2O_3 catalysts for dibenzothiophene hydrodesulfurization. Fuel Processing Technology 110 (2013): 8-16.

Leung, D.Y.C., Guo, Y., Transesterification of neat and used frying oil: optimization for biodiesel production. Fuel process. Technol. 87(2006): 883–890.

Leyva Carolina, Mohan S. Rana, Jorge Ancheyta., Surface characterization of Al_2O_3–SiO_2 supported NiMo catalysts: An effect of support composition. Catalysis Today 130 (2008): 345–353.

Li S, Lee JS, Hyeon T, Suslick KS., Catalytic hydrodenitrogenation of indole over molybdenum nitride and carbides with different structures. Applied Catalyst A: General 184 (1999):1–9.

Liu, Y., Sotelo-Boyás, R., Murata, K., Minowa, T., Sakanishi, K., 2009. Hydrotreatment of jatropha oil to produce green diesel over trifunctional Ni–Mo/SiO_2–Al_2O_3 catalyst. Chemistry Letters 38(2009): 552–553.

M. Stumborg, A. Wong, E. Hogan., Hydroprocessed vegetable oils for diesel fuel improvement, Bioresource Technology 56 (1996): 13–18.

Mailhe MA. Sur la décomposition catalytique de l‘huile de requin. Bull Soc Chim France 31 (1922): 249–52.

Man Y.B. Che, T. Haryati, H.M. Ghazali, B.A. Asbi., Composition and Thermal Profile of Crude Palm Oil and Its Products. JAOCS 76 (1999): 237-242.

Maria Carolina Sérgi Gomes, Pedro Augusto Arroyo, Nehemias Curvelo Pereira., Biodiesel production from degummed soybean oil and glycerol removal using ceramic membrane. Journal of Membrane Science 378 (2011): 453– 461.

Meena Marafi, Antony Stanislaus, Edward Furimsky., Handbook of Spent Hydroprocessing Catalysts, 2010: Pages 17-49

N. Laosiripojana, P. Mongkolbovornkij, V. Champreda, W. Sutthisripok., Esterification of industrial-grade palm fatty acid distillate over modified ZrO_2

(with WO_3 – ,SO_4 – and TiO_2 –): Effects of co-solvent adding and water removal. Fuel Processing Technology 91 (2010): 1510 –1516

Oleg V. Kikhtyanin, Anton E. Rubanov, Artem B. Ayupov, Gennadii V. Echevsky., Hydroconversion of sunflower oil on Pd/SAPO-31 catalyst. Fuel 89 (2010): 3085–3092.

Patil PD, Deng S., Optimization of biodiesel production from edible and non-edible vegetable oils. Fuel 88 (2009): 1302–1306.

Pavel Šimáčˇek, David Kubicˇka, Gustav Šebora, Milan Pospíšil., Fuel properties of hydroprocessed rapeseed oil. Fuel 89 (2010): 611–615.

Petrobras.[online].2009:http://www2.petrobras.com.br/ingles/ads/ads_Tecnologia.html [2 January 2011]

Priecel Peter, David Kubicka, Libor Capek, Zdenek Bastl, Petr Rysánek., The role of Ni species in the deoxygenation of rapeseed oil over NiMo-alumina catalysts. Applied Catalysis A: General 397 (2011): 127–137.

Q. Smejkal, L. Smejkalova, and D. Kubicka., Thermodynamic balance in reaction system of total vegetable oil hydrogenation. Chemical Engineering Journal 146 (2009): 155–160.

Rana Mohan S., J. Ancheyta, P. Rayo, S.K. Maity., Effect of alumina preparation on hydrodemetallization and hydrodesulfurization of Maya crude. Catalysis Today 98 (2004): 151–160.

R.C. Santana, P.T. Do, M. Santikunaporn, W.E. Alvarez, J.D. Taylor, E.L. Sughrue, and D.E. Resasco., Evaluation of different reaction strategies for the improvement of cetane number in diesel fuels. Fuel 85 (2006): 643-656.

Ramadhas, A.S., Jayaraj, S., Muraleedharan, C., Biodiesel production from high FFA rubber seed oil. Fuel 84(2005): 335–340.

Seamans J.D., J.G. Gasser., Method of presulfiding a hydrotreating catalyst. US Patent 4 (1990).

S. Bezergianni, and A. Kalogianni., Hydroprocessing of used cooking oil for biofuels production. Bioresource Technology 100 (2009): 3927-3932.

S.Bezergianni, A. Dimitriadis, A. Kalogianni, and P.A. Pilavachi., Hydrotreating of waste cooking oil for biodiesel production Part I: Effect of temperature on

product yields and heteroatom removal. Bioresource Technology 101 (2010): 6651–6656.

S.Bezergianni, A. Dimitriadis, T. Sfetsas, and A. Kalogianni., Hydrotreating of waste cooking oil for biodiesel production Part II: Effect of temperature on hydrocarbon composition. Bioresource Technology 101 (2010): 7658–7660.

S. Chongkhong, C. Tongurai, P. Chetpattananondh, C. Bunyakan., Biodiesel production by esterification of palm fatty acid distillate. Biomass and Bioenergy 31 (2007): 563 – 568.

S. Chongkhong, C. Tongurai, P. Chetpattananondh., Continuous esterification for biodiesel production from palm fatty acid distillate using economical process. Renewable Energy 34 (2009): 1059–1063

S.P. Santos, S.H. Santos, and S.P. Toledo., Standard transition aluminas. Electron microscopy studies. Materials Research 3, 4 (2000): 104-114.

S. Ramanathan, and S.T. Oyama., J. Phys. Chem. 99 (1995): 16365.

S.T. Oyama, G. Ertl, H. Knozinger, J. Wcitkamp., Handbook of Heterogeneous Catalysis, vol. 1, VCH, Verlagsgesellschaft mbH, Weinheim< Germany, 1997, p. 39.

S. Izhar, H. Kanesugi, H. Tominaga, and M. Nagai., Cobalt molybdenum carbides: Surface properties and reactivity for methane decomposition. Applied Catalysis A: General 317 (2007): 82–90.

S. Mikkonen., Second-generation renewable diesel offers advantages. Hydrocarbon Processing February (2008): 63–66.

Scherzer, J., Gruia, A.J., Hydrocracking Science and Technology. Marcel Dekker Inc., New York. (1996)

Sebos I, Matsoukas A, Apostolopoulos V, Papayannakos N., Catalytic hydroprocessing of cottonseed oil in petroleum diesel mixtures for production of renewable diesel. Fuel 2009(88):145–9.

Senol O, Viljava T, Krause A. Hydrodeoxygenation of aliphatic esters on sulphided NiMo/ ɣ-AlO and CoMo/ ɣ-AlO catalyst: the effect of water. Catalyst Today 106 (2005): 186–9.

Senol OI, Ryymin EM, Viljava T-R, Krause AOI. Reactions of methyl heptanoate hydrodeoxygenation on sulphided catalysts. Journal Molecular Catalyst A 268 (2007): 1–8.

Šimácek P, Kubicka D, Šebor G, Pospíšil M. Hydroprocessed rapeseed oil as a source of hydrocarbon-based biodiesel. Fuel 88 (2009): 456–60.

Šimácek Pavel, David Kubicka, Gustav Šebor, Milan Pospíšil., Hydroprocessed rapeseed oil as a source of hydrocarbon-based biodiesel. Fuel 88 (2009): 456–460.

Šimácek Pavel, David Kubicka., Hydrocracking of petroleum vacuum distillate containing rapeseed oil: Evaluation of diesel fuel. Fuel 89 (2010): 1508–1513.

Šimácek Pavel, David Kubicka, Gustav Šebor, Milan Pospíšil., Fuel properties of hydroprocessed rapeseed oil. Fuel 89 (2010): 611–615.

Šimácek Pavel, David Kubicka, Iva Kubicková, František Homola, Milan Pospíšil, Josef Chudoba., Premium quality renewable diesel fuel by hydroprocessing of sunflower oil. Fuel 90 (2011): 2473–2479.

Singh SP, Singh D., Biodiesel production through the use of different sources and characterization of oils and their esters as the substitute of diesel: a review. Renewable & Sustainable Energy Reviews 14(1) (2010): 200–216.

Sundaramurthy V., A.K. Dalai, J. Adjaye., Comparison of P-containing ɣ-Al_2O_3 supported Ni-Mo bimetallic carbide, nitride and sulfide catalysts for HDN and HDS of gas oils derived from Athabasca bitumen. Applied Catalysis A: General 311 (2006): 155–163.

Takuya Ito, Yusuke Sakurai, Yusuke Kakuta, Motoyuki Sugano, Katsumi Hirano., Biodiesel production from waste animal fats using pyrolysis method. Fuel Processing Technology 94 (2012): 47 – 52.

Tominaga H, Nagai M. Theoretical study of methane reforming on molybdenum carbide. Applied Catalyst A: General 328 (2007): 35–42.

Topsøe H, Clausen B. S, Massoth F. E, Hydrotreating Catalysis. Science and Technology. Springer-Verlag: Berlin, 1996.

V.Schwartz, S. T. Oyama, and J. G. Chen., Supported Bimetallic Nb-Mo Carbide: Synthesis, Characterization, and Reactivity. J. Phys. Chem. B (2000): 104 8800-8006

V.Sundaramurthy, A.K.Dalai, and J.Adjaye., Effect of phosphorus addition on the hydrotreating activity of NiMo/Al2O3 carbide catalyst. Catalysis Today 125 (2007): 239-247.

Veriansyah Bambang, Jae Young Han, Seok Ki Kim, Seung-Ah Hong, Young Jun Kim, Jong Sung Limb, Young-Wong Shu, Seong-Geun Oh, Jaehoon Kim., Production of renewable diesel by hydroprocessing of soybean oil: Effect of catalysts. Fuel 94 (2012): 578–585.

Veljkovic, V.B., Lakicevic, S.H., Stamenkovic, O.S., Todorovic, Z.B., Lazic, M.L., Biodiesel production from tobacco (Nicotiana tabacum L.) seed oil with a high content of free fatty acids. Fuel 85(2006): 2671–2675.

Viljava T.-R., R.S. Komulainen, A.O.I. Krause., Effect of H2S on the stability of $CoMo/Al_2O_3$ catalysts during hydrodeoxygenation. Catalysis Today 60 (2000): 83–92.

W. Kiatkittipong, S. Suwanmanee, N. Laosiripojana, P.Praserthdam and S. Assabumrungrat., Cleaner gasoline production by using glycerol as fuel extender. Fuel Processing Technology 91 (2010): 456–460.

X. Yang, and NJ. Edison., Stabilized flash calcined gibbsite as a catalyst support. United States: Patent Application Publication, 2007.

Yao Z, Shi C., Development of a catalytic cycle in molybdenum carbide catalyzed NO/CO reaction. Catalyst Lett 130 (2009): 239–45.

Zhou Zheng, Zhou, Sheng-Li Chen, Derun Hua, Ai-Cheng Chen, Zhi-Gang Wang, Jun-Hui Zhang, Jinsen Gao., Structure and activity of NiMo/alumina hydrodesulfurization model catalyst with ordered opal-like pores. Catalysis Communications 19 (2012): 5–9.

Zhu Xinli, Lance L. Lobban, Richard G. Mallinson, Daniel E. Resasco., Tailoring the mesopore structure of HZSM-5 to control product distribution n the conversion of propanal. Journal of Catalysis 271 (2010): 88–98.

APPENDICES

APPENDIX A

CALCULATION FOR CATALYST PREPARTION

Preparation of 2.5Ni10Mo/ γ-Al_2O_3 is shown as follows:

Calculation for the preparation of Nickel and Molybdenum loading catalyst for 2.5Ni10Mo

Example calculation for the preparation of 2.5Ni10Mo/ γ-Al_2O_3

Based on 100 g of catalyst used, the composition of the catalyst will be as follows:

Nickel	=	2.5 g		
Molybdenum	=	10 g		
Al_2O_3	=	100 – (2.5+10)	=	87.5 g

For 2 g of Al_2O_3

Weight of catalyst	=	2 × (100/87.5)	=	2.2857 g
Nickel required	=	2.2857 × (2.5/100)	=	0.0571 g

Nickel 0.0571 g was prepared from $Ni(NO_3)_2 \cdot 6H_2O$ and molecular weight of Ni is 58.6934 g/mol which molecular weight of $Ni(NO_3)_2 \cdot 6H_2O$ is 290.79.

$$Ni(NO_3)_2 \cdot 6H_2O \text{ required} = \frac{\text{MW of } Ni(NO3)2 \cdot 6H2O \times \text{Nickel required}}{\text{MW of Nickel}}$$

$$= (290.79/58.6934) \times 0.0571 = 0.2829g$$

For 10Mo from 2 g of Al_2O_3

Molybdenum required = $2.2857 \times (10/100)$ = 0.2285g

Molybdenum 0.2285 g was prepared from $(NH_4)_6Mo_7O_{24} \cdot 4H_2O$ molecular weight is 1,234.58 g/mol and molecular weight of Mo is 95.94 g/mol

$$NH_4)_6Mo_7O_{24} \cdot 4H_2O \text{ required} = \frac{\text{MW of } (NH4)6Mo7O24.4H2O) \times \text{Molybdenum required}}{\text{MW of Molybdenum}}$$

$$= (1{,}234.58 \times 0.2285)/(95.94 \times 7)$$

$$= 00.4200 \text{ g}$$

Preparation of 2.5Co10Mo/γ-Al_2O_3 is shown as follows:

Calculation for the preparation of Cobalt and Molybdenum loading catalyst for 2.5Co10Mo

Example calculation for the preparation of 2.5Co10Mo/γ-Al_2O_3

Based on 100 g of catalyst used, the composition of the catalyst will be as follows:

Cobalt = 2.5 g

Molybdenum = 10 g

Al_2O_3 = 100 - (2.5 + 10) = 87.5 g

For 2 g of Al_2O_3

Weight of catalyst = 2 × (100/87.5) = 2.2857 g

Cobalt required = 2.2857 × (2.5/100) = 0.0571 g

Cobalt 0.0571 g was prepared from $Co(NO_3)_2 \cdot 6H_2O$ molecular weight is 291.03 g/mol and molecular weight of Co is 58.93 g/mol

$$Co(NO_3)_2 \cdot 6H_2O \text{ required} = \frac{\text{MW of } Co(NO3)2 \cdot 6H2O \times \text{Cobalt required}}{\text{MW of Cobalt}}$$

= (291.03/58.93) × 0.0571 = 0.2819 g

Molybdenum required = 2.2857 × (10/100) = 0.2285 g

Molybdenum 0.2285 g was prepared from $(NH_4)_6Mo_7O_{24} \cdot 4H_2O$ molecular weight is 1,234.58 g/mol and molecular weight of Mo is 95.94 g/mol

$$NH_4)_6Mo_7O_{24} \cdot 4H_2O \text{ required} = \frac{\text{MW of } (NH4)6Mo7O24.4H2O) \times \text{Molyb denum required}}{\text{MW of Molybdenum}}$$

= (1,234.58 × 0.2285)/(95.94× 7)

= 00.4200 g

APPENDIX B

PROGRAM SIMULATED DISTILLATION OF GAS CHROMATOGRAPHY WITH FLAME IONIZATION DETECTOR

This appendix showed the program Simulated distillation (SimDist) for calculation of composition of hydrocarbon components in hydroprocessing reaction.

A flame ionization detector (FID) is used for detection and measurement of the hydrocarbon analytes. The result of SimDist analysis provides a quantitative percent mass yield as a function of boiling point of the hydrocarbon components of the sample. The chromatographic elution times of the hydrocarbons are calibrated to the atmospheric equivalent boiling point (AEBP) of the paraffins reference material. The SimDist method ASTM (American Society for Testing and Materials) D2887 covers the boiling range 55–538°C (100–1000°F) which covers the n-alkanes (n-paraffins) of chain length about C_5–C_{44}.

In this study, we used simulated distillation to analyze the temperature range of products following by ASTM-2887-D86 procedure. It was found, at temperature range of 250-380°C is a suitable for diesel range (n-C_{15}-n-C_{18}). Table B.1 – Table B.3 and Figure B.1 – Figure B.2 are shown conditions use in gas chromatography with flame ionization detector, chromatogram of calibration mixture reference and data analysis.

Table B.1 Conditions use in gas chromatography with flame ionization detector.

Parameters	**Condition**
Width	5 sec
Slope	2,000 uV/min
Drift	0 uV/min
T.DBL	1,000 min
Min.Area/Hight	10,000 counts
Quantitation	
Quantitative Method	Corrected Area Normalization
	External Standard
Calculated by	Area
# of Calib. Levels	1
Curve Fit Type	Liner
Unit	%(w/w)
X Axis of Calib. Curve	Conc.
Identification	
Window	5 %
Default Band Time	0.01 min
Identification Method	Absolute Rt
Peack Select	Closest Peak
Grouping	Not Used
Correction of RT	No Change

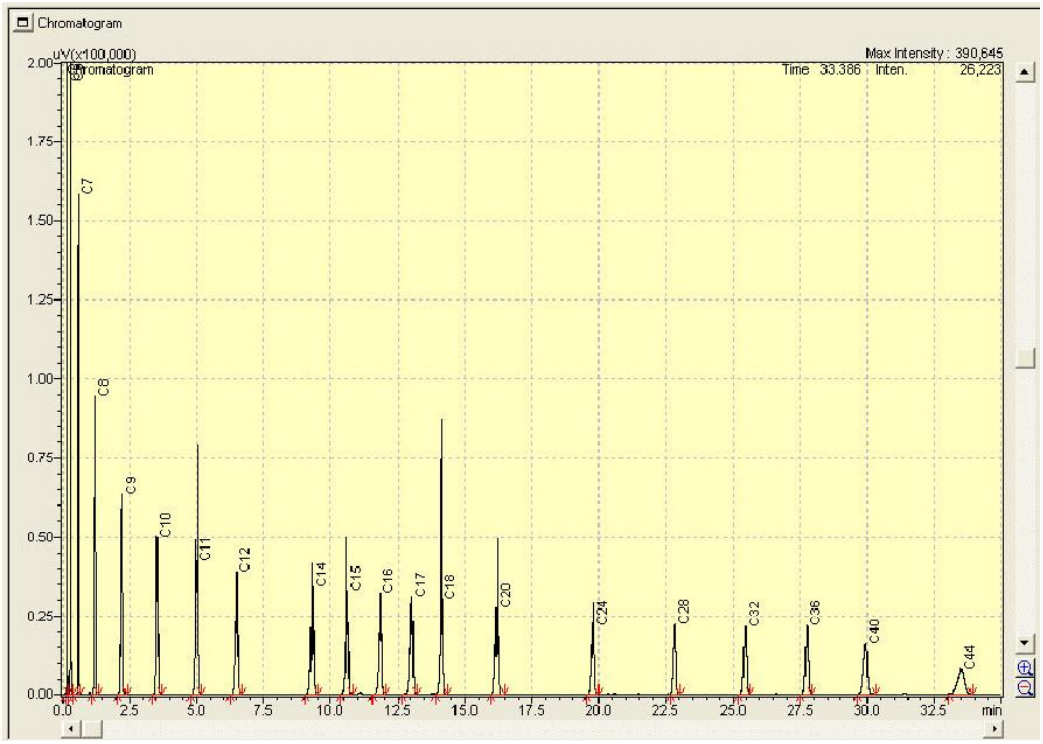

Figure B.1 Chromatogram of calibration mixture reference.

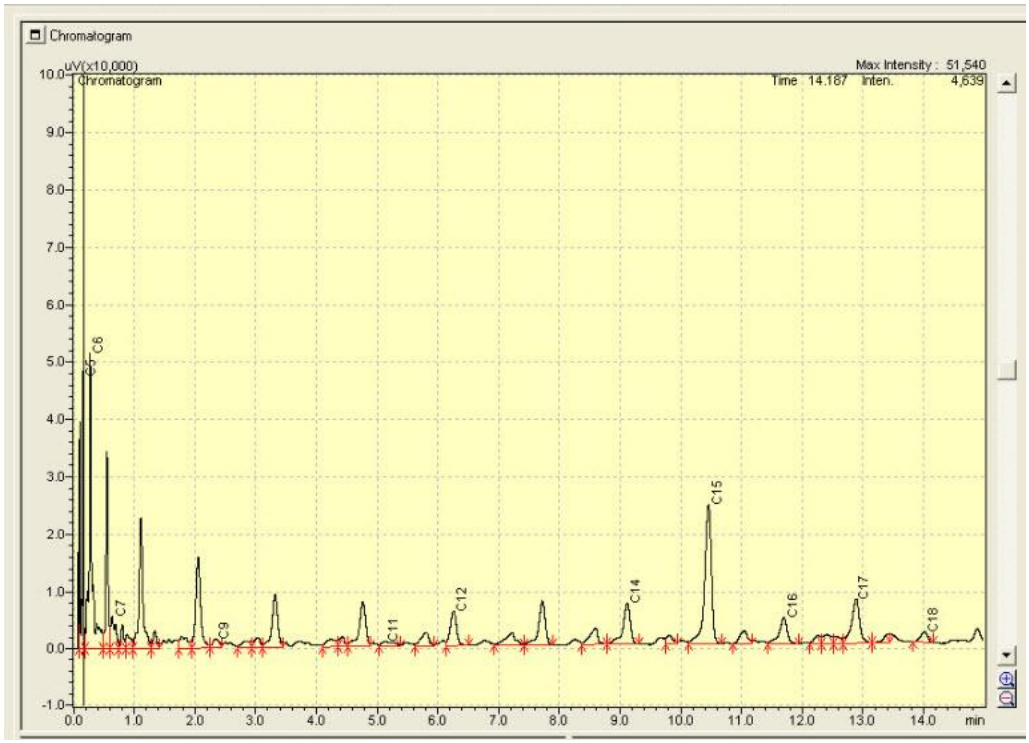

Figure B.2 Chromatogram of data analysis.

Table B.2 Results from chromatogram of calibration mixture reference.

Peak	Component	Rt (min)	Area	Conc.	Conc. (100%)	Units
1	C_5H_{12}	0.163	316798.1	0.9995	5.00033	%(w/w)
2	C_6H_{14}	0.3	345611.2	0.9995	5.00033	%(w/w)
3	C_7H_{16}	0.61	330865.1	0.9995	5.00033	%(w/w)
4	C_8H_{18}	1.22	63212.1	0.9995	5.00033	%(w/w)
5	C_9H_{20}	2.23	300457.4	0.9995	5.00033	%(w/w)
6	$C_{10}H_{22}$	3.55	291602.6	0.9995	5.00033	%(w/w)
7	$C_{11}H_{24}$	5.01	273183.5	0.9995	5.00033	%(w/w)
8	$C_{12}H_{26}$	6.5	262581.8	0.9995	5.00033	%(w/w)
9	$C_{14}H_{30}$	9.32	239842.9	0.9995	5.00033	%(w/w)
10	$C_{15}H_{32}$	10.62	233431.4	0.9995	5.00033	%(w/w)
11	$C_{16}H_{34}$	11.85	225150.5	0.9995	5.00033	%(w/w)
12	$C_{17}H_{36}$	13.02	216383.8	0.9995	5.00033	%(w/w)
13	$C_{18}H_{38}$	14.13	205113.8	0.9995	5.00033	%(w/w)
14	$C_{20}H_{42}$	16.19	187065.4	0.9995	5.00033	%(w/w)
15	$C_{24}H_{50}$	19.76	160614.5	0.9995	5.00033	%(w/w)
16	$C_{28}H_{58}$	22.83	160561.9	0.9995	5.00033	%(w/w)
17	$C_{32}H_{66}$	25.45	157273.7	0.9991	4.99832	%(w/w)
18	$C_{36}H_{74}$	27.76	153387.5	0.9995	5.00033	%(w/w)
19	$C_{40}H_{82}$	29.94	158740	0.9986	4.99582	%(w/w)
20	$C_{44}H_{90}$	33.52	146186.8	0.9995	5.00033	%(w/w)

Data analysis can be converted from GC postrun to program GC distillation data calibration by batch table for calculated distillation data, distillation curve, distillation data in specified temperature range and ASTM D-86. Result analysis form program simulated distillation is shown in Figure D.3 – Figure D.6 respectively.

Table B.3 Distillation GC calibration initial setting.

ID	Component	Rt (min)	Boiling point (˚C)
1	C_5H_{12}	0.163	36
2	C_6H_{14}	0.3	69
3	C_7H_{16}	0.61	98
4	C_8H_{18}	1.22	126
5	C_9H_{20}	2.23	151
6	$C_{10}H_{22}$	3.55	174
7	$C_{11}H_{24}$	5.01	196
8	$C_{12}H_{26}$	6.5	216
9	$C_{14}H_{30}$	9.32	254
10	$C_{15}H_{32}$	10.62	271
11	$C_{16}H_{34}$	11.85	287
12	$C_{17}H_{36}$	13.02	302
13	$C_{18}H_{38}$	14.13	316
14	$C_{20}H_{42}$	16.19	344
15	$C_{24}H_{50}$	19.76	391
16	$C_{28}H_{58}$	22.83	431
17	$C_{32}H_{66}$	25.45	466
18	$C_{36}H_{74}$	27.76	496
19	$C_{40}H_{82}$	29.94	522
20	$C_{44}H_{90}$	33.52	545

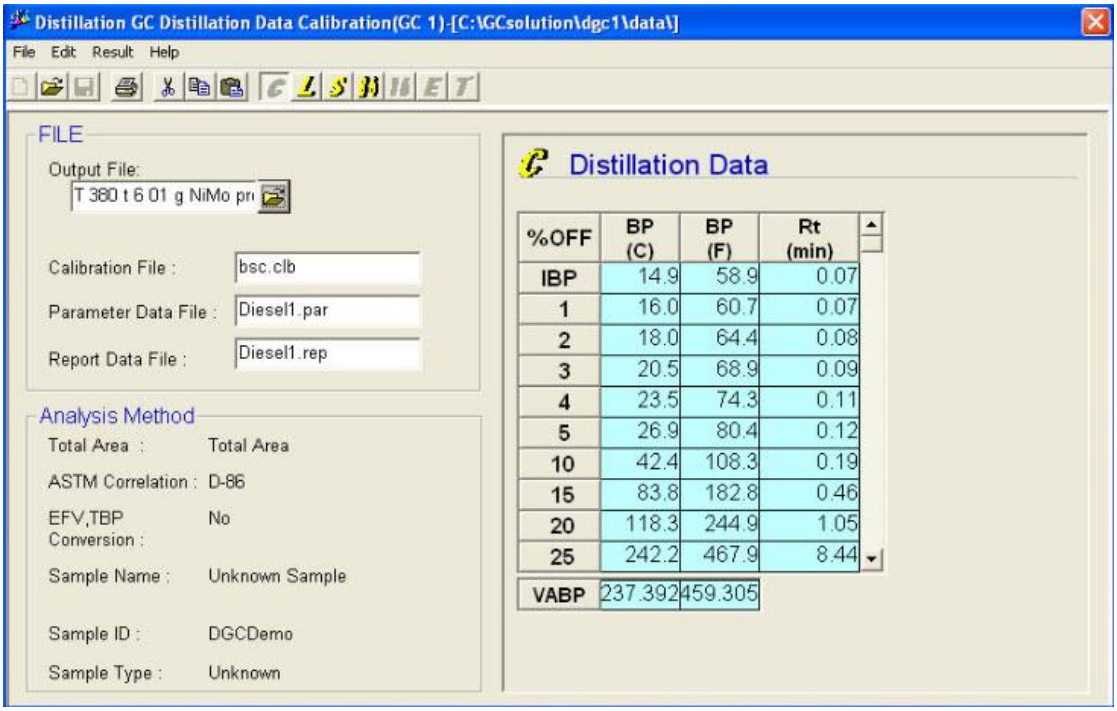

Figure B.3 Calculated distillation data.

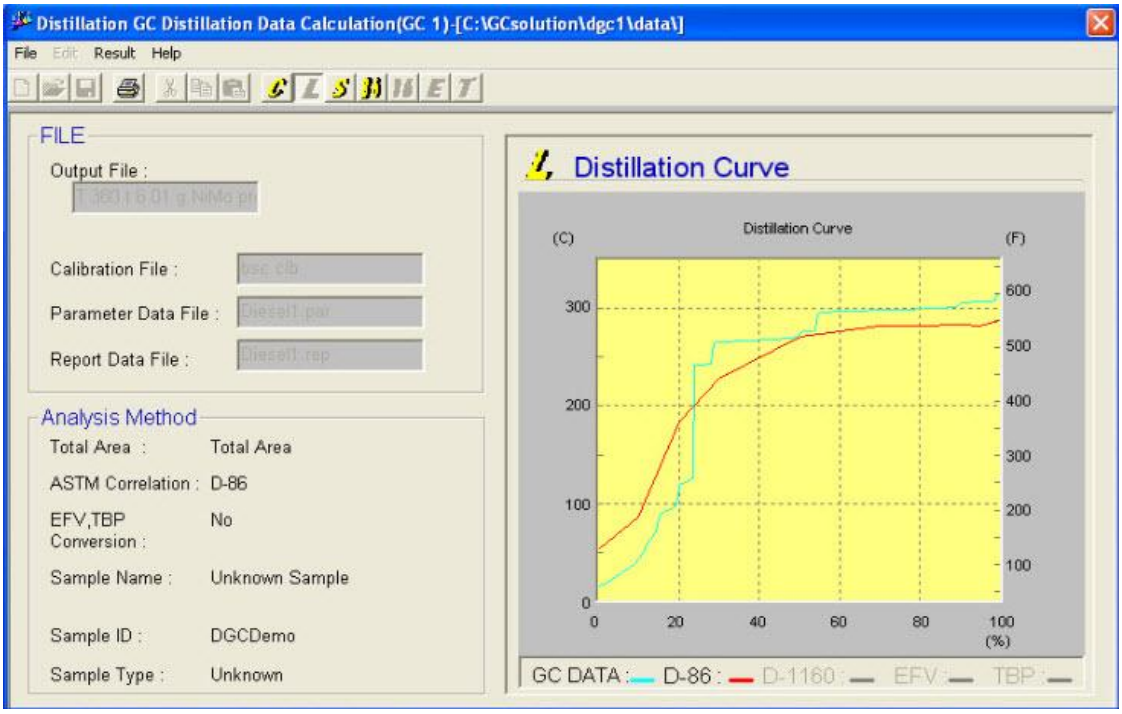

Figure B.4 Distillation curve.

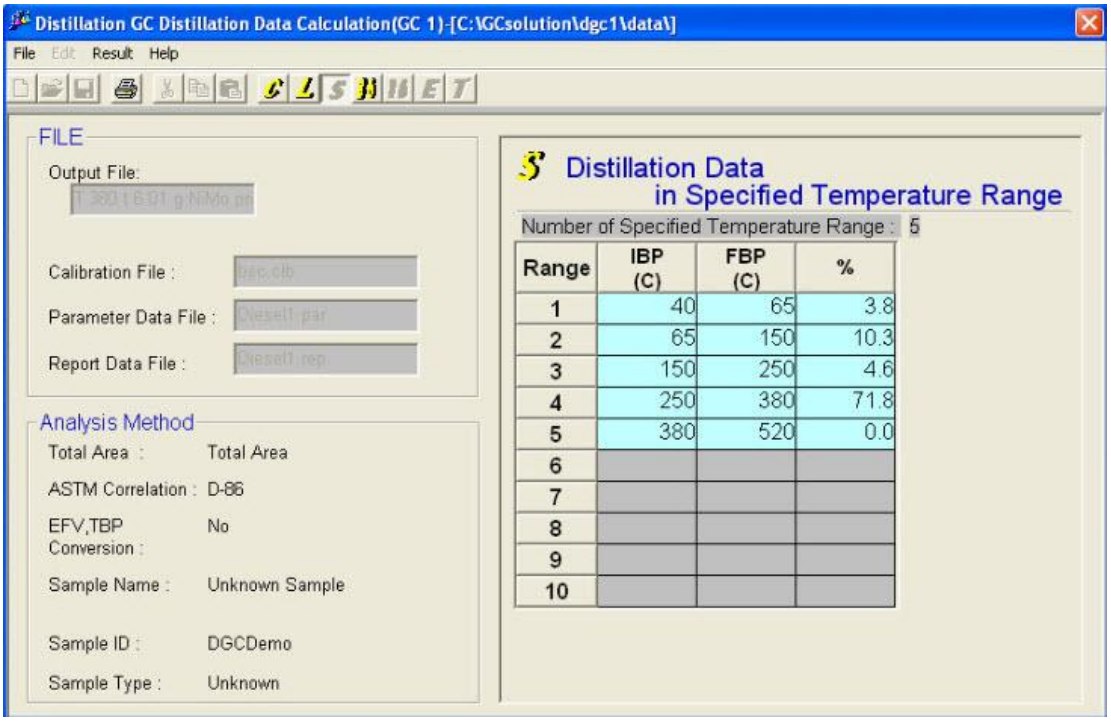

Figure B.5 Distillation data in specified temperature range.

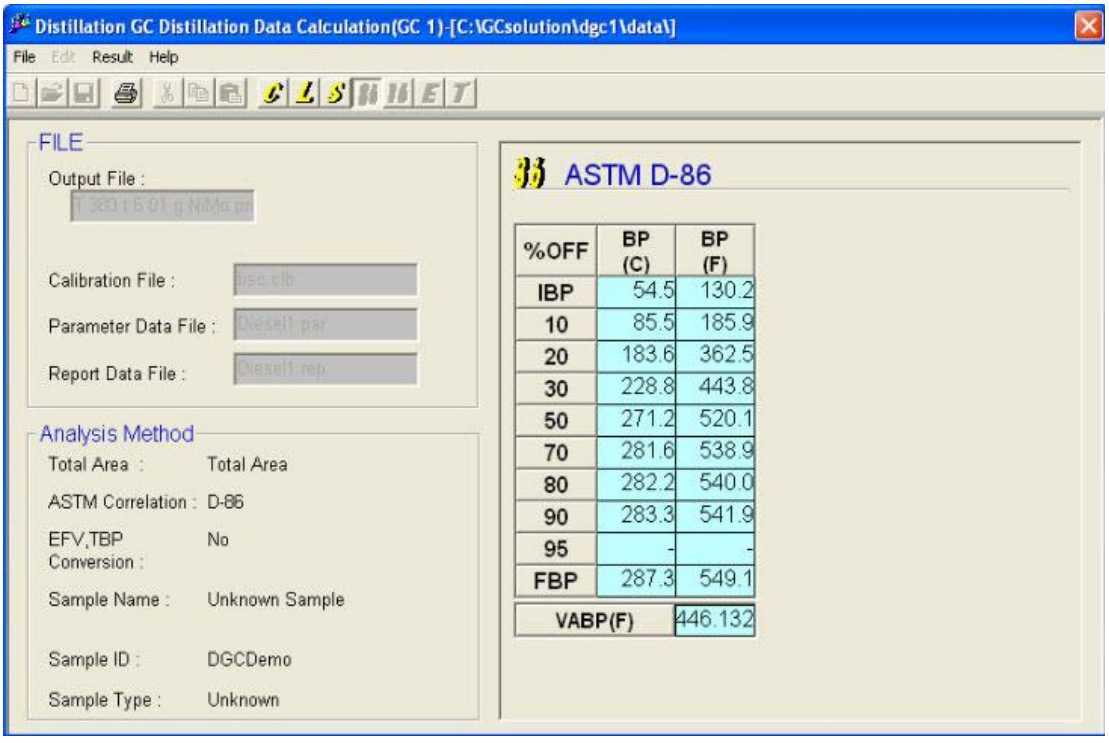

Figure B.6 ASTM D-86.

APPENDIX C

DATA OF CALCULATION OF TOTAL ACID SITE

Table C.1 Area of NH_3 TPD curve for calculation of total acid site

Sample	Temperature (°C)	area	Total area
$NiMo/Al_2O_3$	238.7	0.33607	0.33607
$CoMo/Al_2O_3$	181.3	0.0093	0.11865
	209.4	0.10935	

Calculation of total acid sites

For example, $NiMo/Al_2O_3$ sample, total acid site is calculated from the following step

1. Calculation of total peak area to peak volume

From Figure C.1 below, the volume of NH_3 calculates from equation y = 35.847x

The volume of NH3 = 35.847 x area

(Total acid strength = 35.847 x 0.33607

= 12.047 ml

2. Calculation for adsorbed volume of 15%NH_3

Adsorbed volume of 15% NH_3 = 0.15x total peak volume

= 0.15 x 12.047ml

= 1.807ml

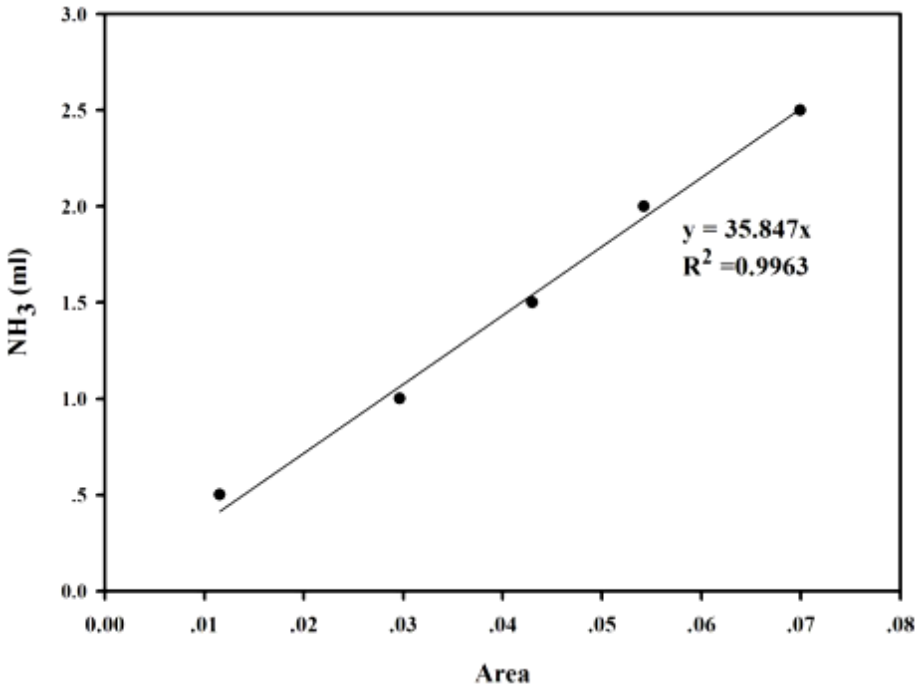

Figure C.1 The calibration curve of ammonia.

3. The acid sites are calculated from the following equation

$$\text{The acid sites} = \frac{\text{Adsorbed volume(ml)} \times 101.325\ \text{Pa}}{3.314 \times 10^{-3}\ \frac{\text{Pa} \cdot \text{ml}}{\text{K} \cdot \mu\text{mol}} \times 298\text{K} \times \text{weight of catalyst(g)}}$$

For $NiMo/Al_2O_3$ sample, 0.0522 g of this sample was measured, therefore

$$\text{The acid sites} = \frac{1.807\text{ml} \times 101.325\ \text{Pa}}{3.314 \times 10^{-3}\ \frac{\text{Pa} \cdot \text{ml}}{\text{K} \cdot \mu\text{mol}} \times 298\text{K} \times 0.0522\ \text{g}}$$

$$= 1.415\ \text{mmol/g}$$

VITA

Miss. Narisara Rodboon was born on 7th November 1987, in Bangkok Thailland. She studies high school from Navamintrachinuthid Suankularb Wittayalai Samutprakarn. Her graduated Bachelor degree of Chemical Engineering from King Mongkut University of Technology Thonburi, Thailand in April 2010. She has studying for her Master degree of Engineering from the department of Chemical Engineering, Chulalongkorn University.

List of Plublication:

Narisara Rodboon, Worapon Kiatkittipong, and Suttichai Assabumrungrat, "THE HYDROPROCESSING OF WASTE COOKING PALM OIL FOR DIESEL LIKE HYDROCARBONS PRODUCTION OVER NiMo/Al_2O_3 CARBIDE CATALYST", Proceedings of Pure and Applied Chemistry International Conference 2012, Chiang Mai, Thailand, Jan.10-12,2012.